UNIVERSIDAD NACIONAL AUTÓNOMA DE MÉXICO

PROGRAMA DE MAESTRÍA Y DOCTORADO EN INGENIERÍA

INGENIERÍA EN EXPLORACIÓN Y EXPLOTACIÓN DE
RECURSOS NATURALES – YACIMIENTOS

DYNAMIC RESERVOIR CHARACTERIZATION USING FLOWING PRESSURE AND PRODUCTION RATE

TESIS
QUE PARA OPTAR POR EL GRADO DE:
DOCTOR EN INGENIERÍA

PRESENTA:
JOSÉ ERNESTO PARRA PÉREZ

TUTOR PRINCIPAL
DR. FERNANDO SAMANIEGO VERDUZCO
FACULTAD DE INGENIERÍA UNAM

CIUDAD UNIVERSITARIA, CDMX, ENERO 2024

Abstract

This work presents macroscopic and microscopic analytical flow models for dynamic reservoir characterization. The models use production rate and flowing pressure data acquired from reservoir monitoring and surveillance, i.e., without the need to shut-in wells or perform dedicated tests.

The main purpose of the macroscopic models is to calculate the original oil in place (OOIP), both, for volumetric and natural water drive reservoirs, but they can also calculate the productivity index (PI), average pressure, water influx and heterogeneity factor. The microscopic model is mainly used to estimate the directional permeability from a multiwell reservoir.

The macroscopic models are dynamic material balance, also known as zero-order or tank models. They consider average properties within large control volumes, such as the drainage volume of a well, or the entire reservoir. Microscopic models are solutions to the diffusivity equation, they are applied at each point in the reservoir and in multiple dimensions.

The macroscopic models are derived from physical principles, in the same manner as the well-known capacitance resistance models (CRM): a production analysis technique that has been widely used to characterize reservoirs during injection processes, such as waterflooding, however, most applications neglect bottomhole pressure and only a few have focused on primary recovery.

The first macroscopic model is referred to as the Capacitance Resistance Producer-Based Model (CRMP). It is used to characterize volumetric undersaturated oil reservoirs in primary recovery. The model accounts for production due to depletion and pressure fluctuations from operational changes. CRMP enables the calculation of the drainage pore volume (PV) and the PI, analogous to the classical flowing material balance (FMB) methods used in production/rate transient analysis (RTA). The major differences between them are in the derivation and solution method; CRMP is derived from an instantaneous macroscopic balance and solved via nonlinear regression, whereas the FMB is derived using superposition and provides some diagnostics when the data is not too noisy. CRMP was improved by incorporating PI definitions, and also using successive time windows that enable to capture of time-varying parameters. The model was extensively investigated by comparison with various synthetic and real field cases of single and multiwell reservoirs, with results well within engineering accuracy.

Next, CRMP was extended to characterize oil reservoirs with natural water influx; thus, it was coupled with the Fetkovich aquifer model resulting in the Capacitance Resistance Producer-Based Aquifer Model (CRMPA). The Fetkovich model and CRM fit nicely together, because they are derived from the same assumptions. Other oil reservoir-aquifer models have been reported in the field of RTA and pressure transient analysis (PTA); however, they are not widely applied because the oil

reservoir and aquifer properties are generally similar and may not show distinct features in diagnostic plots. CRMPA was constrained and solved, using simple storage and transmissibility relationships between an equivalent (single permeability) and the composite (reservoir and aquifer) medium. The model enables calculating the reservoir PV, PI, and water influx. Thus, it also helps to identify the reservoir recovery mechanisms.

Furthermore, CRMPA was coupled with the Koval fractional flow model yielding the CRMPAF. Incorporating the fractional flow model enables to account for the individual oil and water production rates, significantly increasing the accuracy of the solutions. CRMPAF calculates the same properties as CRMPA and additionally estimates a parameter describing the heterogeneity associated with each production well. CRMPAF was compared with numerical reservoir-aquifer models with different properties and geometries, and it was also used to characterize a field case. The OOIP estimations using CRMPAF for reservoirs with water influx and two-phase production were in excellent agreement with the validation and field case data.

Finally, this work presents a novel application of a microscopic analytical model of a 2D multiwell volumetric reservoir. The model also uses production rate and flowing pressure data to characterize the reservoir. The model handles variable flow rates, damaged or stimulated wells, single or dual porosity, and permeability anisotropy. The novel approach uses the model in an inverse way to characterize the directional permeability at the interwell scale, this approach has been possible with the advent of permanent downhole gauges (PDG). Various synthetic and real cases are discussed. This model is most useful for studying interwell communication in small reservoirs, or within a group of wells in a block or pattern in large fields.

The analytical macroscopic and microscopic flow models presented in this thesis can serve as a proxy before reservoir simulation, however, they have important differences; e.g., they are more easily programmed and their computing times are much faster; but most importantly, these models are used for dynamic reservoir characterization, i.e., they provide the OOIP and interwell permeability as output values, whereas these are usually the input data used for prediction purposes in reservoir simulation.

Acknowledgments

I want to thank my supervisor Dr. Fernando Samaniego, for all the support, challenge, motivation and guidance throughout all these years. I am very grateful to have worked with one of the greatest minds in our industry and with an excellent human being.

I am also very grateful with Dr. Larry Lake from the University of Texas at Austin. Our collaboration was extremely valuable; thanks for the ideas and suggestions for this research, and for always having an amazing charisma.

I want to thank the members of my PhD Dissertation Committee and the professors who have greatly encouraged my graduate studies: Dr. Fernando Rodríguez de la Garza, Dr. Héber Cinco Ley, Dr. José Luis Bashbush and Dr. Néstor Martínez Romero.

I also want to thank Dr. Gary Pope, a great mentor who has always motivated and cared for me.

I want to thank my sister Mariana for always being there. I am also very grateful with my parents Leticia and José; you are my greatest examples and the people that I most admire.

Most importantly, I want to thank my wife Lorena, thanks for all your love and support throughout these years. I am already looking forward to what's next for us.

Contents

List of Tables

List of Figures

Nomenclature

A	=	area, L^2, ft^2
a	=	Shape factor
B	=	formation volume factor, RB/STB
c	=	compressibility, Lt^2/m, psi^{-1}
D	=	Depth, L, ft
E	=	Viscosity ratio
f	=	Fractional flow
h	=	net pay thickness, L, ft
i	=	injection flow rate, L^3/t, RB/D
J	=	productivity index, L^4t/m, STB/D-psi
K_v	=	Koval factor
k	=	permeability, L^2, md
N	=	Oil in place, L^3/t, STB
N_P	=	Cumulative oil produced, L^3, STB
p	=	pressure, m/Lt^2, psi
Q_p	=	Cumulative production, L^3, STB
q	=	Production flow rate, , L^3/t, STB/D
r	=	radius, L, ft
S	=	Saturation
s	=	skin
t	=	time, t, days or hours
V_p	=	pore volume, L^3, RB
W_e	=	Cumulative water influx, L^3, STB/D
w_e	=	Water influx rate, L^3/t, STB/D
W_p	=	Cumulative water produced, L^3, STB
x	=	coordinates in x direction, L, ft
y	=	coordinates in y direction, L, ft
β	=	Conversion factor, 141.2 in field units
μ	=	viscosity, m/Lt, cp
τ	=	time constant, t, days
λ	=	Interwell connectivity
ϕ	=	porosity
ρ	=	Density, m/L^3, Kg/m^3

Subscripts and superscripts

a	=	aquifer
D	=	dimensionless
e	=	external
f	=	formation
G	=	geometric
H	=	Harmonic
h	=	horizontal
i	=	initial
j	=	producer index
n	=	timestep level
o	=	oil
r	=	reservoir
t	=	total
v	=	vertical
w	=	water

Chapter 1. Introduction

Reservoir characterization is the necessary step before performing any type of physics-based prediction in reservoir engineering; once this is accomplished, production forecasts and reserves estimation can be conducted using analytical or numerical simulation models.

Reservoir characterization is usually divided into static and dynamic, but they must be ultimately used together to yield a single reservoir model. Dynamic reservoir characterization is defined as the identification and evaluation of the properties that affect reservoir flow behavior (Cinco Ley, 2023). It is conducted by simultaneously analyzing rate and pressure data, while also using other available fluid, well, and reservoir information. The most important methods for dynamic characterization are the material balance equation (MBE), capacitance resistance models (CRM), pressure transient analysis (PTA), production data analysis or rate transient analysis (RTA), tracer tests, temperature measurements, and production logging tools (PLT).

This research was motivated by the need to characterize reservoirs using dynamic (pressure and rate) data from flowing wells, i.e., without the need for shut-ins. Production flow rate data is the most abundant information from an oil or gas field. Bottomhole pressure (BHP) data was very limited in the past, but it has become more accessible in recent years, as more wells are now equipped with permanent downhole gauges (PDG), (Houzé et al. 2009).

This work presents new analytical flow models to characterize reservoir properties using production rates and flowing pressures. Flow models can be classified as macroscopic or microscopic (Walsh and Lake, 2003). Macroscopic models (tank or zero order) are dynamic material balance type models used to characterize the whole reservoir or the drainage volume of a well using overall/average properties. Microscopic models, on the other hand, can describe the flow behavior at each point in space and in multiple dimensions.

Analytical flow models are the basis of the MBE, CRM, PTA, and RTA techniques, which stem from the same basic physical principles. However, their derivation, assumptions, and solutions differ. The classic MBE is a cumulative macroscopic model, CRM is an instantaneous macroscopic model, and both PTA and RTA represent microscopic models.

Both, macroscopic and microscopic models are developed in this research, thus important concepts will be reviewed. Chapter 2 starts with a discussion of fluid flow in reservoirs, it presents the derivation, differences, and solutions of the macroscopic and microscopic fluid flow equations that are used throughout the thesis. Reservoir flow behavior goes through different stages or regimes that enable to quantification of different properties, the more general classification divides flow behavior

concerning the reservoir boundary condition as either transient or infinite acting flow (IAF) and boundary-dominated flow (BDF), first discussed by Muskat (1946).

The present work is restricted to conventional (moderate to high permeability, >10 md) undersaturated oil reservoirs; thus, the main emphasis is on BDF, which is the main flow regime of interest for long-term production data. It is important to point out that conventional reservoirs account for about 90% of the total world production of ~95 million barrels per day (BP 2023).

Chapter 2 also discusses some of the classical MBE, PTA and RTA methods. The MBE is discussed along the derivation of the macroscopic flow model, pointing out important concepts about the recovery mechanisms. PTA is briefly discussed with emphasis on the analysis of flow tests. RTA is also discussed focusing on the Decline Curve Analysis (DCA) and the basic modern production analysis methods.

It must be emphasized that PTA and RTA are analogous, the basic models were originally derived from a microscopic balance, and their fundamental solutions date back to the constant terminal rate and the constant terminal pressure solutions for IAF and BDF reservoirs (van Everdingen and Hurst, 1949). They also share similar mathematical procedures and their solutions are related, but the techniques have evolved in different ways and they are also different in practice.

PTA, also referred to as well testing, is a controlled experiment performed in-situ. It is usually a short-term test (hours to days) that analyzes high-frequency pressure measurements. The main regime of interest is transient flow, during which permeability and skin can be determined, but which can also detect other reservoir characteristics, such as faults, boundaries, storativity, and communication between wells. It can also quantify BDF properties such as pore volume (PV) and reservoir geometry, depending on the test type and duration.

PTA has largely evolved from its early days (Theis, 1935) to the technique that it is today. Largely, because of the developments of mathematical and computational methods, as well as hardware tools (Mathews and Russell 1967; Earlougher 1977; Kamal 2009). The majority of tests performed in PTA are pressure buildups (BU) because they result in clean data. The major drawbacks are that the tests require shut-in wells, causing lost production and representing costs and risk to the well, as any other field operation. A minor number of PTA tests are also conducted under flowing conditions, as in drawdown, injection, and multi-rate or deliverability tests. Multiple rate tests could be analyzed with RTA, yielding equivalent results, however, RTA is usually not performed as a dedicated test, but rather as an analysis of routine well surveillance/monitoring production data.

RTA focuses on long-term rate variations (months to years). The flow regime of interest for conventional reservoirs is BDF and transient flow for unconventionals. RTA encompasses the Arps (1944) empirical rate-time equations or DCA, which is still one of (if not) the most widely applied

method for reserves estimation, and modern production analysis, which provides analytical models derived from physical principles using rate-pressure-time, and which also set the theoretical basis for DCA. RTA was first developed assuming the well produces at constant flowing pressure (Fetkovich 1980), as opposed to PTA which assumed constant flow rate. Later it was shown (Blasingame and Lee 1986) that variable rate/pressure can also be handled, analogous to PTA (Kuchuk et al. 2008).

This work uses concepts derived from both PTA and RTA to characterize well-reservoir properties using flowing pressure and rate data, which are jointly referred to as production data throughout the thesis, and which have also been discussed in the CRM literature (Chapter 3).

The Capacitance Resistance Model (CRM); a physics-based mathematical model that is solved with data-driven methods. This modern CRM version was developed by Yousef et al. (2006) to characterize reservoirs under waterflooding processes. CRM bears its name from the analogy between the capacitance-resistance properties of an electric circuit and the storage-transmissibility of a permeable medium; in the past this idea was investigated with experimental models (Bruce 1943). The modern CRM was developed based on the work of Albertoni and Lake (2003), who formulated a purely resistive (steady-state) analytical model to find the connectivity between injection and production wells, solved using regression methods.

The CRM technique has been continuously developed and applied to many reservoirs under secondary and tertiary recovery processes (Holanda et al. 2018). However, there are very few applications of CRM to model reservoirs in primary recovery (Izgec and Kabir 2011; Nguyen 2011). Furthermore, the fluid production caused due to operational changes, which are reflected in the BHP are usually not included in the analyses, either because the BHP data are not available or because the fluctuations are considered negligible in mature reservoirs under injection processes.

Chapter 3 discusses the fundamental concepts of CRM. It presents the control volume representations, the derivation, assumption and solutions, with emphasis in the Capacitance Resistance Producer-Based Model (CRMP). This model was initially formulated by Liang (2007) for waterflooding. It considers that the control volume is the total drainage volume of a well. It differs from the control volume representation originally developed by Yousef et al. (2006), which considers each injector-producer pair drainage volume, whose approach is known as the Capacitance Resistance Injector-Producer Model (CRMIP). Later, Sayarpour (2009) developed and compared rigorous solutions for this and other CRM control volume approaches. The most basic CRM control volume representation considers a tank or “super well”, whereas the more complex representations can include injection-producer pairs in commingled reservoirs that further require individual layer data. CRMP and CRMIP are the most popular approaches, as they provide a good balance between the model complexity, the number of unknowns, and solution quality.

The developments from this dissertation are presented in Chapters 4 to 6. Chapter 4 and 5 present the macroscopic flow modeling approaches for production data analysis while Chapter 6 describes a microscopic model.

Chapter 4 presents improvements to the CRMP approach, which applies to undersaturated volumetric reservoirs in primary recovery (Parra et al. 2023a). The model calculates the production flow rate of a well due to reservoir depletion and BHP changes from operational activities. Characterization is achieved by finding the reservoir PV and the PI that better represent the historical production data, using nonlinear regression. CRMP was improved from the previous works by incorporating PI definitions, thus, accounting for reservoir properties and geometry for ideal cases. It was also extended to include time varying drainage PV or PI by using successive time windows. Furthermore, if the well-reservoir model is known from a PTA test, the time-varying skin or permeability can also be quantified. Several single and multiwell reservoir cases are presented to show the utility of CRMP.

CRMP includes the macroscopic exponential rate decline and the pseudo-steady state (PSS) flow solutions as limiting cases. It is analogous to the flowing material balance (FMB) (Mattar and McNeil, 1996; Mattar and Anderson, 2003), which is a major part of the production analysis toolbox. The differences are that CRM is derived from a macroscopic balance and is solved by history matching, whereas the FMB uses superposition and may offer some diagnostics when production data is not too noisy. Also, pressure-dependent properties can be updated in CRMP, analogous to reservoir simulation, which resembles the use of pseudo-functions in the FMB.

Chapter 5 extends the CRMP approach and presents a novel method to characterize an undersaturated oil reservoir in primary recovery, with natural water influx. CRMP is coupled with the Fetkovich aquifer model to yield the Capacitance Resistance Producer-Based Aquifer Model (CRMPA). This model is a significant improvement from the only previously coupled CRM-aquifer approach (Izgec and Kabir 2010), which required prior estimations of the drainage volume and average pressure from BU tests, whereas, these parameters are obtained as outputs in the new CRMPA. The new model enables the estimation of water influx, aquifer pore volume, and PI, respectively, in addition to the parameters obtained from the simpler CRMP approach.

Next, CRMPA was further improved by coupling it with fractional flow theory, namely, with the Koval (1963) model yielding the CRMPAF approach (Parra et al. 2023b), which enables to account for two-phase production caused by water breakthrough from the aquifer.

Multi-phase production is a complex topic. It is usually incorporated into reservoir flow models, analytical (Pope 1980) or numerical, via relative permeability and sometimes capillary pressure equations; although one must be aware that these relationships often come from laboratory tests or

empirical models, thus, their model parameters are often treated as history match parameters, as is done in reservoir simulation, where the PV, permeability, compressibility, and other reservoir/aquifer parameters are fixed. Conversely, in CRMPA the reservoir and aquifer PV and PI, are unknown, thus, adding more matching parameters will complicate the problem.

Recently, Cao et al. (2015) used the Koval fractional flow model to describe waterflooding processes, yielding accurate results. The major advantage of the Koval model is that it is a one parameter model. It has been amply validated and utilized in Enhanced Oil Recovery (Lake et al. 2014). The Koval method is also equivalent to the Buckley-Leverett (1942) model for the case of straight-line relative permeabilities, which is a reasonable assumption considering that relative permeabilities tend to stretch out as a function of scale, e.g., going from a representative elementary volume (REV) such as a core to a field scale, thus, the Koval factor can also be regarded as a measure of reservoir heterogeneity (Salazar and Lake, 2020). CRMPAF estimates the Koval or heterogeneity factor, in addition to the previous CRMPA parameters. The CRMPAF models were validated and used to characterize synthetic and real field cases with very good results.

The CRMP, CRMPA and CRMPAF approach strictly apply to single-well reservoirs, however, this work shows that approximate solutions can also be obtained for multiwell reservoirs for BDF/stabilized flow, i.e., when the wells have established no-flow boundaries. Attempts were also made throughout this research to include the effect of connectivity between multiple production wells, using the macroscopic models, however, the results were highly non-unique. This was one of the motivations to use a microscopic model as presented in Chapter 6.

The microscopic model is a solution of the diffusivity equation for a 2D homogeneous reservoir in cartesian coordinates, under PSS flow. It incorporates the effect of multiple wells and variable flow rates using superposition. The model and similar versions were previously presented in the literature (Ozkan 1986; Rodríguez and Cinco-Ley 1993, Camacho et al. 1996, Umnuayponwiwat and Ozkan, 2000; Valko et al. 2002), but it was only used in a forward manner and not in a reservoir characterization sense. The main objective of applying this model was to characterize the directional permeabilities using long-term rate and flowing pressure data, which was not available in the past.

Permeability anisotropy has been commonly investigated with multiwell interference or pulse tests assuming IAF (Kamal, 2009) and performing tracer tests. The latter provides more direct evidence of connectivity; however, some operators are still reluctant to conduct them because they take longer and cost more than pressure tests. Ramey (1975) introduced the most popular form of interference test for anisotropic reservoirs; the method requires an active well and at least three shut-in observation wells. The more general theory does not preclude that the observation wells are opened, but the analysis becomes more difficult when the wells have varying rates (Kamal, 2009; Houzé et al. 2022).

The microscopic model used here assumes BDF, thus, it can incorporate longer periods of production data as compared to the transient method, however, it requires an estimation of the reservoir PV, usually from volumetrics or any other source, e.g., CRM. The model is solved by history matching the directional permeabilities using the historical rate and BHP data, preferably coming from a PDG. Cases are presented to demonstrate this approach.

Finally, Chapter 7 provides the conclusions of this work, as well as recommendations for future research.

Chapter 2. Flow Models in Reservoir Engineering

Flow models are obtained by combining conservation equations with constitutive relations and equations of state. The fundamental principle in reservoir engineering is the conservation of mass or continuity, expressed as:

$$[\text{Rate of mass in}] - [\text{Rate of mass out}] = [\text{Rate of mass accumulation}]. \quad (2.1)$$

The principle can be expressed mathematically, the first step is to assume a control volume, often considered in cartesian or cylindrical coordinates (Fig. 2.1).

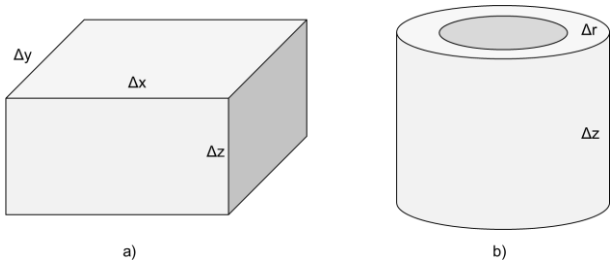

Fig. 2.1—Control volume for a) cartesian and b) cylindrical coordinate system models.

The mass balance for Fig. 2.1a, assuming single phase 1D flow in cartesian coordinates is:

$$\left[(\rho u_x)|_{x,y,z} - (\rho u_x)|_{x+\Delta x,y,z}\right]\Delta y\Delta z\Delta t = [(\rho\phi)|_{t+\Delta t} - (\rho\phi)|_t]\Delta x\Delta y\Delta z, \quad (2.2)$$

where ρ is the density of the fluid and u is the superficial or Darcy velocity, ϕ is the porosity, x, y and z are the space variables in cartesian coordinates, and t is time. Dividing by $\Delta x\Delta y\Delta z\Delta t$ and taking the limit as the space and time increments approach zero:

$$\frac{\partial \rho u_x}{\partial x} = -\frac{\partial \phi\rho}{\partial t}. \quad (2.3)$$

Alternatively, assuming single phase 1D radial flow through the control volume (Fig. 2.1b):

$$\left[(\rho u_r A_r)|_{r,\theta,z} - (\rho u_r A_r)|_{r+\Delta r,\theta,z}\right]\Delta t = [(\rho\phi)|_{t+\Delta t} - (\rho\phi)|_t]2\pi r\Delta r h, \quad (2.4)$$

where A_r is the cross-sectional area in the r direction, h is the thickness, and r, θ and z are space variables. The area term is inside the parenthesis because it is not constant in cylindrical coordinates. Dividing by $2\pi r\Delta r h\Delta t$ and taking the limits as both Δr and Δt approach zero leads to:

$$\frac{1}{r}\frac{\partial (r\rho u_r)}{\partial r} = -\frac{\partial \phi\rho}{\partial t}. \quad (2.5)$$

The generalization of the principle of mass continuity in a porous medium for any geometry and dimensions is expressed in vector notation as:

$$\nabla \cdot \rho u = -\frac{\partial \phi\rho}{\partial t}. \quad (2.6)$$

Eq. 2.6 is classified as a microscopic balance. The only assumption so far is single phase flow.

Microscopic models assume a continuum domain and enable calculations at any position and in multiple dimensions. Examples of microscopic balances are the diffusivity equation, and the pseudocomponent/modified black oil or beta models used in reservoir simulation. The diffusivity equation will be discussed in the next section, while the latter can be expressed for any phase *j* in a multiphase medium as follows:

$$\frac{d(\phi S_j \rho_j)}{dt} = -\nabla \cdot \rho_j u_j. \tag{2.7}$$

Eq. 2.7 is also known as the strong form of the conservation equation.

Alternatively, the continuity equation can be used to formulate macroscopic balances, which may be derived directly or from the integration of microscopic balances. Macroscopic models deal with finite systems and provide overall balances, independent of space. The material balance equation (MBE) and the Capacitance Resistance Model (CRM) represent cumulative and instantaneous macroscopic balances, respectively. The basic macroscopic and microscopic equations used throughout this thesis are derived next.

Macroscopic Balance

The macroscopic continuity equation can be derived by a spatial integration of Eq. 2.6 or 2.7 in any coordinate system, e.g., starting from the radial continuity in Eq. 2.5 and integrating from r_w to r_e, multiplying by $2\pi r \Delta r h$ and recalling $q = Au$ is the volumetric flow rate, results in the net rate of flux:

$$-\int_{r_w}^{r_e} 2\pi h \frac{\partial(\rho u_r)}{\partial r} dr = \rho q|_{r_e} - \rho q|_{r_w} = \rho \tilde{q}, \tag{2.8}$$

where we have assumed fluid density is the same in the whole control volume.

The time derivative integral over space multiplied by the annular control volume gives:

$$\frac{d}{dt}\int_{r_w}^{r_e} 2\pi h r \phi \rho \, dr = V_b \frac{d(\phi\rho)}{dt}, \tag{2.9}$$

where V_b is the bulk volume.

Thus, the macroscopic continuity equation is:

$$V_b \frac{d(\phi\rho)}{dt} = \rho \tilde{q}, \tag{2.10}$$

it is an overall balance; also known as the weak form of the conservation equation. It is valid regardless of the coordinate system.

The macroscopic equation for a multiphase medium for a phase *j* is:

$$V_b \frac{d(\phi S_j \rho_j)}{dt} = \rho_j \tilde{q}_j. \tag{2.11}$$

The macroscopic equations for the oil and water in an undersaturated oil reservoir are:

$$V_b \frac{d(\phi S_o \rho_o)}{dt} = \rho_o \tilde{q}_o, \tag{2.12}$$

$$V_b \frac{d(\phi S_w \rho_w)}{dt} = \rho_w \tilde{q}_w. \tag{2.13}$$

These equations can be combined to yield a total fluid material balance; the basis of CRM or MBE techniques. First, we use the product rule, divide Eq. 2.12 by $\phi S_o \rho_o$ and define $V_p = V_b \phi$ to yield

$$\frac{1}{\phi}\frac{d\phi}{dt} + \frac{1}{S_o}\frac{dS_o}{dt} + \frac{1}{\rho_o}\frac{d\rho_o}{dt} = \frac{\tilde{q}_o}{V_p S_o}, \tag{2.14}$$

applying the chain rule and defining an average pressure ($\bar{p}$) in the control volume:

$$\frac{1}{\phi}\frac{d\phi}{d\bar{p}}\frac{d\bar{p}}{dt} + \frac{1}{S_o}\frac{dS_o}{dt} + \frac{1}{\rho_o}\frac{d\rho_o}{d\bar{p}}\frac{d\bar{p}}{dt} = \frac{\tilde{q}_o}{V_p S_o}, \tag{2.15}$$

using the definitions of fluid and modified formation compressibility:

$$c_f \frac{d\bar{p}}{dt} + \frac{1}{S_o}\frac{dS_o}{dt} + c_o \frac{d\bar{p}}{dt} = \frac{\tilde{q}_o}{V_p S_o}, \tag{2.16}$$

leads to:

$$V_p S_o (c_o + c_f)\frac{d\bar{p}}{dt} + V_p \frac{dS_o}{dt} = \tilde{q}_o, \tag{2.17}$$

and analogously for the water:

$$V_p S_w (c_w + c_f)\frac{d\bar{p}}{dt} + V_p \frac{dS_w}{dt} = \tilde{q}_w. \tag{2.18}$$

Summing these equations and using the following expressions:

$$c_t = c_o S_o + c_w S_w + c_f, \tag{2.19}$$

$$S_o + S_w = 1, \tag{2.20}$$

$$\frac{dS_o}{dt} + \frac{dS_w}{dt} = 0, \tag{2.21}$$

leads to the total fluid balance at reservoir conditions as:

$$V_p c_t \frac{d\bar{p}}{dt} = \tilde{q}_o + \tilde{q}_w. \tag{2.22}$$

Substituting the net rate definitions:

$$V_p c_t \frac{d\bar{p}}{dt} = i_w - q_w - q_o. \tag{2.23}$$

or using the formation volume factor *B* and the subscript *sc* for standard conditions:

$$V_p c_t \frac{d\bar{p}}{dt} = \tilde{q}_{iwsc} B_w - \tilde{q}_{wsc} B_w - \tilde{q}_{osc} B_o. \tag{2.24}$$

Eq. 2.24 is the starting point of the CRM techniques. It is an instantaneous macroscopic expression relating the average pressure with time. Further, assuming no water is injected or produced:

$$V_p c_t \frac{d\bar{p}}{dt} = -q_{osc} B_o. \tag{2.25}$$

rearranging leads to:

$$\frac{d\bar{p}}{dt} = -\frac{q_{osc} B_o}{V_p c_t}. \tag{2.26}$$

The right term also appears in the solution of the microscopic pseudosteady state (PSS) flow equation.

It must be emphasized that solutions to microscopic and macroscopic balances are independent, which allows to use them together to solve reservoir engineering problems as will be described throughout this work.

Integrating Eq. 2.24 assuming B, V_p, c_t are constant with respect to pressure and rearranging yields an expression relating the average pressure with cumulative production:

$$V_p c_t (p_i - \bar{p}) = N_p B_o + W_p B_w - W_i. \tag{2.27}$$

where N_p, W_p, Wi are the cumulative oil, water, and water injection volumes. Eq. 2.27 is more commonly written as:

$$\frac{N B_{oi} c_t \Delta p}{S_o} = N_p B_o + W_p B_w - W_i, \tag{2.28}$$

which is well-known as the MBE for an undersatured oil reservoir.

Microscopic equation

The single-phase microscopic continuity equation (Eq. 2.6) is the starting point of the diffusivity equation, which is the basis of PTA/RTA techniques for reservoir characterization. This equation is coupled with a constitutive relation (usually Darcys Law) and an equation of state to reach a description of flow in permeable media.

Darcys law relates the potential with flux in a porous medium. The more general expression only assumes laminar flow and is written as:

$$u = -\frac{k}{\mu} \nabla \Phi, \tag{2.29}$$

where k and μ are permeability and viscosity, $\Phi = p \pm \rho g h$. Substituting Darcys law into the continuity equation:

$$\nabla \cdot \left(\frac{\rho k}{\mu} \nabla \Phi \right) = \frac{\partial \phi \rho}{\partial t}, \tag{2.30}$$

which applies for any coordinate system. Assuming isothermal conditions, no gravity effects and a constant viscosity, which is reasonable for most liquids:

$$\nabla \cdot \rho k \nabla p = \mu \frac{\partial \phi \rho}{\partial t}. \tag{2.31}$$

Applying the product and chain rules for ρ and ϕ in the time derivatives and rearranging:

$$\nabla \cdot \rho k \nabla p = \phi \rho \mu \left(\frac{1}{\rho} \frac{\partial \rho}{\partial p} \frac{\partial p}{\partial t} + \frac{1}{\phi} \frac{\partial \phi}{\partial p} \frac{\partial p}{\partial t} \right). \tag{2.32}$$

Using the definitions of small and constant compressibility for the fluid and rock:

$$\nabla \cdot \rho k \nabla p = \phi \rho \mu c_t \frac{\partial p}{\partial t}. \tag{2.33}$$

Applying the product and chain rule for the divergence terms:

$$\rho k \nabla^2 p + k \frac{\partial \rho}{\partial p} \nabla p^2 + \rho \nabla p \nabla k = \phi \rho \mu c_t \frac{\partial p}{\partial t}. \tag{2.34}$$

Neglecting pressure square terms (they are small for liquid flow in permeable media) and dividing by density:

$$k \nabla^2 p + \nabla p \nabla k = \phi \mu c_t \frac{\partial p}{\partial t}. \tag{2.35}$$

For a homogeneous and isotropic medium Eq. 2. leads to the well-known diffusivity equation:

$$\nabla^2 p = \frac{\phi \mu c_t}{k} \frac{\partial p}{\partial t}. \tag{2.36}$$

The diffusivity equation been solved for different geometries, initial and boundary conditions. Its application leads to the estimation of well-reservoir characteristics and enables to conduct modelling forecasts; it is the basis of PTA/RTA methods. Their solutions can also include the macroscopic responses as special cases.

The isotropic assumption can often be relaxed, e.g., using the following coordinate transformation and the geometric mean for a 3D cartesian medium when the permeability axes are aligned with the coordinate axes:

$$\bar{\xi} = \xi \sqrt{\frac{k}{k_\xi}} \quad \text{for} \quad \xi = x, y, z, \tag{2.37}$$

$$k = \sqrt[3]{k_x k_y k_z}. \tag{2.38}$$

These transformations enable to reduce the anisotropic problem to the isotropic case. Thus, the final form of the 3D diffusivity equation for an anisotropic medium is:

$$\frac{\partial^2 p}{\partial \bar{x}^2} + \frac{\partial^2 p}{\partial \bar{y}^2} + \frac{\partial^2 p}{\partial \bar{z}^2} = \frac{\phi \mu c_t}{k} \frac{\partial p}{\partial t}. \tag{2.39}$$

Flow stages

Fluid flow from petroleum reservoirs can be categorized in different stages or regimes. The main stages are transient, unsteady state or infinite acting flow (IAF) and boundary dominated flow (BDF) which is further divided into PSS, depletion and steady state (SS) flow.

As the names suggest, the major difference between the two flow regimes is the boundary condition. The main driving force during transient flow is diffusion, which is governed by the fluid and rock petrophysical properties, namely the hydraulic diffusivity $\eta = k/\phi\mu c_t$. Further, during the so-called late transient or semi-infinite acting-flow period some but not all of the boundaries affect the flow behavior. Conversely, during BDF the main driving force is the reservoir expansion, which depends on the storage/capacitance ($V_p c_t$), and on some contribution related to the reservoir inflow properties.

Several different flow geometries can occur during the IAF and BDF regimes, depending on the well completion and reservoir properties. For example, radial, spherical, linear, and bilinear flow geometries can be detected during transient flow. Radial or linear flow generally occur under BDF conditions. The microscopic models can be used to model both transient and BDF conditions. The macroscopic models are useful to describe BDF independent of the flow geometry.

Microscopic solutions to the flow equations can be found by considering an inner boundary condition (IBC), either constant pressure or constant rate, although most wells operate with variable rate and pressure. Macroscopic models, on the other hand, are usually independent of the IBC.

Fig. 2.2 shows the typical behavior of the production rate and bottomhole pressure (BHP) corresponding to the IAF, PSS and depletion flow stages of a well in a conventional oil reservoir. Note that the well is initially produced at a constant (maximum economic) rate while the BHP drops until it reaches the minimum BHP to lift the fluids to the surface: when the rate starts declining. In theory, wells can also be produced at constant pressure with a declining rate and go through the IAF and BDF stages, however this is rarely seen in practice, except in unconventional reservoirs. Next, the characteristics of these flow regimes are discussed, afterwards, some popular practical applications for estimating the OOIP (analogous to CRM) are discussed.

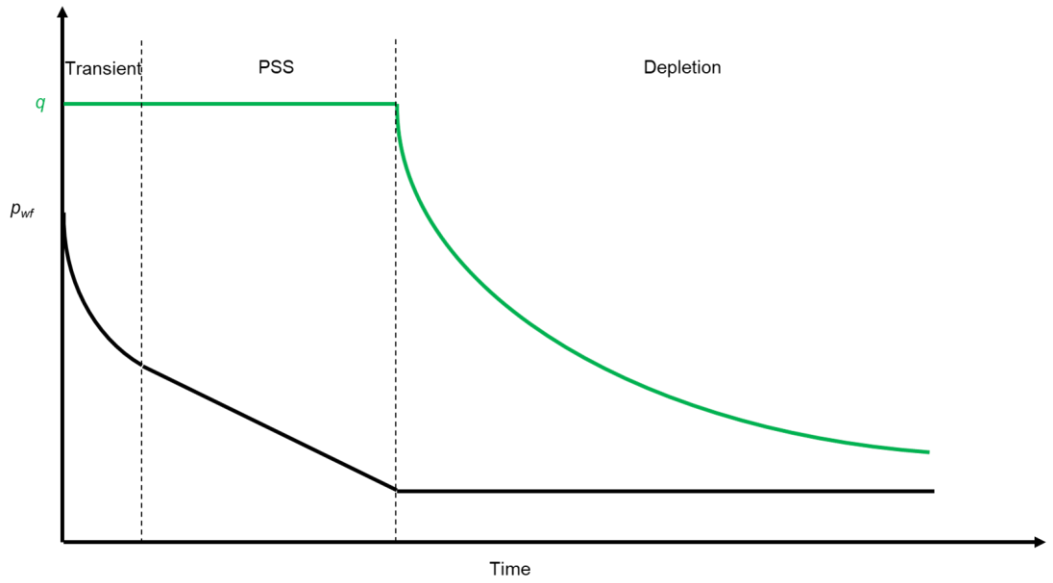

Fig. 2.2—Fluid flow stages in a conventional undersaturated volumetric oil reservoir, indicating the theoretical rate and flowing pressure at a production well.

Transient flow

This flow regime assumes an infinite acting reservoir. Although no reservoir is truly infinite, transient flow provides a nice flow description during the early production or shut-in periods of a well. Transient flow is relatively short as compared to the BDF regime duration (Fig. 2.2), at least in conventional reservoirs. It usually lasts from days to weeks in oil reservoirs or from weeks to months in gas reservoirs depending on the reservoir properties, namely permeability. On the other hand, transient flow is the main regime of interest in unconventional (low permeability) reservoirs, where it can last several years.

A transient occurs every time there is a major operational change in a reservoir, such as opening or shutting in a well or one of its neighbors, until stabilized flow conditions are reached again. Transient flow is of major importance for reservoir characterization; this is because the reservoir boundaries do not affect the flow behavior, simplifying the mathematical problem, the number of unknowns and the complexity of solutions (Dake, 1994).

During transient flow, the production condition at the wellbore is most often constant rate. It is characterized by a pressure drop that depends on both time and distance from the well as follows:

$$\frac{dp}{dt} = f(x,t) \tag{2.40}$$

where f is an arbitrary function that depends on flow geometry and x is a space variable.

Unsteady state flow also assumes that the pressure at the external boundary is constant and equal to its initial pressure, regardless of the time elapsed. Of course, this statement is not in agreement with

the laws of physics which establish that diffusion is an instantaneous process (Salsa, 2016), i.e., a pressure disturbance causes an immediate response in the entire domain, however, the previous consideration has been empirically validated and successfully applied in practice (Earlougher, 1977).

The CRM equations developed in this work are not strictly applicable to unsteady state flow, however, Chapter 4 shows that using some data that falls within this flow regime can still provide reasonable responses, especially during the late-transient flow regime (Matthews and Russell 1967). The microscopic model in Chapter 6 also assumes BDF, which is very useful from a practical perspective in conventional oil reservoirs, however, it could be expanded to include transient flow (Umnuayponwiwat and Ozkan 2000; Medeiros et al. 2010).

Pseudo-steady state (PSS) flow

The beginning of PSS or semi-steady state is shown in Fig. 2.2. At this moment the pressure disturbance has reached all the outer boundaries; either natural (structural/stratigraphical) or the no-flow boundaries arising from the interaction with other wells in multiwell reservoirs. The IBC in PSS flow is constant production rate as in Fig. 2.2. Hence, the two conditions for PSS flow are constant production rate, and a closed outer boundary/finite reservoir, i.e., the pressure gradient and the flow rate are both zero at the boundary. Furthermore, Fig. 2.2 shows that the BHP declines linearly with respect to time, thus, the pressure derivative is constant:

$$\frac{dp_{wf}}{dt} = C. \tag{2.41}$$

In fact, during PSS flow the entire pressure distribution in the reservoir (not only the BHP) declines uniformly and at the same constant rate as the average reservoir pressure:

$$\frac{dp_{wf}}{dt} = C = \frac{d\bar{p}}{dt} = -\frac{q_{osc}B_o}{V_p c_t}, \tag{2.42}$$

which is the same expression as was previously derived from the MBE (Eq. 2.26) for a volumetric undersaturated oil reservoir of small and constant compressibility.

PSS is one of the main flow regimes of interest in Production Analysis. It is generally longer than transient flow but shorter than depletion flow. It usually lasts from months to years in oil reservoirs, and years to decades in the case of gas reservoirs.

In multiwell reservoirs at PSS, the wells will establish their drainage volumes proportional to their production flow rate as required by Eq. 2.3. Matthews, Brons and Hazebroek (1956) used these concepts to calculate the average pressure in a bounded reservoir composed of multiple wells. The MBH method as is commonly known, uses individual drainage volume pressures obtained from buildup (BU) tests which are then volumetrically averaged to find the average reservoir pressure. The

drainage volumes for each well are obtained using the production rate from each well and the whole reservoir volume and total rate, satisfying:

$$\frac{V_{pj}}{V_{pt}} = \frac{q_j}{q_t}. \tag{2.43}$$

This equality holds as long as the rates of withdrawal remain reasonably constant. The authors concluded that their method is simpler and of sounder theoretical basis than averaging well pressures based on contour maps. They also stated that skin and the shape of the drainage volume do not affect this calculation, as expected for a macroscopic model.

The MBH relationship is used during this work to compare results from CRM calculations. The major limitation of the MBH method in estimating the individual drainage volumes of each well, is that the total reservoir volume can have significant uncertainty. Conversely, the main output of the CRMs developed in this research is the estimation of individual drainage volumes.

PSS flow is the flow regime of interest during Reservoir Limit Tests (Jones 1956), popularly used in PTA, whose main output is the estimation of the reservoir PV or OOIP as the models developed in this research.

PSS is also often called stabilized flow, which is more general and also includes SS flow. The difference between the two is in the outer boundary condition (OBC). PSS assumes a closed boundary, thus the reservoir pressure is in a state of depletion, whereas SS considers a constant outer pressure boundary which maintains the same reservoir pressure profile independent of time, for example, SS occurs in reservoirs with very strong aquifers and during a flooding process with a voidage replacement ratio of one.

The PSS and SS represent the extreme cases of the constant terminal rate BDF model. The CRM and the 2D microscopic model presented in this thesis assume PSS at each timestep, thus, PSS is the main flow regime of interest in this work. CRM cannot handle SS flow, because it requires some form of pressure or rate fluctuation to work adequately. The microscopic model could also be solved assuming SS flow as described by Ozkan (1986).

Depletion flow

Also known as constant terminal pressure BDF. It occurs when the BHP reaches its minimum value to lift the fluids from the wellbore to the surface (Fig. 2.2). This stage is characterized by a declining production flow rate as opposed to PSS flow where the rate is constant. However, the average pressure depletes in both cases. Unfortunately for operators, the depletion period dominates ~85% of a well's life (Walsh and Lake 2003). Also, there are cases in which the minimum BHP is reached before PSS flow can be attained.

Fetkovich (1973 and 1980) was the first to present a method for production analysis including the solutions for wells producing at constant BHP during IAF and BDF (depletion flow). Later, Blasingame and collaborators (1986;1991) demonstrated that the behavior of PSS and depletion flow can be described in an equivalent manner, and set the basis for the development of production/rate transient analysis (PA/RTA) techniques. CRM includes both PSS and depletion flow as special cases. Its main purpose (analogous to RTA) is to calculate the reservoir OOIP and can also estimate reserves as long as the model assumptions are reasonably satisfied.

Pressure Transient Analysis (PTA)

PTA is the most popular technique used for dynamic reservoir characterization. Excellent references have been published, such as Matthews and Russell (1967), Earlougher (1977); Raghavan (1995); Horne (1995); Lee et al. (2002) Bourdet (2002); Kamal (2009); Kuchuk et al. (2010); Houzé (2022) and thousands of technical papers.

PTA consist of a short-term test performed in-situ in which the rate and pressure data are monitored. Most of these tests are pressure BU tests, which require shut-in wells but which yield high-quality data. Other type of tests can include drawdown, multiple-rate and interference tests.

During a drawdown test a well at a stable static pressure is put on constant rate production for a specific time. In fact, most PTA analysis methods are based on solutions of the pressure drawdown equation. When the test is long enough that the pressure signal can reach all the reservoir boundaries it is known as a Reservoir Limit Test (RLT) as described by Jones (1956).

Drawdown tests are almost exclusively conducted in exploration or appraisal wells and they are usually restricted to small reservoirs or reservoirs with small diffusivity because in this case the test can take a very long time to reach the reservoir boundaries, becoming economically unviable.

Interpretation of the RLT can be conducted from a linear plot of the well flowing pressure (or pressure drop) versus time, yielding a linear response represented by the PSS flow period in Fig. 2.2. The reservoir PV can be estimated from the slope of Eq. 2. Interpretation can be conducted in a more robust manner using the pressure derivative function (Bourdet 1983), where PSS flow is characterized by the late time unit slope pressure and pressure derivative behavior. The specialized and diagnostic plots are straightforward to apply, however, there are some practical limitations, mainly that it is hard to maintain a stable/constant rate during the test, thus requiring to use some averaging, normalization, convolution/superposition or deconvolution technique to handle variable rate conditions.

Another limitation of the classical PSS flow theory for the analysis of RLT in conventional undersaturated oil reservoirs is the presence of an aquifer, which result in a composite medium. Composite models and methods of analysis for these cases have been extensively developed for use

in PTA (Carter 1966; Satman 1985; Ambastha 1988; Abbaszadeh and Kamal 1989; Abbaszadeh and Hegeman 1990; Kaczorowski 1993; Chen et al. 1998; El-Khatib 1999). These models work effectively for the case of gas reservoir-aquifer systems (matching almost any flow problems as they have more degrees of freedom, so they should be used with care), however, in the case of oil reservoirs, the analysis becomes more difficult since the oil and water are generally similar in terms of viscosity and compressibility, roughly, an order of magnitude, which may not enable to distinguish the two media in a diagnostic or specialized plot. Further complicating the analysis in these reservoirs, is the fact that water can breakthrough and be produced from the aquifer, thus, requiring multiphase flow models. Multiple formulations have been developed to handle multiphase flow (Martin 1959; Perrine 1959; Raghavan 2009), but there is still not a single fit-all representation.

Chapter 4 uses a CRM technique that handles variable pressure/rate production conditions for a volumetric reservoir as most PTA models do, offering yet another method to the reservoir engineer toolbox. In principle PTA, RTA and CRM will lead to analogous reservoir PV solutions as they are obtained from the same physical principles, only they differ in their considerations and solutions procedures. Chapter 5 presents a new model that uses time-rate-pressure data to estimate the OOIP from reservoirs with natural water influx and two-phase production.

The other form of test that is important for this thesis is the interference test as named by Jacob (1941), which is actually the oldest type of PTA test (Theis 1935). Interference tests are used to establish communication between wells and determine interwell properties. The simplest form of interference test is conducted using two dedicated wells, one active and one observation well, which is usually shut-in to record high quality data.

Interference tests have been used to determine yes/no answers with respect to interwell communication and to establish the magnitudes of the interwell reservoir properties. Initially the models used the line source solution, but later considered other well geometries (Martínez Romero and Samaniego 2010) analogous to single- well cases. Interference tests can determine the interwell permeability and compressibility. They have also been used to determine the permeability anisotropy. Collins (1961) first presented a microscopic solution to calculate the permeability anisotropy between two observation points caused by a pressure disturbance at the origin, assuming that the permeability axes are aligned with the well axes. Later, Papadopulos (1965) presented a more general method to characterize permeability anisotropy, which enables the calculation of the orientation of the permeability axes, in addition to their magnitude. The method was incorporated to the petroleum industry by Ramey (1975). The model is simple to apply and extremely useful to obtain interwell properties. Unfortunately, this type of interference test is not systematically applied. This is because the test requires to shut-in at least three observation wells aligned in different directions from the

active well, or two when the ϕc_t product is known. Since the method was developed assuming the observation wells are shut-in, thus, it is difficult to apply in practice. In principle, the method could be extended using superposition to include more active/observation wells producing/injecting at variable rate, analogous to Kamal (2009) for isotropic reservoirs. Theory states that one can solve this type of problem, however, experience shows this is often a myth (Houze et al. 2022). This is because the pressure fluctuations are usually small between wells, especially in large permeability reservoirs and when the spacing is large. Furthermore, these solutions use superposition assuming that transient flow governs the entire test duration, which might not always be the case (Dake 1994). Chapter 6 discusses a method that uses a solution to the diffusivity equation in a closed reservoir to characterize the directional permeabilities, the model also assumes that the permeability directions are aligned with the well axes, as is done in reservoir simulation (and as done by Collins). The model accounts for multiple wells and multiple rates, thus, it is best solved with nonlinear regression, a widely use approach (Earlougher 1972; Horne 1996; Ramey 1992; El-Khatib 1990). The 2D finite reservoir model was originally used to predict reservoir performance as described in the next section.

Rate Transient Analysis (RTA)

Another reservoir engineering technique to characterize reservoir properties is rate transient analysis (RTA), also known as production analysis or well performance analysis (Blasingame 2023). RTA is based on the same theory as PTA, but focuses on the analysis of long-term pressure-rate data from routine production operations. In conventional reservoirs the main flow regime is BDF, analogous to CRM. A major breakthrough in RTA was the development of the PI-material balance time technique (Blasingame and Lee 1986), which enables to quantify the reservoir size and PI from a well using pressure-rate data for any variable pressure/rate production schedule. This technique was initially derived from the full solution of the radial flow problem (IAF and BDF) towards a well in a cylindrical reservoir. This solution includes a depletion and an inflow component that add up to the total pressure difference in a well. The simplified expression for an oil well assuming constant properties is:

$$\frac{p_i - p_{wf}}{q} = \frac{1}{J} + \frac{N_p}{V_p c_t q}, \tag{2.44}$$

which can be analogously written as:

$$\frac{q}{p_i - p_{wf}} = J - J\frac{N_p}{V_p c_t \left(p_i - p_{wf}\right)}. \tag{2.45}$$

known as the Flowing Material Balance (FMB), as described by Mattar and Anderson (2005) following the gas formulation of Mattar and McNeil (1998).

The term N_p/q is known as material balance time, it is superposition time for BDF and enables to characterize variable rate/pressure data yielding the reservoir PV. In any of the previous cases using the MBE leads to:

$$\bar{p} = p_{wf} + \frac{q}{J}, \tag{2.46}$$

which states that the average pressure can be obtained from knowledge of well's pressure/rate and PI. Chapter 3 shows that the integral form of the CRMP solution is equal to the FMB.

Many more analysis methods have been developed in the field of RTA (Agarwal et al. 1999; Anderson and Mattar 2004; Ilk et al. 2010). Recently it has also found great utility in unconventional reservoirs (Clarkson 2021), however, as in PTA, it has been mainly dedicated to analyzing single well scenarios, with only few publications dealing with multiwell reservoirs and for oil reservoirs with an associated aquifer.

The multiwell applications generated reservoir pressure profiles for specified production constraints and predicted future production flow rates (Rodríguez and Cinco-Ley 1993, Camacho et al. 1996; Umnuayponwiwat and Ozkan 2000; Valkó et al. 2000; Marhaendrajana and Blasingame 2001). In all the cases it is assumed that the reservoir is hydraulically connected and that it is homogeneous and isotropic.

CRM was originally developed without any assumption regarding the connectivity between injection and production wells. This same idea was applied here and considered unsuccessful to characterize the interwell connectivity between producers in primary production, however, the simpler CRMP version presented in Chapter 4 can at least provide a yes/no answer of the connectivity between the wells, which can assure the correct application of the microscopic multiwell models in Chapter 6, and whose main purpose is to characterize the magnitude of the 2D permeabilities in an anisotropic medium, analogous to an interference test in BDF.

The water-influx problem was first investigated for production analysis by Doublet and Blasingame (1995) who developed analytical solutions to the diffusivity equation with prescribed boundary conditions that represented water influx. Their solution provided good accuracy when compared to single and multiphase numerical simulations; however, accurate descriptions of real cases required very long production periods. Currently, a common approach is to couple the classical Van Everdingen and Hurst (1949) or Fetkovich (1971) aquifer models to the transient or PSS well-reservoir models, respectively (Anderson and Mattar 2004; Harmony 2022). This approach has been useful for gas wells, but is less satisfactory for oil reservoirs, again, because of the small compressibility and mobility contrast between oil and water. The CRMPAF approach in Chapter 5 was developed to aid the characterization of these type of reservoirs including two-phase production.

Chapter 3. Capacitance Resistance Model

The Capacitance Resistance Model (CRM) is a relatively new technique for dynamic reservoir characterization. It can be classified as a production analysis technique, because it uses rate and pressure data from flowing (production/injection) wells for reservoir characterization and performance prediction.

The modern CRM was developed by Yousef et al. (2006), who followed on the work of Albertoni and Lake (2003). It is a physics-based analytical technique, as opposed to the experimental CRMs (**Fig. 3.1**) developed in the past (Bruce 1943; Wahl et al. 1962). However, the physical principles remain the same: the analogy between the capacitance and resistance of an electric circuit with the storage and transmissibility of fluid flow in a petroleum reservoir.

As with most reservoir engineering models, CRM is derived from the coupling of a material balance/continuity equation and a rate equation, as is often done with reservoir engineering models. The most general CRM equation enables quantifying the well production flow rate because of reservoir depletion, fluid injection or natural water influx, and producer bottomhole pressure (BHP) fluctuations caused by field operations. The models are then solved via robust data-driven approaches using historical pressure-production data.

As reported in the excellent review by Holanda et al. (2018a), CRM has become increasingly popular over the last few years. Hundreds of publications have appeared discussing various improvements to the original formulation and several field applications. CRM was initially developed to characterize reservoir properties during mature waterfloods, mainly with the purpose of quantifying inter-well connectivity between the injector and producer pairs. Later, several more applications were reported for use in other flooding methods during secondary and tertiary recovery, and few applications were developed for reservoirs in primary recovery (Izgec and Kabir 2010; Izgec and Kabir 2011, Nguyen et al. 2011; Soroush and Rasaei 2018).

Reservoirs in primary recovery are the focus of the CRM developments of this research. This chapter presents the general CRM derivation, assumptions, its physical meaning, and solutions. It also describes some of the previous publications of CRM for primary recovery. The chapter finishes with a discussion of the current limitations of CRM, which are addressed in the next chapters. Chapter 4 discusses new developments for the single-phase volumetric undersaturated oil reservoir model, Chapter 5 presents a more complex natural water-drive reservoir model with two-phase production.

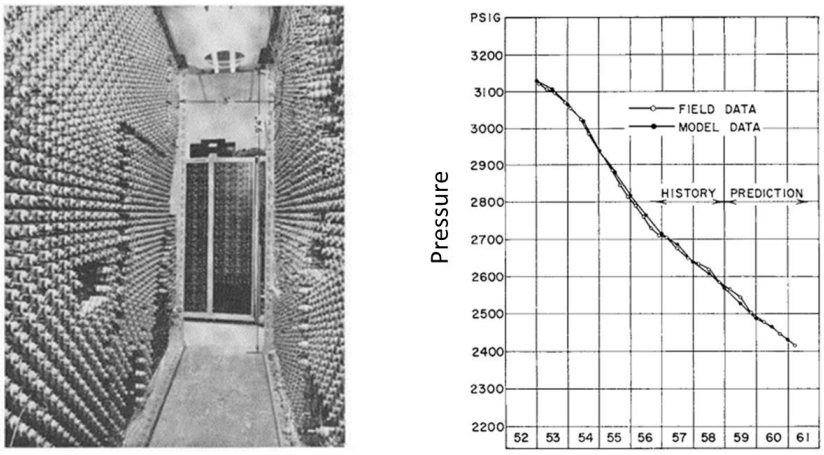

Fig. 3.1—Capacitance-Resistance Model (left) and reservoir pressure match from a reservoir in the Ghawar field (right), (from Wahl et al. 1962).

Control volume representation

CRM can be classified as an instantaneous macroscopic model because it assumes an overall control volume that only requires average properties. Different control volumes can be assumed, which lead to distinct CRM representations and solutions. **Fig. 3.2** shows four common control volume representations, the Capacitance Resistance Tank Model (CRMT), Capacitance Resistance Producer-Based Model (CRMP), Capacitance-Resistance Producer-Aquifer Model (CRMPA), and the Capacitance-Resistance Injector-Producer Pair Model (CRMIP).

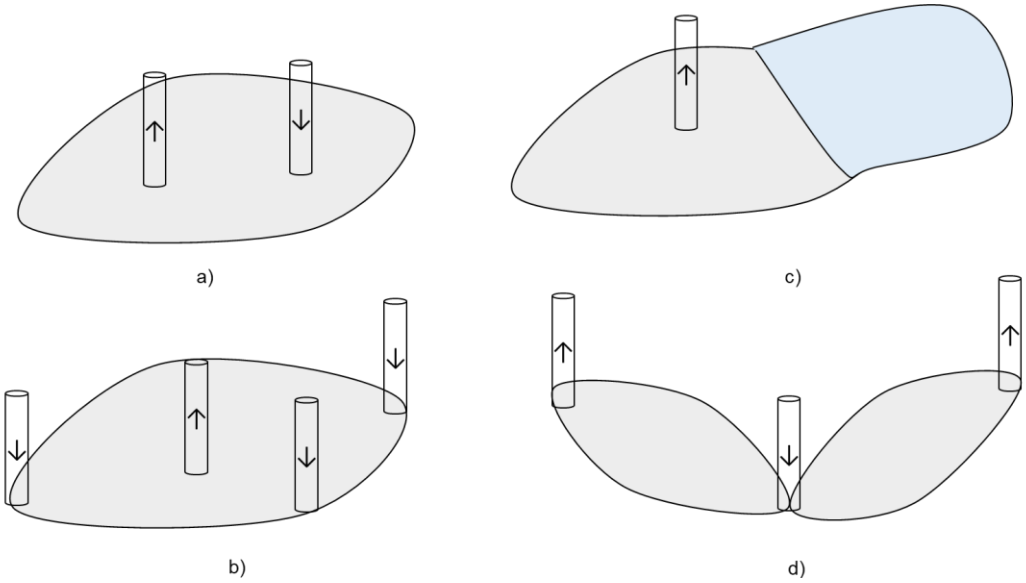

Fig. 3.2—Reservoir control volumes representations: a) Capacitance-Resistance Tank Model (CRMT) b) Capacitance resistance producer model (CRMP), c) Capacitance Resistance Producer-Aquifer Model (CRMP), and d) Capacitance-Resistance Model Injector-Producer (CRMIP).

Note that the control volume is represented arbitrarily. It does not need to have a specific shape, and may have various input/outputs. CRMT assumes a single input and output source from a control volume. It can be used to model the reservoir as a "super well", in this case all the production and injection rates are added and an average BHP is assumed for the whole reservoir. CRMP assumes that the control volume is the drainage volume of a producer either during primary recovery, or including all of its surrounding injectors during flooding processes. CRMP is the most widely used formulation. CRMP collapses to CRMT for the case of a single production well or the case of a single injector-producer pair. CRMPA assumes the control volume is a composite medium, with two tanks (representing the reservoir and aquifer) that are hydraulically connected. Finally, CRMIP assumes that the control volume is the connected volume between each injector-production pair.

The CRM representations differ in complexity. CRMT is the simplest formulation, while CRMIP requires the largest number of parameters, but provides more detail in the solution.. There are many other possible control volume representations, including the use of multiple control volumes in series or in parallel non-communicating layers, developed for heterogeneous and commingled reservoirs, respectively. These models increase in complexity, but they are limited in practical application.

Derivation

CRM is derived from a macroscopic mass conservation equation (Eq. 2.23) and a rate/inflow equation. The mass conservation or continuity is:

$$V_p c_t \frac{d\bar{p}}{dt} = w(t) - q(t), \tag{3.1}$$

where $V_p =$ pore volume, $c_t =$ total compressibility, $\bar{p} =$ average control volume pressure, $t =$time, $w =$ total injection flow rate and $q =$ total production rate expressed at reservoir conditions. The assumptions invoked to reach Eq. 3.1 are closed/finite reservoir, constant pore volume, and small and constant total compressibility.

The rate equation is the classical productivity index (PI), an empirical and universal equation that relates flow rate with the pressure drawdown:

$$J = \frac{q}{\bar{p} - p_{wf}} \tag{3.2}$$

where p_{wf} is the bottomhole flowing pressure.

The major difficulty in applying Eq. 3.1 is that it includes the average pressure term, which is generally unknown, except when it is estimated by pressure buildup (BU) tests in shut-in wells. Combining Eqs. 3.1 and 3.2 leads to:

$$V_p c_t \frac{d}{dt}\left[\frac{q}{J} + p_{wf}\right] = w(t) - q(t). \tag{3.3}$$

Assuming a constant PI, which is true during PSS flow and approximately valid during the constant-pressure boundary-dominated flow (BDF) regime, results in the general CRM equation:

$$q(t) = -\frac{V_p c_t}{J}\frac{dq(t)}{dt} - V_p c_t \frac{dp_{wf}(t)}{dt} + w(t). \tag{3.4}$$

Eq 3.3 can also be solved assuming *J* is not constant yielding:

$$q(t) = -V_p c_t \left[\frac{1}{J}\frac{dq(t)}{dt} + q(t)\frac{d\left(\frac{1}{J(t)}\right)}{dt} + \frac{dp_{wf}(t)}{dt}\right] + w(t). \tag{3.5}$$

Eq. 3.5 enables the incorporation of transient *J* effects, as was done by Pan (2016) for the purpose of characterizing unconventional reservoirs. This work uses Eq. 3.4 since it focuses on long-term production data from conventional reservoirs, which spent most of their production life in BDF.

The reservoir properties in Eq. 3.4 can be grouped together resulting in the time constant:

$$\tau = \frac{V_p c_t}{J}. \tag{3.6}$$

The time constant is a fundamental property of a porous medium, it is also the inverse of the decline rate during primary production. Substituting its definition in Eq. 3.4 leads to:

$$q(t) = -\tau\frac{dq(t)}{dt} + w(t) - \tau J\frac{dp_{wf}(t)}{dt}. \tag{3.7}$$

Eq. 3.7 is an ordinary differential equation (ODE) of order one. It has the familiar form:

$$y' + P(x)y = Q(x) \tag{3.8}$$

that can be solved with standard methods (integrating factor), and whose solution is:

$$y = e^{-\int P(x)dx}\left(\int Q(x)\, e^{\int P(x)dx}dx\right) + Ce^{-\int P(x)dx}. \tag{3.9}$$

For CRM, the integrating factor is $e^{-\int\frac{dt}{\tau}}$ and $C = q_0$. Thus, the analytical solution for CRM (Yousef 2005 and Sayarpour 2008) is:

$$q(t) = q(t_0)e^{-\frac{t-t_0}{\tau}} + e^{-\frac{t}{\tau}}\int_{t_0}^{t} e^{\frac{\xi}{\tau}}\frac{w}{\tau}d\xi - e^{-\frac{t}{\tau}}\int_{t_0}^{t} e^{\frac{\xi}{\tau}}J\frac{dp_{wf}}{d\xi}d\xi. \tag{3.10}$$

Next, integration by parts using $\int udv = uv - \int vdu$ for the influx term leads to:

$$q(t) = q(t_0)e^{-\frac{t-t_0}{\tau}} + e^{-\frac{t}{\tau}}\left[e^{\frac{\xi}{\tau}}w\right]_{t_0}^{t} - e^{-\frac{t}{\tau}}\int_{t_0}^{t} e^{\frac{\xi}{\tau}}\frac{dw}{d\xi}d\xi - e^{-\frac{t}{\tau}}\int_{t_0}^{t} e^{\frac{\xi}{\tau}}J\frac{dp_{wf}}{d\xi}d\xi. \tag{3.11}$$

Yousef (2005) solved Eq. 3.11 discretizing the integrals. Instead, Sayarpour (2008) solved it analytically considering that between two timesteps, the injection rate and the pressure drop can be represented by a stepwise or a linear variation in the injection rate, and a linear variation for the BHP.

The one timestep analytical solution for the case of a linear variation in the influx term and a linear BHP variation is:

$$q^n = q^{n-1}e^{-\left(\frac{\Delta t}{\tau}\right)} + \left[w^n - e^{-\left(\frac{\Delta t}{\tau}\right)}w^{n-1}\right] - \tau\left[\frac{w^n - w^{n-1}}{\Delta t}\right]e^{-\left(\frac{t^n}{\tau}\right)}e^{\left(\frac{\Delta t}{\tau}\right)} - \tau J e^{-\frac{t^n}{\tau}}\left[\frac{p_{wf,j}^n - p_{wf,j}^{n-1}}{\Delta t}\right]e^{\left(\frac{\Delta t}{\tau}\right)}, \tag{3.12}$$

where n denotes the timestep level and Δt is the time difference between timesteps. Using the properties of exponentials and rearranging:

$$q^n = q^{n-1}e^{-\left(\frac{\Delta t}{\tau}\right)} + \left[w^n - e^{-\left(\frac{\Delta t}{\tau}\right)}w^{n-1}\right] - \tau\left[\frac{w^n - w^{n-1}}{\Delta t}\right]\left(1 - e^{-\left(\frac{\Delta t}{\tau}\right)}\right) - \tau J\left(1 - e^{-\left(\frac{\Delta t}{\tau}\right)}\right)\left[\frac{p_{wf,j}^n - p_{wf,j}^{n-1}}{\Delta t}\right]. \tag{3.13}$$

Simplifying:

$$q^n = q^{n-1}e^{-\frac{\Delta t}{\tau}} + \left[w^n - e^{-\frac{\Delta t}{\tau}}w^{n-1}\right] - \tau\left(1 - e^{-\frac{\Delta t}{\tau}}\right)\left\{\left[\frac{w^n - w^{n-1}}{\Delta t}\right] + J\left[\frac{p_{wf}^n - p_{wf}^{n-1}}{\Delta t}\right]\right\}. \tag{3.14}$$

In a similar manner, the one timestep analytical solution for the case of a stepwise variation in the influx term and a linear BHP variation results in:

$$q^n = q^{n-1}e^{-\frac{\Delta t}{\tau}} + \left(1 - e^{-\frac{\Delta t}{\tau}}\right)\left\{w^n - \tau J\left[\frac{p_{wf}^n - p_{wf}^{n-1}}{\Delta t}\right]\right\}. \tag{3.15}$$

Eqs. 3.14 and 3.15 apply for a single timestep. Although, not initially noted, the linear variation in BHP is consistent with PSS flow. CRM assumes a constant production rate at each timestep and since the control volume is closed, CRM also assumes PSS flow at each timestep.

Sayarpour (2009) also presented solutions for the case of multiple rates using superposition in time, thus, assuming linearity. An alternative approach, followed in this work, is to apply this equation for each timestep within a time window having multiple pressure-rate data, analogous to Fetkovich (1971) or to reservoir simulation, which can further enable to update properties at each timestep (see Cao 2014), such as pressure-dependent parameters that are evaluated at the average drainage pressure.

The general CRM (Eq. 3.7) can also be used to describe the production flow rate from a well with multiple injectors resulting in the CRMP representation:

$$q_j(t) = -\tau_j \frac{dq_j(t)}{dt} + \sum_{i=1}^{N_i} \lambda_{ij} w_i(t) - \tau_j J_j \frac{dp_{wf,j}(t)}{dt}, \tag{3.16}$$

where λ, is the interwell connectivity between injector and producer (also known as gain, connectivity or allocation factor). It is defined as the fraction of injected fluid from an injector *i* that supports production in producer *j*. It is dependent on reservoir geology and relative position between the wells, i.e., it does not depend on the injection flow rate, analogous to the radius of investigation during pressure well tests. The solution of Eq. 3. 16 is analogous to Eq. 3.15 but with multiple wells, i.e., applying superposition in space:

$$q_j^{\,n} = q_j^{n-1} e^{\left(-\frac{\Delta t}{\tau_j}\right)} + \left[1 - e^{\left(-\frac{\Delta t}{\tau_j}\right)}\right] \left\{ \sum_{i=1}^{N_i} \lambda_{ij} w_i^n - \tau_j J_j \left[\frac{p_{wf,j}^{\,n} - p_{wf,j}^{n-1}}{\Delta t}\right] \right\}. \tag{3.17}$$

In CRMP there is one time constant for the whole drainage volume, one productivity index for each producer, and one connectivity for each producer-injector pair, whereas for the CRMIP representation there is one time constant, one connectivity and one productivity index for each injector-producer pair. CRMP is the most widely used representation for characterizing reservoirs in secondary or tertiary recovery. CRMIP is often used for heterogeneous media or irregular flood patterns.

The ODE for a production well with natural water influx (CRMPA) in primary recovery is:

$$q_j(t) = -\tau_j \frac{dq_j(t)}{dt} + w_e(t) - \tau_j J_j \frac{dp_{wf,j}(t)}{dt}. \tag{3.18}$$

The subscript e denotes the influx from the aquifer. The CRMPA solutions are the same as given in Eqs. 3.14-15.

In the case of a single-well volumetric reservoirs (no influx) during primary recovery. CRMP is:

$$q^n = q^{n-1} e^{-\frac{\Delta t}{\tau}} - \left(1 - e^{-\frac{\Delta t}{\tau}}\right) \tau J \left[\frac{p_{wf}^{\,n} - p_{wf}^{n-1}}{\Delta t}\right]. \tag{3.19}$$

Furthermore, when the BHP is constant, Eq. 3.19, becomes the well- known exponential decline:

$$q^n = q^{n-1} e^{-\frac{\Delta t}{\tau}}. \tag{3.20}$$

Verifying that τ is the inverse of the decline rate (*D*) used in decline curve analysis (DCA). Conversely, when the flow rate is approximately constant between timesteps, the second term on the ight-hand side of Eq. 3.19, representing the attenuated production rate due to BHP changes collapses to the PSS flow equation:

$$q^n = \tau J \left[\frac{p_{wf}^{\,n} - p_{wf}^{n-1}}{\Delta t}\right]. \tag{3.21}$$

If V_p or c_t can be reasonably estimated from the time constant (Eq. 3.6) definition, the CRMP single-well volumetric reservoir during primary recovery (CRMP) in Eq. 3.19 can be written explicitly as:

$$q^n = q^{n-1} e^{-\frac{J\Delta t}{V_p c_t}} - \left(1 - e^{-\frac{J\Delta t}{V_p c_t}}\right) V_p c_t \frac{p_{wf}^n - p_{wf}^{n-1}}{\Delta t}; \tag{3.22}$$

analogously, for the drainage volume of a well with an aquifer as:

$$q^n = q^{n-1} e^{-\frac{J_r\Delta t}{V_{pr} c_{tr}}} + \left(1 - e^{-\frac{J_r\Delta t}{V_{pr} c_{tr}}}\right)\left\{w_e^n - V_{pr} c_{tr}\left[\frac{p_{wf}^n - p_{wf}^{n-1}}{\Delta t}\right]\right\}, \tag{3.23}$$

where the subscript *r* denotes reservoir properties.

The analytical solutions can handle variable rate and variable BHP with changing timesteps. They are straightforward to apply for real field cases, analogous, but more robust than traditional DCA.

Solution procedures

The previous equations can be conveniently solved by nonlinear regression through a fitting process that minimizes the sum of the squared errors (SSE) between all measured and calculated production flow rates (assumed constant during each timestep), over a time window with *N* timesteps.

$$\min\left[\sum_{n=1}^{N}(q_{measured} - q_{CRM})^2\right]. \tag{3.24}$$

In this work the total error minimization was conducted using the fmincon function in MATLAB Optimization Toolbox, which uses an interior point algorithm, a gradient-based method. This function can also be expanded for the case of two-phase flow as is described in Chapter 5.

Nonlinear optimization is a powerful technique. It has become the most popular method for solving dynamic reservoir characterization problems (Horne, 2002).

The CRM matching parameters are τ or V_p, J and λ. There is usually some geoscience/reservoir information that enable to constrain these parameters, which reduces non-uniqueness and improves the computational speed of the solution. Also, depending on the recovery stage and the available information, some parameters might be more relevant, for example, during primary recovery λ does not appear in the equations, whereas J might be reasonably known and fixed during secondary recovery, to reduce the number of parameters to be estimated during the solution procedure.

It must be noted that since the optimization is performed over a series of timesteps, the history match parameters are average values for each time window. The optimization can also be performed using successive time intervals, in this manner; time-varying properties can be monitored as described in Chapter 4. Thus, the CRM solution serves as a reservoir characterization tool, with the major advantage of only requiring discrete (daily, weekly or monthly) rate and bottomhole pressure data (no shut-in or dedicated tests required), which are usually available from reservoir surveillance.

With respect to the solution quality and procedures, several researchers (Sayarpour 2008, Kaviani et al. 2014) have pointed out that CRM can perform adequately when the number of production data points is four times the number of unknowns. CRM has also been tested by adding random errors in production datasets, as would be expected from the noise and measurement error from field data. CRM estimations have been sufficiently accurate, demonstrating its robustness. Furthermore, for adequate estimations, CRM requires at least one rate variation of large-magnitude, or a series of rate variations of at least higher magnitude than the measurement error.

CRM for primary recovery

As previously discussed, most CRM applications have focused on characterizing reservoirs under secondary and tertiary recovery processes. However, it can also be used to characterize reservoirs in primary recovery, analogous to PTA or RTA.

Nguyen et al. (2011) first applied CRM for primary recovery. They developed the integrated CRM, which uses an integral form of the CRMP material balance equation (Eq. 3.22). The integrated CRM enables the calculation of the storage capacity and PI for each well in a producing reservoir:

$$N_p = V_p c_t \left(p^0 - p_{wf}(t)\right) - \frac{V_p c_t}{J} q(t), \tag{3.25}$$

which can be simplified using the average pressure definition to reach the same equation as the single-phase oil flowing material balance (FMB) (Mattar and Anderson 2005):

$$\bar{p}(t) = p_{wf}(t) + \frac{q(t)}{J}. \tag{3.26}$$

The authors validated the model against synthetic and real field numerical simulation models and studied the effects of field size, oil saturation, and permeability.

Izgec and Kabir (2011) first used the instantaneous CRMP (Eq. 3.22) to calculate the time constant, the drainage PV and PI of a single well in a multiwell reservoir. They also calculated the average pressure associated with each well at each timestep as follows:

$$\bar{p}_j^{\,n} = \bar{p}_j^{\,n-1} - \frac{q_j^{\,n-1}\Delta t}{V_{p,j} c_t}. \tag{3.27}$$

Izgec and Kabir (2011) compared CRMP with synthetic cases using a streamline simulator and used it to characterize a real gas field using pseudopressure, **Fig.3.3**. They also proposed a diagnostic plot to analyze reservoir compartmentalization by comparing the calculated drainage volume fraction from CRMP with those from a reservoir at pseudosteady state (PSS), as described by Matthews et al. (1954). Deviations from a 45º straight-line indicate reservoir compartmentalization.

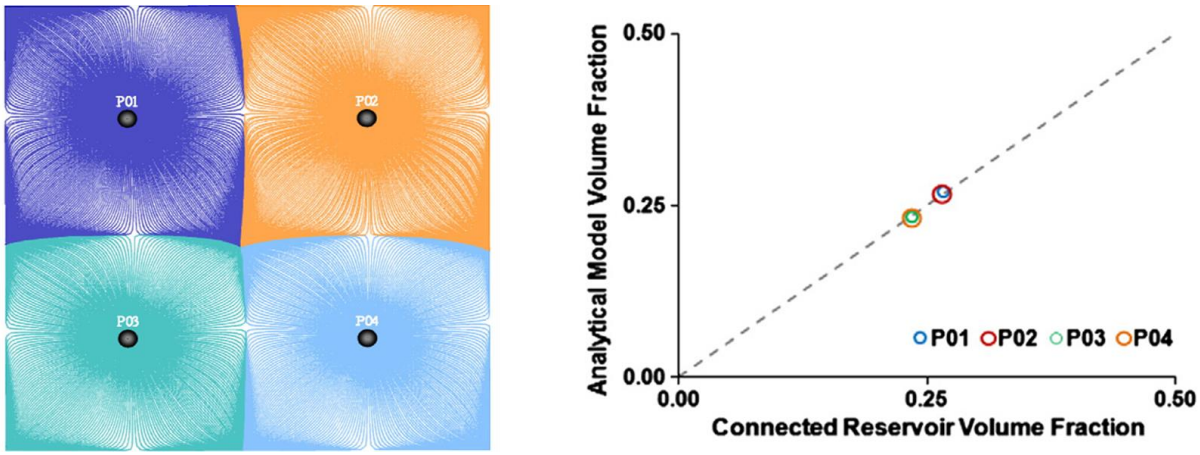

Fig. 3.3—Comparison between the streamline simulation of a multiwell reservoir (left), and the MBH and CRMP volume fractions (right) displaying communication between the wells (from Izgec and Kabir, 2011).

More recently, Soroush and Rasaei (2018) introduced two new CRM formulations (pseudo-injector and BHP) to estimate the interwell connectivity during primary recovery. The former is a heuristic approach that assumes some producers act as injectors with negative rates, analogous to the CRMIP used during flooding applications (Yousef et al. 2006). This formulation also incorporated a new parameter to account for the fractional aquifer contribution to each well. The BHP approach was derived from the multiwell PI (Kaviani and Valkó 2010). Both formulations provided good results on synthetic numerical reservoir models. The pseudo-injector approach was considered adequate during a field application.

The previous references show the feasibility of CRM to characterize reservoirs in primary recovery. The three approaches are useful, but CRMP will be used as the basis for the developments of this research; it provides an excellent balance between the model complexity and solution quality (Holanda et al. 2018).

Limitations

The CRM review presented by Holanda et al. (2018) pointed out some of the unresolved issues and suggestions for future research. Among others, they include incorporating the well orientation and completion type, accounting for the time varying behavior of CRM parameters and improving the coupling of CRM with fractional flow models. This research elaborates on these topics. First incorporating the well-reservoir model to CRM and also an approach using successive time windows to account for the reservoir time-varying properties. Then introducing aa novel approach to characterize undersaturated oil reservoirs with natural water influx and two-phase production.

Chapter 4. Capacitance-Resistance Producer-Based Model (CRMP)

Introduction

This chapter investigates the application and usefulness of the capacitance resistance producer-based model (CRMP) to characterize single and multiwell undersaturated oil reservoirs in primary recovery.

As already stated, the capacitance resistance model (CRM) has been amply used to model reservoirs under different recovery stages, particularly during flooding processes. However, there have been very few applications to primary recovery. The previous work on primary recovery used the rate and bottomhole pressure data to calculate the time constant or storage capacity, and the productivity index (PI) associated with each production well.

Here, popular productivity models are incorporated into CRM, making the results comparable with those from pressure or rate transient analysis. Also, new topics are discussed including constant and variable rate wells, transient flow, well location, well geometry, anisotropy, and different types of reservoir heterogeneity. This explanation helps to clarify the model capabilities and limitations in order to include CRM in the reservoir engineering toolbox.

CRMP is systematically compared and validated against analytical and numerical models of single and multiwell reservoirs, and it is also used to characterize flow in a real oil reservoir. The results demonstrate that CRM can provide important parameters for reservoir characterization using bottomhole pressure and rate data acquired from routine production operations, i.e., without the need to shut in wells or perform dedicated tests. It yields reasonable estimates of flow properties that depend on reservoir geology, petrophysics, and well condition. The chapter also presents an approach using successive time intervals to assess changes in well-reservoirs properties, such as drainage radius or PI, an indication of well damage. Most importantly, it is shown that for several well-reservoir cases with multiple complexities, CRM can accurately capture the reservoir size, or the drainage pore volume associated with each well in developed fields, which enables the calculation of average pressure, and helps asses inter-well communication and opportunities for infill drilling.

CRMP (Eq. 3.22) represents the dynamic performance of a volumetric undersaturated oil reservoir:

$$q^n = q^{n-1} e^{-\frac{J\Delta t}{V_p c_t}} - \left(1 - e^{-\frac{J\Delta t}{V_p c_t}}\right) V_p c_t \frac{p_{wf}^n - p_{wf}^{n-1}}{\Delta t}, \tag{4.1}$$

The model calculates the production flow rate as a function of depletion and bottomhole pressure changes incorporating storage and transmissibility properties. CRMP can be easily solved via nonlinear regression by finding the parameters (usually V_p and J) that best represent the historical

rate-pressure dataset. Note that since the model estimates the drainage pore volume (PV) one can also readily calculate the average pressure in the drainage volume using the MBE:

$$\bar{p}^n = \bar{p}^{n-1} - \frac{q^{n-1}\Delta t}{V_p c_t}. \tag{4.2}$$

The major benefit of this CRMP version is that it can be programmed in a spreadsheet, making it accessible to any engineer worldwide, still yielding important answers. Fig. 4.1 shows an example comparing CRMP with the example of Blasingame and Lee (1986), which set the foundations of modern production data analysis. The CRMP rate estimation is almost identical, but most importantly, it leads to a reservoir PV of 660 million barrels and a PI of 3.87 bpd/psi, approximately equal to the original reference.

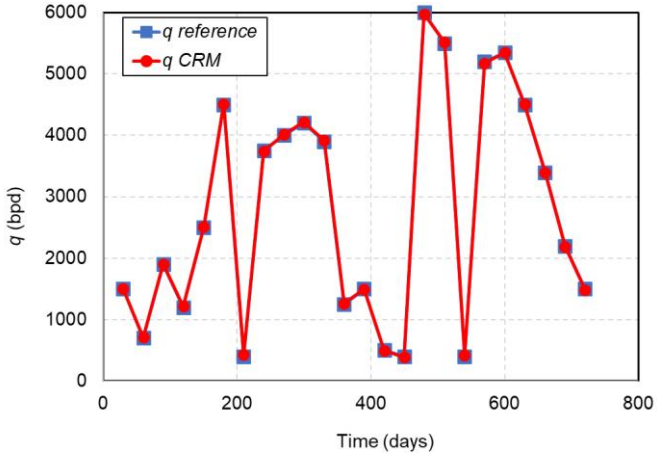

Fig. 4.1—Production flow rate comparison between CRMP and example case given in Blasingame and Lee (1986).

Productivity index (PI) models

A first addition to CRMP is to incorporate a well-reservoir model via the PI definition. These models are defined by integrating geological, petrophysical or reservoir engineering data (Matthews and Russell 1967). Next, the well-reservoir model can be incorporated in CRMP (Eq. 4.1). In this work, we introduce PI definitions (Economides et al. 2012) for three widely used well-reservoir models (Table 4.1). The formation volume factor (B) converts the rates from reservoir (CRM domain) to surface conditions. The first two PI models assume a vertical well at pseudo-steady state (PSS) flow and the third assumes a horizontal well at steady state (SS) flow. The latter is used because of its simplicity and widespread application, but we recall that the difference between PI models at PSS and SS flow is very small (Walsh and Lake 2003).

Reservoir model	Productivity index (STB/D-psi)	Eq.
Vertical well in the center of a closed cylindrical reservoir	$J = \frac{\alpha k h}{\mu B\left[\ln\left(\frac{r_e}{r_w}\right) - 3/4 + s\right]}$	(4.3)
Vertical well at an arbitrary position in a closed reservoir	$J = \frac{\beta k h}{\mu B\left[\frac{1}{2}\ln\left(\frac{4A}{\gamma C_a r_w^2}\right) + s\right]}$	(4.4)
Horizontal well at the center of an equivalent cylindrical reservoir with constant outer pressure	$J = \frac{\beta k h}{\mu B\left[\ln\left(\frac{a + \sqrt{a^2 - \left(\frac{L}{2}\right)^2}}{\frac{L}{2}}\right) + \frac{h}{L}\ln\left(\frac{h}{2r_w}\right)\right]}$ $a = \frac{L}{2}\left\{0.5 + \left[0.25 + \left(\frac{2r_e}{L}\right)^4\right]^{0.5}\right\}^{0.5}$	(4.5)
γ = 1.781, β = 0.00708		

Table 4.1—Productivity index for three popular reservoir models.

The approach of incorporating the PI model in terms of well-reservoir properties resembles those followed by Fetkovich (1971), or by Chitsiripanich (2015) for linear flow during flooding processes or in RTA applications. Hence, the matching parameters for capacitance and resistance can be the drainage radius or area for the capacitance, and permeability or skin for the resistance. Matching the permeability or skin, rather than the PI requires knowing or assuming the other, whereas the PI includes both as composite properties. Also, as illustrated in the chapter, anisotropy and some forms of heterogeneity can be modeled adequately with the equations in Table 4.1 if the correct definition of permeability is used, e.g., the geometric mean (and a change of coordinates) for anisotropic reservoirs, and the arithmetic or harmonic average permeability for layered and composite reservoirs.

Solution procedure

In this chapter, the CRMP solution was obtained using V_p and J or r_e and k from the PI models (**Table 4.1**) as matching parameters. The fitting process (**Fig. 4.2**) was conducted with an objective function that minimizes the sum of the squared errors (SSE) between all the measured and calculated production rates (assumed constant during each timestep) over a time window with N timesteps:

$$\min\left[\sum_{n=1}^{N}(q_{measured} - q_{CRM})^2\right]. \tag{4.6}$$

The minimization of Eq. 4.6, or optimization, was conducted for each production well using the fmincon function in the MATLAB Optimization Toolbox. This function uses an interior point algorithm, a gradient-based method. The parameters were only constrained to be positive and less

than very high upper bounds: 100,000 ft and 10,000 md, for the drainage radius and permeability, respectively. Because the optimization is performed over a series of timesteps, the history match parameters are average values for each time window. The optimization can also be performed using successive time intervals, in this manner, time-varying properties can be monitored. Thus, the CRM solution serves as a reservoir characterization tool, with the major advantage of only requiring discrete (daily, weekly or monthly) rate and bottomhole pressure (BHP) data (no shut-in or dedicated tests required), which are usually available from reservoir surveillance.

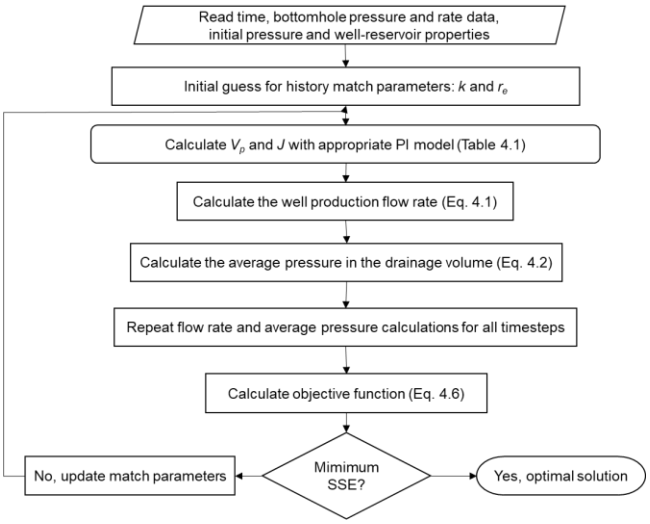

Fig. 4.2—Flow diagram for CRMP with productivity index models.

Validation

In this section, CRM is compared and validated against analytical and numerical models. The analytical model is the microscopic model described in Chapter 6, it assumes a 2D, homogeneous, single-phase reservoir flowing at pseudosteady state (PSS) with multiple wells (Ozkan 1988; Umnuayponwiwat and Ozkan 2000) that are fully penetrated and that can operate at variable rate. The analytical model is referred to as the PSS model throughout the chapter. The CMG IMEX reservoir simulator was used for the numerical model. The base reservoir properties used for the validation models are in **Table 4.2.** Symbols are defined in the Nomenclature section. The main numerical model had 41×41×1 cells in the x, y and z directions, respectively.

Various cases of single and multiwell reservoirs are discussed next, with emphasis on topics such as constant and variable rate wells, transient flow, well location, well geometry, reservoir anisotropy and some types of reservoir heterogeneity.

Property	Value and units
x_e	10,000 ft
y_e	10,000 ft
r_{eq}	5640 ft
h	100 ft
ϕ	0.10
k	100 md
c_t	3×10^{-5} psi^{-1}
μ	1 cp
B_o	1 RB/STB
V_p	178 million barrels
p_i	2000 psi
r_w	0.5 ft
s	0

Table 4.2—Base case well and reservoir properties.

Constant rate production

The first case corresponds to a single-well reservoir producing at a constant rate. The well is located at the center of the reservoir (Table 4.2). It produces at a constant rate of 1000 B/D for one year. The bottomhole flowing pressure is calculated with the PSS analytical model; transient flow is neglected for now. The pressure profile at the end of the flow period and the corresponding monthly BHP are in **Figs. 4.3a** and **4.3b,** respectively. As expected, the reservoir develops a symmetrical pressure profile and the bottomhole pressure decreases linearly.

The analytical BHP data was used as the input for CRM in Eq. 4.1, with Eq. 4.3 representing J. A radial geometry model was used for this square reservoir, however, the differences between the two are negligible. The CRM rate history match is in Fig. 4.3b. The result seems satisfactory at first, however, it is highly nonunique, i.e., this is an inverse problem and there are infinite combinations of r_e and k that reach a local minimum depending on the initial guesses, whereas, the real reservoir parameters are r_{eq} = 5640 ft and k = 100 md. This is because CRM depends on the amplitude and frequency of the input signals (Moreno and Lake, 2014), and requires at least one rate variation to perform adequately. It also depends on the amount and quality of information.

Kaviani et al. (2014) performed an extensive analysis about data sufficiency and noise in CRM and concluded that accurate results are achieved when the number of data measurements is four times greater than the number of parameters to be estimated (a rule of thumb). For the present primary recovery CRMP application, eight timesteps suffice to estimate two model parameters. Using more data improves the solution quality and is more relevant for cases with noise and measurement error. However, using very long datasets may lead to deviations from the model assumptions, e.g., pressure

dependent properties and time-varying skin. Using different time windows for analysis can also aid in the estimation of time-varying properties.

All of the next cases follow the previous guidelines, which are not major limitations, since real wells exhibit rate fluctuations throughout their life and long-term production data is generally available, as well as BHP for wells with permanent downhole gauges (PDGs). In addition, the optimization procedure was made more robust by using multiple initial guesses during each realization. This procedure becomes more important in Chapter 5 since the number of model parameters increases for the aquifer case.

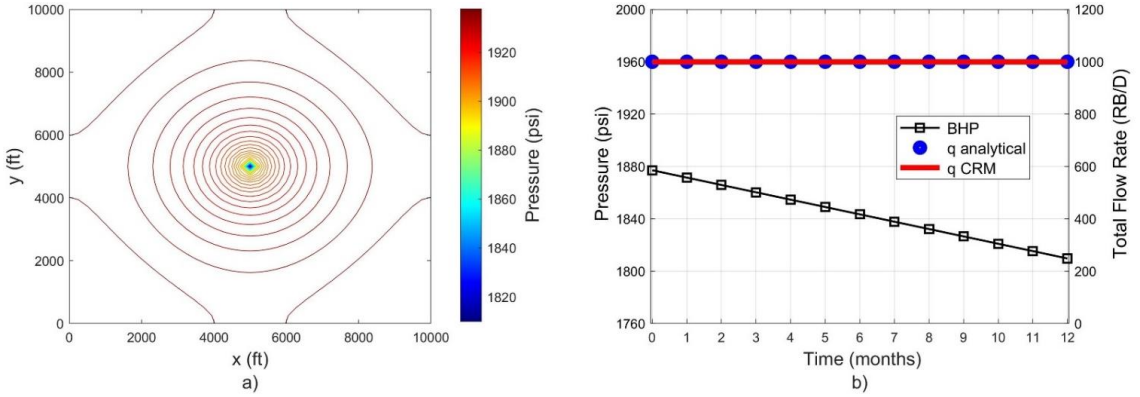

Fig. 4.3—a) Pressure profile from the PSS analytical model after one year, for a well producing at a constant rate, and b) declining BHP, analytical and CRM production flow rate comparison.

Variable rate production

Two cases are considered to start analyzing production rate variations which are composed by 1) high-amplitude and 2) high-frequency signals. The BHP data used as input for CRM is again calculated with the PSS analytical model.

The high-amplitude rate variation case differs from the previous example, because now the well is initially closed with $q(t = 0) = 0$ and $\text{BHP}(t = 0) = p_i$ (these values are used as input data for the history match, differing from the previous example). The well is instantaneously opened to production at a constant rate of 1000 B/D (**Fig. 4.4a**), creating the necessary rate variation. In the high-frequency rate variation case, the rate fluctuates monthly within ±10% from the base 1000 B/D (Fig. 4.4b).

The CRM calculated rate for the high-amplitude case is also in Fig. 4.4a. The matching parameters are r_e = 5639 ft and k=98.6 md. The relative error between the calculated and real values is 0.1 and 1.4%, respectively, and the coefficient of determination (R^2), which quantifies the goodness of the fit between the input and calculated CRM rates is > 0.99. The CRM calculated rates for the high-frequency variation case is in Fig. 4.4b. The matching parameters and R^2 are almost identical to the high-amplitude case. The same results were obtained after performing multiple realizations. Thus, it

can be concluded that both high-amplitude and high-frequency signals are useful for CRM and that non-uniqueness was minimized as compared with the previous example.

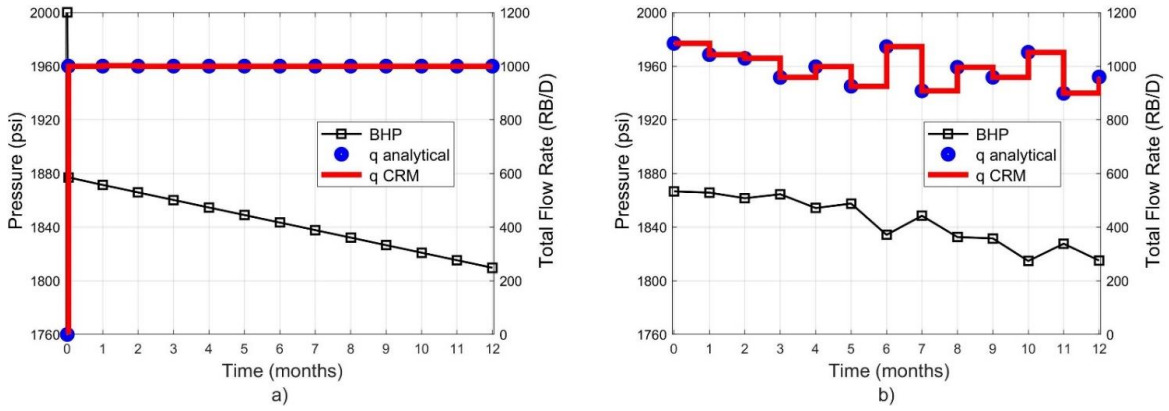

Fig. 4.4—BHP, analytical and CRM production rate for a a) well initially shut-in (high-amplitude signal) and b) well producing at variable rate (high-frequency signal).

Furthermore, it must be noted that rate measurements at the field always contain some error; to analyze this issue, we added a 10% zero mean Gaussian error (from 1000 B/D) to the rates of the high-amplitude and the high-frequency variation examples, and performed 50 realizations with each. The former case resulted in a mean for the drainage radius and permeability of 5653 and 98.9 md, respectively, and a standard deviation of 155 ft and 1.8 md. The R^2 between the input and calculated rates was 0.98. The high-frequency rate variation case achieved about the same mean for the matching parameters, but with a larger standard deviation, 216 ft for the drainage radius and 22 md for permeability. It also achieved a lower R^2 coefficient of 0.79, still within engineering accuracy.

Transient Flow

This example examines the utility of CRM to model a well using transient flow data. The intention is not to propose CRM (rigorously developed for bounded reservoirs) as an alternative to pressure transient tests, which are indispensable for well-reservoir analysis (Earlougher 1977; Kamal 2009), but rather to investigate whether incorporating rate-pressure data within this flow regime can be used for accurate CRM analyses.

To capture transient effects, we used the numerical reservoir model with the properties in Table 4.2. The production flow rate schedule used in the simulation was the same as in the high-frequency rate schedule from the previous example. The numerical rates change every month and are represented by the discrete points in Fig. 4.5. the calculated BHP represented by the solid black curve. There is a period of transience for every rate change. The time to reach the end of transient flow is calculated from the well-known approximation: $t_{eia} = 300\phi\mu c_t A/24k$ to be 37 days.

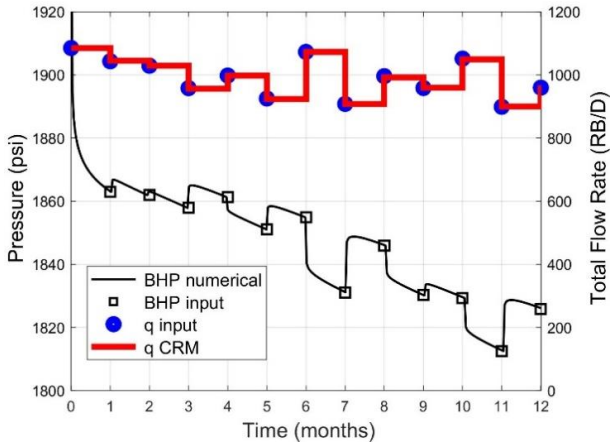

Fig. 4.5—Numerical BHP, discrete BHP and production rate extracted from the numerical model and used as the input for CRM, and CRM production rate history match for a well using transient flow data.

The initial CRM application considers only the last pressure measurement corresponding to every constant rate period as input for CRM. Fig. 4.5 shows these discrete pressure measurements (squares). Note that the last pressure measurement for each rate change is the closest possible value to PSS flow. Next the CRM is used to calculate the production rates, also shown in Fig. 4.5. The matching parameters were 5698 ft and 99 md for the drainage radius and permeability, respectively. The relative error between them and the true values are about 1%. The R^2 of the rate match is 0.99.

Next, a discrete pressure measurement was randomly selected from each of the continuous transient BHP data corresponding to every constant rate period, i.e., the input pressure for CRM can be taken from any day from each month. Once again, multiple realizations (50) were performed and the statistics were calculated for the matching parameters and the goodness of the fit (**Table 4.3**). Using transient data introduces some errors to the model as compared to using only PSS or close (late transient) to PSS data, however, CRM is still able to provide results with engineering accuracy.

Parameter	Mean	Standard deviation	Relative error
k	93.1	14.9	6.9%
r_e	5472	357	3.0%
R^2	0.84	0.19	

Table 4.3—Statistics for the CRM history match parameters and goodness of the fit after 50 realizations using random transient BHP data during each flow period for a well producing with the high-frequency rate schedule.

Off-center well

The problem now considers a well located at coordinates (2500, 2500) ft of the reservoir described in Table 4.2. The production rate schedule is the same as in the high-frequency variation case used previously. Pressure was calculated with the PSS analytical model. The pressure profile at the end of

the production period and the monthly BHP are in **Figs. 4.6a** and **4.6b**, respectively. The analytical BHP data was used as input for CRM. Permeability and drainage radius in Eq. 4.3 were used as matching parameters. The rate history match is in Fig. 4.6b. The calculated permeability and drainage radius are 91 md and 5642 ft, respectively. The radius estimation is excellent, but permeability is slightly off. This is because the well is not located at the center. If the shape factor is known a priori then the PI model given by Eq. 4.4 can be used, which results in match parameters of 101 and 5641 ft, both in excellent agreement with the real values.

This case shows that adding reservoir complexities degrades the permeability, or more generally the resistance estimation. A similar compensating effect in the permeability estimation would occur in a well where skin is not accounted for, whereas the storage capacity remains unaffected, as expected for a PSS model. This case also suggests that CRM can be used to directly calculate the time-varying permeability or skin (if the other is known) if successive time intervals are used. Following this example one might suggest increasing the number of matching parameters, but this will also increase the non-uniqueness of the solution, and it is better to limit the solution for two matching parameters alone which can often lead to satisfactory results, as shown in these calculations.

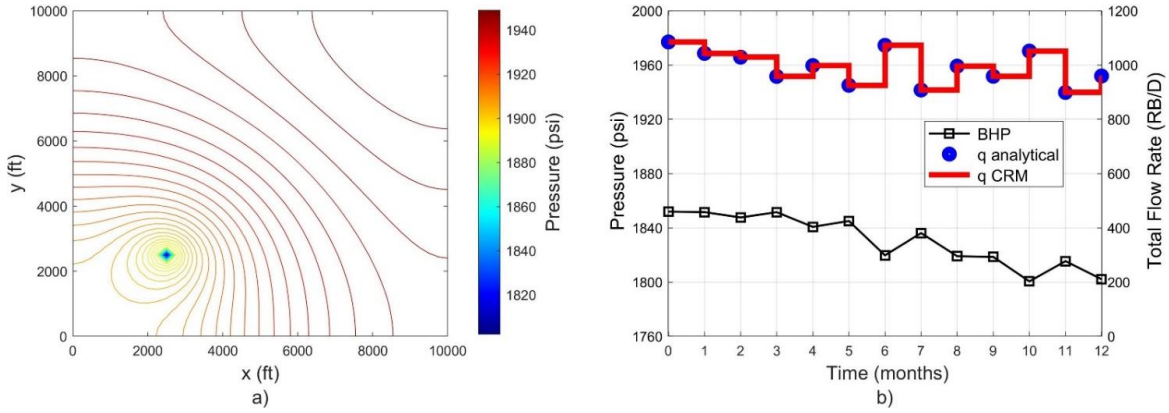

Fig. 4.6—a) Pressure profile and b) BHP, analytical and CRM rate comparison for an off-center well.

Anisotropic reservoir

This example comprises a well located at the center of an anisotropic reservoir with properties in Table 4.2, except that the *y* direction permeability is changed from 100 to 50, 20 and 10 md, while the *x* direction permeability remains constant at 100 md. We used the high-frequency rate variation schedule and calculated the pressure response using the PSS analytical model. The PSS model uses anisotropy as described in Chapter 2: through a change of coordinates and a geometric mean permeability defined by $\bar{k}_G = \sqrt{k_x k_y}$. As an example, the pressure profile at the end of the production period and the bottomhole pressure for the case with $k_x/k_y = 5$ is presented in **Figs. 4.7a**

and **4.7b**, respectively. Permeability and drainage radius were used as CRM matching parameters in Eqs. 4.1 and 4.3. The CRM calculated rate is also in Fig. 4.7b. The solutions for all anisotropic cases are in **Table 4.4**. CRM is adequately capturing the geometric mean permeability and exactly calculating the same equivalent drainage radius (or drainage pore volume) for this anisotropic reservoir; a remarkable result, since it would be difficult with conventional well tests.

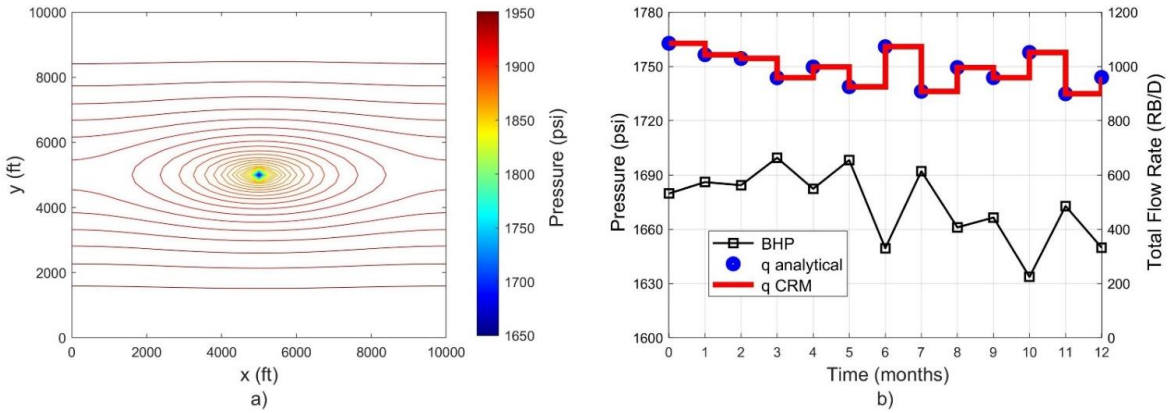

Fig. 4.7—a) Pressure profile, b) BHP, analytical and CRM production rates for an anisotropic reservoir with k_x/k_y=5.

k_x/k_y	$\bar{k}_G$ (md)	k_{CRM} (md)	$r_{e\,CRM}$ (ft)	$V_{p\,CRM}$ (million barrels)
1	100	101	5642	178
2	71	69	5642	178
5	45	41	5642	178
10	32	28	5642	178

Table 4.4—CRM parameters calculated for single-well anisotropic reservoirs.

Heterogeneous Composite Reservoir

A heterogeneous case was constructed using the numerical reservoir simulation model with the properties in Table 4.2. The vertical well was located at the center of the reservoir, which is comprised of two concentric zones of different but isotropic permeability (**Fig. 4.8a**). The outer zone had a constant permeability of 100 md and the inner zone permeability was changed from 200 to 150, 100 (homogeneous), 75, 50 and 25 md. The inner zone drainage volume represents one tenth of the total pore volume and has an equivalent drainage radius of 1790 ft, while the equivalent outer radius is 5640 ft from the well. The harmonic mean permeability was estimated as follows:

$$\bar{k}_H = \frac{\ln(r_e/r_w)}{\frac{\ln(r_e/r_{in})}{k_{out}} + \frac{\ln(r_{in}/r_w)}{k_{in}}}, \tag{4.7}$$

where the subscripts *in* and *out* denote the inner and outer concentric zones, respectively.

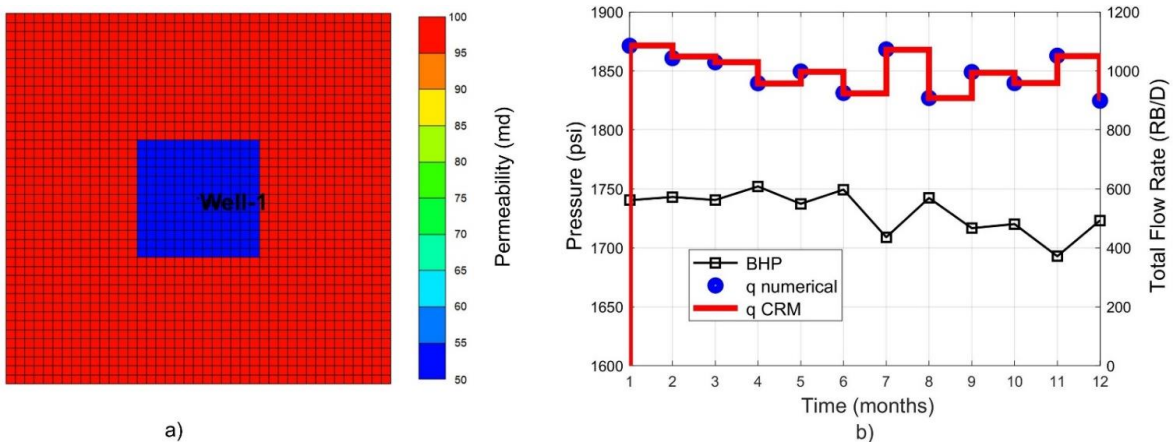

Fig. 4.8—a) Permeability and b) BHP from the numerical model, numerical and CRM production rate comparison for a two-zone composite reservoir with outer permeability of 100 md and inner permeability of 50 md.

The numerical simulation was performed for one year using the variable rate schedule. The discrete monthly BHP from the simulations was the input for CRM. Permeability and drainage radius were used as matching parameters for each heterogeneous case. Fig. 4.8b shows the calculated production rate from CRM for the case of an inner zone permeability of 50 md. **Table 4.5** shows that in all cases, the calculated CRM permeability is very similar to the harmonic mean permeability characteristic of composite reservoirs, which means that CRM is adequately capturing this reservoir property. The drainage pore volume is once again very exact, with 1% accuracy of the real value, except for the case of 25 md. The minor differences between the numerical and CRM model in the k_{in} = 25 md case is because it has a longer transient period resulting in a smaller drainage radius estimation.

k_{in} (md)	$\bar{k}_H$ (md)	k_{CRM} (md)	$r_{e\,CRM}$ (ft)	$V_{p\,CRM}$ (million barrels)
200	178	182	5665	180
150	141	141	5664	180
100	100	98	5660	179
75	77	75	5655	179
50	53	51	5637	178
25	28	26	5508	170

The outer zone permeability (k_{out}) is 100 md in all cases.

Table 4.5—CRM parameters calculated for single-well composite reservoirs.

Layered Reservoirs

Cases of production from layered reservoirs with and without crossflow were also investigated. The layered reservoir cases for comparison were built using the numerical simulation model (**Fig. 4.9**). The base reservoir properties are again in Table 4.2. The reservoir is produced by a vertical well

located at the center and completed in all the layers. The well produces with the same variable rate schedule as in the previous examples. The layers have a constant thickness of 10 ft, but the layer permeability changes in each case.

The base case is a homogeneous isotropic reservoir with a permeability of 100 md for each layer. The other cases consider permeability stratification. Beginning with the case of a multilayer reservoir with an isotropic (horizontal = vertical) permeability of 20 and 180 md, for odd and evenly numbered layers, respectively, starting from top to bottom of the reservoir. The arithmetic average permeability for this and all subsequent cases is 100 md. This case represents an extreme condition of crossflow since k_h is usually thought to be larger than k_v, but it is useful for illustrative purposes. The pressure profile at the end of the simulation is in Fig. 4.9a. The pressure profile is essentially identical to the base homogeneous case (not shown).

The next case considered a multilayer reservoir without crossflow, i.e., the vertical permeability is zero in all the layers, while all the other inputs are the same as before. The pressure profile at the end of the simulation is in **Fig. 4.9b**. The pressure in the low permeability layers depletes much slower in this case, indicating that they are not fully drained as in the previous crossflow case.

Next, we studied the case of a multilayer reservoir with flow barriers between the producing layers, as is often seen in real reservoirs. The flow barrier layers have zero permeability in all directions. The producing layers have equal and isotropic permeability of 200 md, resulting in an average arithmetic permeability of 100 md for the whole reservoir. The pressure profile at the end of the production period is in Fig. 4.9c.

Finally, we have the case of a commingled reservoir that has a major flow barrier represented by two layers of zero permeability and that separate the reservoir in two halves. The other eight producing layers have an equal and isotropic permeability of 125 md and once again an average arithmetic permeability of 100 md considering all the layers. The pressure profile at the end of the simulation is in Fig. 4.9d.

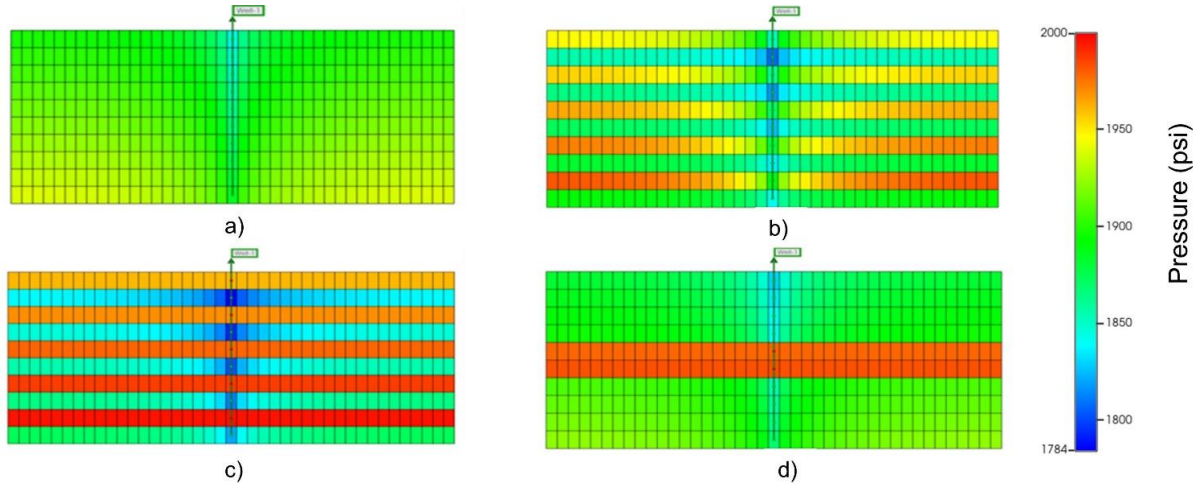

Fig. 4.9—Pressure profiles after one year of production from a well in: a) multilayer reservoir with crossflow and isotropic permeability of 20 and 180 md for odd and evenly numbered layers; b) multilayer reservoir without crossflow: (same as a) except the vertical permeability is zero in all layers); c) multilayer reservoir with flow barriers between producing layers with an isotropic permeability of 200 md; d) commingled reservoir with two no-flow layers at the middle, dividing eight layers with isotropic permeability of 125 md.

The discrete monthly numerical BHP was used as input for CRM. Permeability and drainage radius (converted and reported as pore volume) were calculated and reported in **Table 4.6**. For all investigated cases, the CRM rate comparison with the numerical input has a coefficient of determination $R^2 > 0.99$. The estimated CRM permeability for all cases is well within engineering accuracy of the average arithmetic value of 100 md. However, the PV estimation varies between the cases as explained next. In the multilayer with crossflow case, the reservoir is fully connected and drained. The CRM estimation is very close to the numerical total reservoir PV of 178 million barrels. In the multilayer without crossflow case, the well barely drains the low permeability layers, which results in a smaller CRM drainage PV estimation of 102 million barrels. The estimated drainage volume for the multilayer reservoir with flow barriers and for the commingled reservoir cases are 90 and 144 million barrels, respectively. For both cases, CRM is exactly capturing the real value of the connected/effective reservoir PV; static volumetrics which are most the most popular method to estimate the reservoir size and OOIP will not preserve this connectivity.

Case	Odd layers $k_x = k_y$ (md)	Even layers $k_x = k_y$ (md)	All layers k_z (md)	$\bar{k}_A$ (md)	k_{CRM} (md)	$V_{p\,CRM}$ (million barrels)
a) Multilayer with crossflow	20	180	k_x	100	99	179
b) Multilayer without crossflow	20	180	0	100	95	114
c) Multilayer with flow barriers	0	200	k_x	100	93	90
d) Commingled reservoir	125*	125*	k_x	100	97	144
Homogeneous	100	100	k_x	100	99	179

*Except for the two inner layers which have zero permeability

Table 4.6—CRM parameters calculated for single-well multilayer reservoirs.

Multiwell Reservoirs

The previous section demonstrated CRM utility to accurately capture the drainage/reservoir PV for multiple cases of single-well reservoirs. In this section, CRM is used to model multiwell reservoirs. It must be noted that estimating the drainage pore volume of single wells in developed fields with multiple active wells is a difficult task, e.g., conventional reservoir limit tests (Jones 1956) are not performed for these conditions. Several new CRM approaches were tested to model multiwell reservoirs, leading to the conclusion that using CRMP on a well by well basis achieves the best performance, even in a multiwell setting. For example, using CRMP was used to match all the wells at once (applying superposition in space) with limited accuracy as the number of unknowns increases, even when the number of data measurements was also increased. Another approach developed a so-called capacitance resistance producer-based model with interference (CRMPI) that incorporates a new parameter that accounts for the transmissibility between production wells, resembling previous approaches (Fox et al.1988; Hagoort and Hoogstra 1999), however, the results are also highly non-unique even for the simplest case of a two-well reservoir. Therefore, CRMP was used in the same manner as for single well cases, estimating both a capacitance (PV) and a resistance parameter (permeability, using a productivity model associated to each well). Next, CRMP is compare and validated against analytical and numerical models of multiwell reservoirs.

Four-Well Homogeneous Reservoir

This example presents a four-well homogeneous isotropic reservoir with the wells located at the center of the symmetrical quadrants of the square reservoir with the properties in Table 4.2. Three production cases were considered. The first assumes that at time zero all the wells are opened and produced at a constant rate of 1000 B/D, for one year (similar to the high-amplitude rate variation case discussed for single wells). In the second case, the wells are opened and produced at constant but unequal rates of 1000, 2000, 3000, and 4000 B/D for wells 1 to 4, respectively. In the third and more realistic case, the wells produce with variable rates; their yearly averages are in **Table 4.7**.

The PSS analytical model was used to calculate the BHP data that was used as CRM input for the three cases. The reservoir pressure profile for the first and second cases at the end of the year are in **Figs. 4.10a** and **4.10b**, respectively. Permeability and drainage radius (converted and reported as drainage PV) were used as matching parameters in CRM. The results are in Table 4.7. CRM parameters are in excellent agreement for the first case; permeability is very close to the real value, and the drainage PV associated to each well, exactly corresponds to the expected drainage volume for a reservoir flowing at PSS. CRM also provides very accurate drainage volume estimations for the

constant but unequal rate case, but has some error in the permeability estimations. This is because the wells develop irregular drainage configurations, which must be accounted for in the permeability (flow resistance) estimation. The present CRM formulation, as all PSS models for primary recovery, is best used for calculation of storage parameters, however, CRM is still able to provide order of magnitude resistance estimates for this and more complex cases discussed next.

Dataset description	Well	q (B/D)	k_{CRM} (md)	$V_{p\ CRM}$ (Million barrels)	$V_{p\ total\ reservoir}$ (Million barrels)
Constant equal rates	1	1000	99	44.5	178.0
	2	1000	99	44.5	
	3	1000	99	44.5	
	4	1000	99	44.5	
Constant unequal rates	1	1000	129	17.8	178.0
	2	2000	94	35.6	
	3	3000	88	53.4	
	4	4000	86	71.2	
Variable rate with input from the PSS model	1	1699	85	47.9	172.9
	2	1168	81	32.7	
	3	1746	83	49.4	
	4	1526	75	42.9	
Variable rate with input from the numerical model	1	1699	89	49.2	178.3
	2	1168	66	33.6	
	3	1746	95	50.7	
	4	1526	81	44.8	

The base permeability and total reservoir pore volume are 100 md and 178 million barrels. The production flow rate for the variable-rate cases are average values.

Table 4.7—CRM calculated parameters for a homogeneous reservoir with wells producing at constant or variable rate.

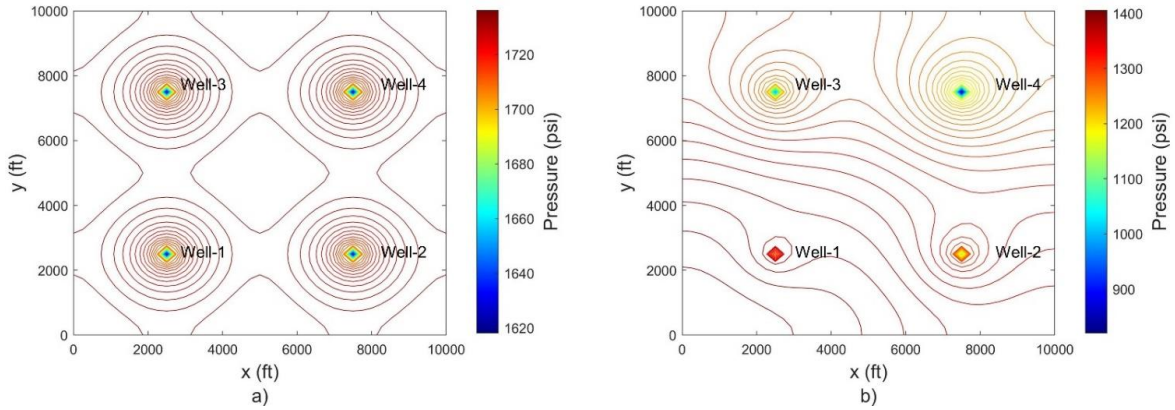

Fig. 4.10—Pressure profile after one year of production from a four-well reservoir with wells producing at a) constant and equal rate and b) constant but unequal rates.

The variable-rate case is finally discussed. The input production rate is represented by the scatter data in **Fig. 4.11**. CRM is slightly less accurate when estimating the total reservoir PV (173 million barrels) with respect to the real value of 178 million barrels, which was perfectly matched in the

previous cases. One possible reason is that the PSS analytical model used for validation, assumes a uniform reservoir pressure at the start of each timestep, and that PSS/stabilized flow is reached instantaneously. To relax this limitation, we used the numerical simulation model to investigate the same variable-rate case, and extracted the discrete monthly BHP data as input for CRM. The CRM rate history match for the four variable-rate wells using the numerical BHP input data is also in Fig. 4.11. The goodness of the fits for all the wells is quantified by an $R^2 > 0.98$. The CRM match parameters are in the last entry of Table 4.7. The results are very similar to those obtained with the PSS model input, demonstrating that CRM can lead to accurate reservoir characterization as long as consistent data is used.

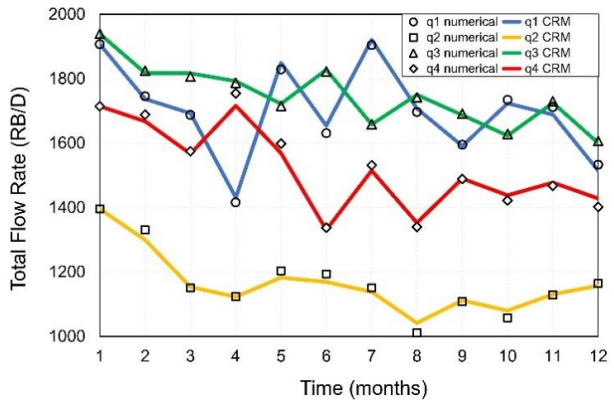

Fig. 4.11—CRM production rate history match for a four-well reservoir with wells producing at variable rate, using numerical bottomhole pressure data as input.

Four-Well Heterogeneous Reservoir

A four-well reservoir with four symmetrical zones of different permeability (**Fig. 4.12a**) is now investigated. The permeability for each quadrant/zone is in **Table 4.8**. The numerical validation model used the variable-rate production history from the previous example. **Fig. 4.12b** shows the pressure profile at the end of the simulation. The discrete BHP monthly numerical data was used as the CRM pressure input. The CRM rate comparison with the numerical input once again has an $R^2 > 0.98$ for all the wells. Table 4.8 shows the average rate values and the CRM reservoir property estimates. The CRM permeability is not equal to the zone permeability, but the estimates are in the right order of magnitude; this is because of non-idealities, such as interference between the wells and off-centered positions in the developed drainage areas. The total PV estimation is in excellent agreement with the real value of 178 million barrels, indicating the wells are effectively draining all the reservoir, but most importantly, demonstrating the effectiveness of CRM for estimating single-well drainage volumes in multiwell heterogeneous reservoirs.

Well	$\bar{q}$ (B/D)	$k_{well\ zone}$ (md)	k_{CRM} (md)	$V_{p\ CRM}$ (Million barrels)
1	1699	200	161	49.8
2	1168	100	70	33.5
3	1746	250	190	51.1
4	1526	150	111	44.6

Table 4.8—CRM calculated parameters for a heterogeneous reservoir with four wells producing at variable rate.

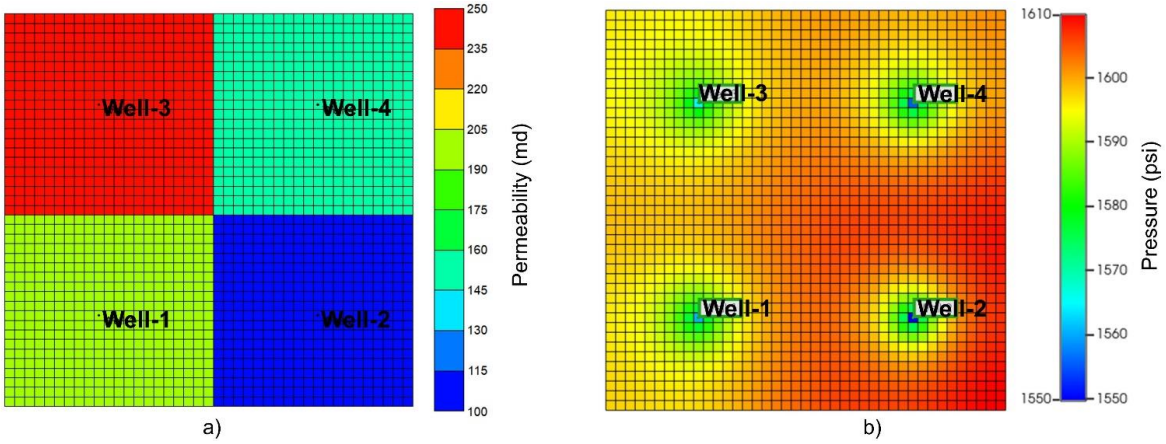

Fig. 4.12—a) Permeability and b) pressure profile for a heterogeneous reservoir with wells producing at variable rate.

It must be noted that in this and the previous example, the reservoir volume is exactly known from the numerical input, however, in a real reservoir it is uncertain. Comparing CRM with other techniques, can help identify undrained zones, e.g., when CRM calculated volumes are smaller than those from static volumetrics.

Four-Well Reservoir with a High Permeability Streak

This validation case begins with a numerical model of a heterogeneous reservoir with the same variable-rate production data as the previous multiwell examples. The model has a constant and isotropic permeability of 100 md, except in a high permeability streak that goes from South to North intersecting Wells -1 and 3 (**Fig. 4.13a**), represented by cells with a y-direction permeability of 1000 md. The pressure profile at the end of the simulation is in Fig. 4.13b.

Using the numerical BHP data into CRM results in the property estimates in **Table 4.9**. The R^2 values for the rate fits are again greater than 0.98. The drainage PV estimates are very similar to the two previous multiwell well cases of homogeneous and heterogeneous reservoirs, however, the permeability estimates are different. The CRM calculated permeability of both wells intersected by the high permeability streak is greater than for the two other wells, demonstrating that using long-

term pressure and rate data, CRM can capture distinct flow resistance properties, in addition to the accurate drainage volume/reservoir size estimations.

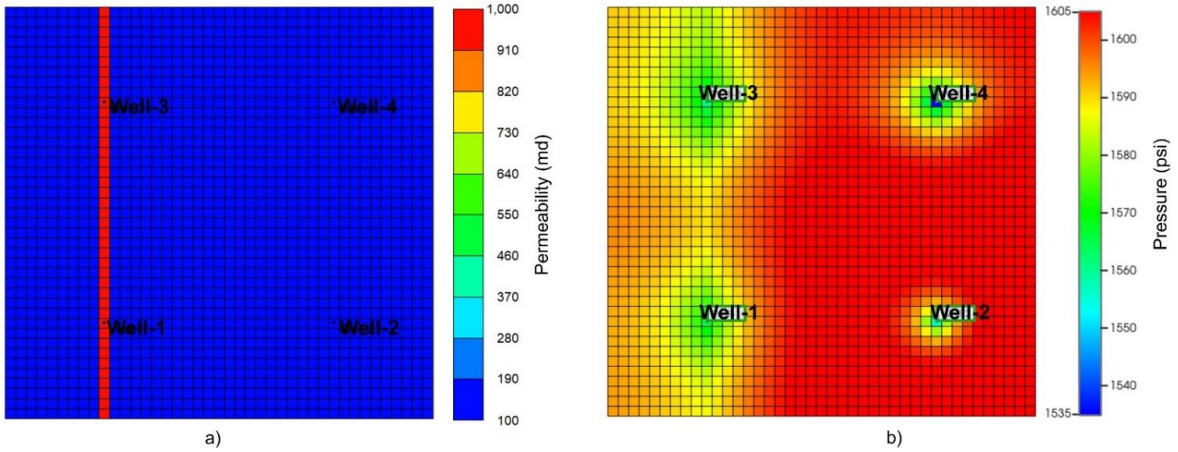

Fig. 4.13—a) Permeability and b) pressure profile for a high permeability streak reservoir, with four-wells producing at variable rates.

Well	$\bar{q}$ (B/D)	k_{CRM} (md)	$V_{p\,CRM}$ (Million barrels)
1	1699	211	49.4
2	1168	66	33.7
3	1746	228	50.7
4	1526	81	45.0

Table 4.9—CRM calculated parameters for a four-well reservoir with a high permeability streak.

Horizontal Wells and Infill Drilling

This case discusses a homogeneous reservoir that is produced with two horizontal wells. The same 41×41×1 numerical model was used, as in the previous vertical well examples, except the reservoir has a homogeneous and isotropic permeability of 10 md. The two horizontal wells are symmetrically located with their heel at the center of opposite quadrants of the reservoir. Both wells have a perforated length of 2684 ft and produce with the same variable rate schedule as previous examples. **Fig. 4.14a** shows the pressure profile at the end of the simulation. There are some undrained zones opposite to the well locations. **Fig. 4.14b** shows the numerical BHP data used as input for CRM (BHPs are equal for the two wells).

In this example we incorporated a productivity model for horizontal wells (Joshi, 1988), given by Eq. 4.5, and estimated the permeability and equivalent drainage radius. The estimated values are 15 md and 3305 ft or equivalently 61 million barrels and a PI of 5.9 B/D-psi. The coefficient of

determination between the CRM and numerical production rate is $R^2 = 0.95$. The CRM permeability is in the same order of magnitude as in the numerical model. The total drainage PV for the two wells is 122 million barrels, which is smaller than the total reservoir volume of 178 million barrels. This result illustrates an important application of CRM: finding undrained zones for infill drilling, when other sources of data, e.g., volumetrics suggest the existence of a larger and continuous reservoir as compared to the drainage volumes from CRM.

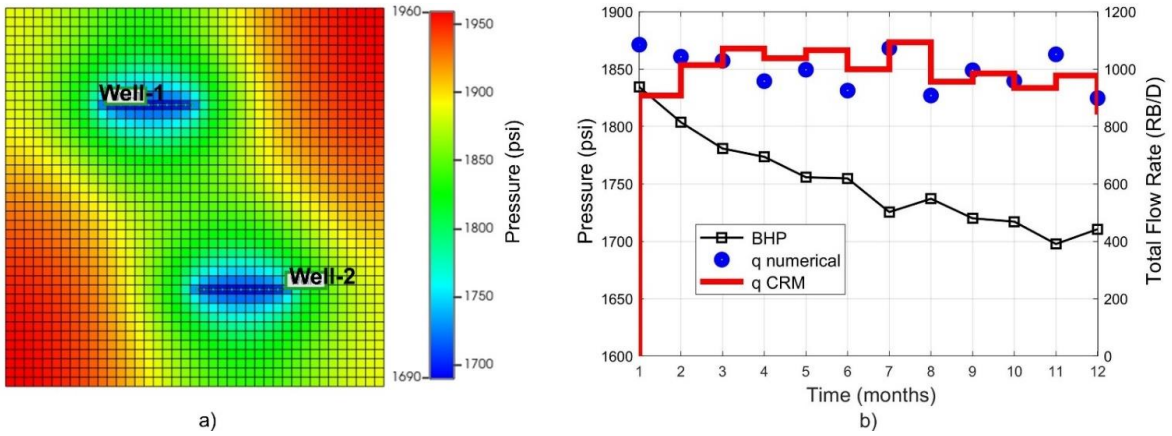

Fig. 4.14—a) Pressure profile for a homogeneous reservoir with two horizontal wells and b) numerical well bottomhole pressure data.

Field case

CRM was used to calculate the storage and resistance parameters, for a multiwell oil reservoir in development stage producing under primary recovery. The objective was to aid in the estimation of reservoir properties, such as field size, average pressure, formation compressibility, time-varying permeability and whether there is communication between wells separated by a fault. The production period for analysis comprised 196 days, during which three vertical wells came into production. Well-1 was the first producer, Wells-2 and 3 started producing at 67 and 123 days, respectively. The wells are located along a Northwest-Southeast direction (**Fig. 4.15)**. The distance between Well-1 and Wells-2 and 3 are 3620 and 2630 ft, respectively. The solid and dashed lines in Fig. 4.14 represent regional faults and approximate stratigraphic boundaries, respectively. Reservoir properties are in **Table 4.10**. From these properties, formation compressibility is generally the parameter with the largest uncertainty. Its value was taken from laboratory measurements of a nearby reservoir; however, CRM could also be used to calculate this parameter (in a similar manner as that of interference tests), when the reservoir size can be estimated from other sources.

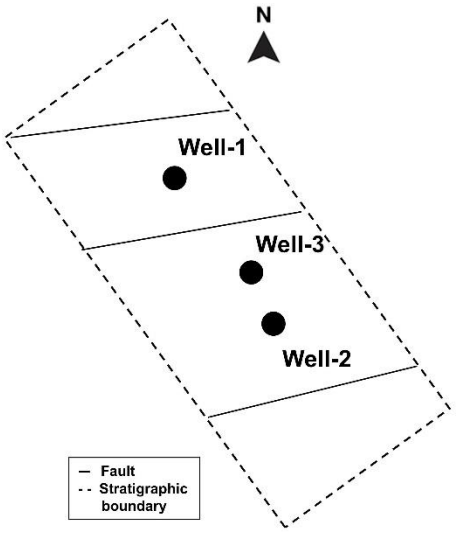

Fig. 4.15—Schematic well location and reservoir boundaries.

Property	Value and units
p_i	4280 psi
p_b	2520 psi
D	5700 ft
h	132 ft
ϕ	0.23
S_w	0.25
c_o	11×10^{-6} psi^{-1}
c_w	3×10^{-6} psi^{-1}
c_f	19×10^{-6} psi^{-1}
c_t	28×10^{-6} psi^{-1}
μ	0.88 cp
B_o	1.33 RB/STB
B_w	1 RB/STB
ρ_o	0.86 g/cm^3 (32º API)

Table 4.10—Field-case oil reservoir properties.

The three wells are equipped with permanent downhole gauges (PDGs). The sensor pressure measurements were converted to the reference depth. All the BHP measurements were above the bubble point pressure. **Fig. 416a** shows the discrete BHP measurements that were used as input for the CRM. The pressure data contains the operational adjustments (choke size), transient, boundary and flowing interference effects. The BHP data shows that Well-1 and Well-2 had about the same initial pressure, regardless that Well-2 commenced production 67 days later. The initial pressure for

Well-3 was 150 psi lower, suggesting interwell communication. Except for this effect, well interference is not evident when analyzed, because the pressure signals are dominated by the production variation from each well. PTA tests indicated that permeability and skin were 399 md and 8.1, 157 md and 4.3, and 100 md and 1.4, for Wells 1 to 3, respectively. Furthermore, the reservoir is known to be connected to an aquifer, as most reservoirs in the region, the wells reach an approximate steady state behavior at late times, as shown by the pressure stabilization in Fig. 4.16a. Production flow rate measurements were performed at discrete times, and in some cases various months apart; prorated data was used for large intervals with no available measurements; this is not a major limitation provided that consistent data is used. The total production flow rate at reservoir conditions is shown by the scatter series in Fig. 15b. The previous conditions are amenable for CRM analysis.

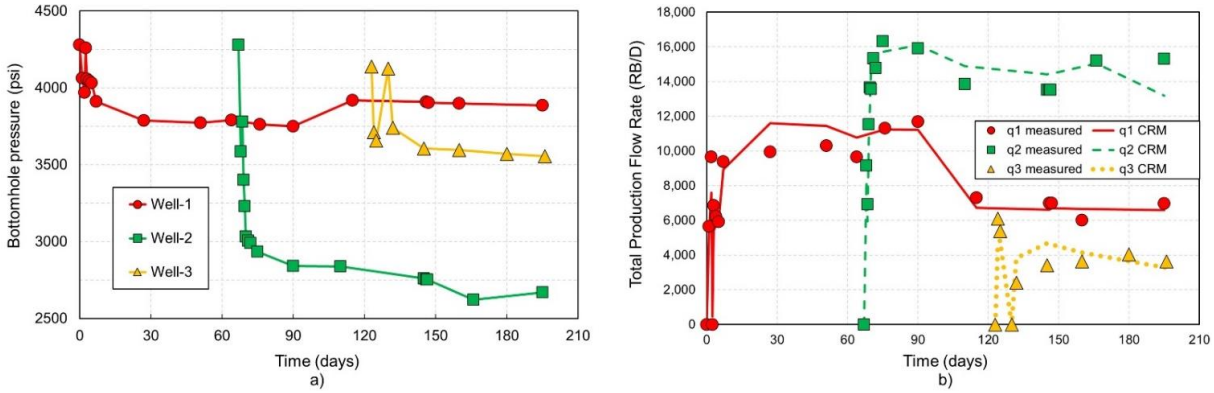

Fig. 4.16—a) Discrete bottomhole flowing pressure and b) measured and CRM production flow rate for a three-well oil reservoir in primary recovery.

CRM was used in conjunction with the PI in E1. 4.3. The skin values obtained from PTA were used, and the permeability and drainage radius were matched, as we have done throughout the paper. Fig. 4.16b shows the CRM rate history match for the three wells considering the complete well production histories. The CRM goodness of the fit as measured by the R^2 coefficient is 0.93, 0.95 and 0.79 for wells 1 to 3, respectively. The lower R^2 value for Well-3 is because it had the fewest available and quality of rate measurements. The CRM history match parameters for the three wells using their whole production history are in the second entry of **Table 4.11**. The permeability estimations have a relative error of 4, 12 and 17% with respect to the PTA results. The drainage radius estimations are higher than expected (from volumetrics). This is because using the complete production history, the drainage volume has reached and extends through the aquifer, leading to the estimation of equivalent (reservoir and aquifer) properties (see Ramey et al. 1973).

To address the previous limitation, CRM analysis was performed for different time windows, i.e., using successive time intervals, starting from the initial data measurement for each well, using at least

six measurements for parameter estimation and increasing the number of data points until all the available pressure-rate measurements were included, which is the case in Fig. 4.16b. The calculation results are in **Figs. 4.17a** and **4.17b**, which show the CRM drainage radius and permeability estimates corresponding to the increasing time windows, respectively. Figs. 4.17c and 4.17d, show the corresponding drainage PV and PI calculated from the matching parameters and known reservoir properties. The storage estimation (r_e or V_p) changes with time, it increases, stabilizes and then increases again, because of the reservoir and aquifer effects. Fig. 4.17b shows that the resistance (k or J) estimation is relatively constant, also indicating that there are no major changes in productivity. Well-1 has the largest productivity, while Wells-2 and 3 have lower and similar productivities.

Well	Production period (days)	k_{CRM} (md)	$r_{e\,CRM}$ (ft)	J_{CRM} (B/D-psi)	$V_{p\,CRM}$ (Million barrels)
1	0 – 27	423	1825	24.0	56
2	67 – 90	138	2234	9.2	85
3	123 – 145	90	722	10.2	9
1	0 – 196*	384	5374	20.3	488
2	67 – 196*	137	2799	9.1	133
3	123 – 196*	83	1490	8.6	38

*Parameters extending through steady state flow, they represent equivalent (reservoir and aquifer) properties.

Table 4.11—CRM calculated parameters corresponding to the reservoir at pseudo steady and steady state (incorporating aquifer effects) flow.

Using multiple time windows with consecutive time intervals enabled to estimate the parameters accounting only for the reservoir (before aquifer effects are felt), which is roughly until about a month of production, as determined from the drainage radii stabilization in Fig. 4.17a and the sensor pressure data in Fig. 4.16a. The first entry of Table 11 shows these history match results. The estimated drainage PV for Wells-1 and 2 before the onset of aquifer effects are in very good agreement with the reservoir compartment volumes estimated from static volumetrics of approximately 50 and 90 million barrels, adding up to a total reservoir volume of 140 million barrels. CRM results were also compared with those following a reservoir limit test procedure, e.g., the slope of the pressure-time data (Fig. 15a) for Well-1 in the period from 7 to 27 days is -6.2 psi/D, and considering a rate of 10,000 RB/D and the known compressibility, results in a pore volume of 57 million barrels. A similar analysis on Well-2 results in a pore volume of ~90 million barrels. The agreement is because the rates are roughly stable. The main difference between CRM and the conventional RLT is that CRM uses long-term variable production data and can be used for multiwell developed reservoirs, whereas RLTs are often used in exploratory wells, requiring long dedicated tests and are more susceptible to rate changes. As

explained throughout this chapter, the PV estimation is the most relevant and accurate information obtained from CRM, serving as an alternate dynamic method for classical material balance, reservoir limit tests (RLTs), and for static volumetrics. The PV comparison also shows that the assumed total compressibility and namely the formation compressibility, is a reasonable value, otherwise significant differences would have existed between the CRM and volumetric estimations; thus, this compressibility can be used in other reservoir engineering analysis, such as in reservoir simulation.

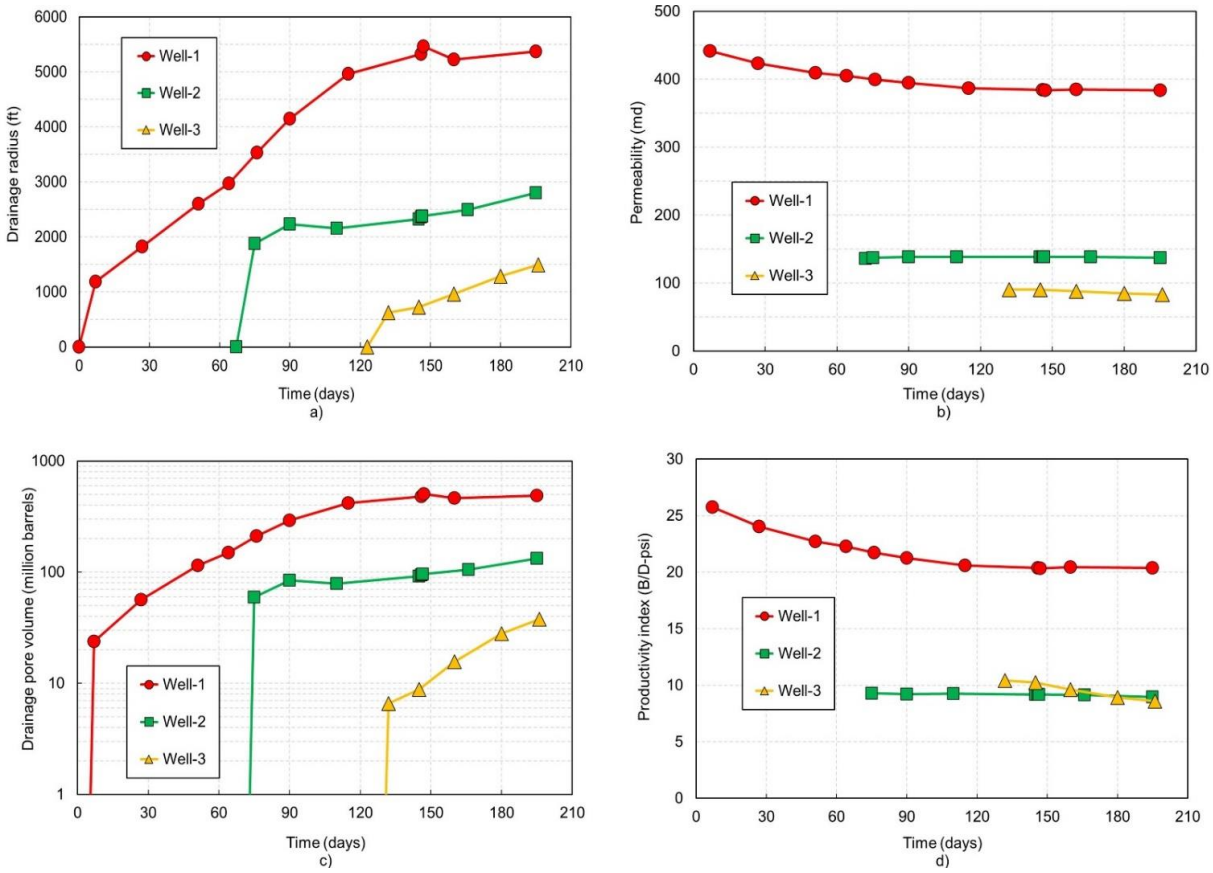

Fig. 4.17—CRM a) drainage radius, b) permeability, c) drainage pore volume and d) productivity index calculated for increasing time windows for a three-well oil reservoir in primary recovery.

Finally, **Fig. 4.18** shows the average drainage pressure for the three wells corresponding to the two different time windows (production periods) given in Table 4.11. The average pressure is calculated from material balance (Eq. 4.2) using the CRM estimated drainage volumes for each time window. The first period for analysis includes approximately the first month of production for each well and is represented by the solid lines in Fig. 4.18. As previously stated, during this time the reservoir displays a volumetric-like behavior and pressure depletion is a function of the reservoir storage capacity. The second time window includes the complete production history for each well and is

represented by the dashed lines in Fig. 4.18; in this case, the average drainage pressures account for the additional pressure support from the aquifer as depicted by the lower depletion rate for the three wells in comparison to the first case. Reservoir behavior displaying a period of PSS flow before water influx becomes dominant has been previously described (Kaczorowski 1993; Chen et al. 1996).

The average drainage pressure calculated from the complete production flow rate histories shows that Wells-2 and 3 have a similar depletion that differs from that of Well-1, which has the lowest depletion rate, because of a stronger aquifer support. As previously stated, under stabilized flow (equilibrium) conditions in a multiwell reservoir. the average pressure in the drainage volume of each well should be equal, otherwise fluid exchange would occur between the drainage volumes. Fig. 4.18 shows that the average drainage pressure is reasonably close between Wells-2 and 3, leading to the conclusion that they are hydraulically connected and that they have negligible communication with Well-1, also indicating that the reservoir is compartmentalized by a major fault shown in Fig. 4.15.

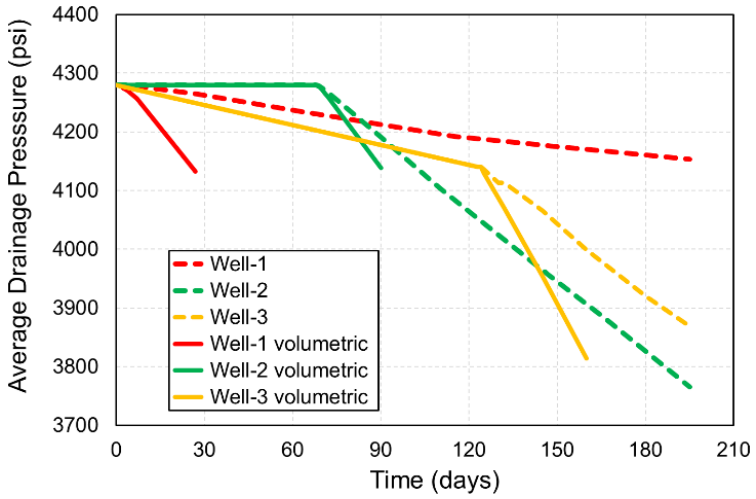

Fig. 4.18—Average drainage pressure calculated from the CRM estimated drainage volumes for a three-well compartmentalized oil reservoir in primary recovery for two different production periods. Solid lines represent the pressure for a production period of about one month, in which the reservoir displays a volumetric behavior. Dashed lines represent the pressure calculated using the full production history, accounting for additional pressure support.

This field example shows that CRM can aid in estimating the drainage PV, total compressibility and average drainage pressure in a multiwell reservoir, without the need to shut in wells. It also serves to estimate resistance properties: the PI or permeability/skin when a well-reservoir model can be defined and one of the two is known. CRM was also used to monitor the time-varying drainage radius and permeability using consecutive time intervals. Finally, this field case demonstrates that CRM analysis of long-term pressure and rate data can help to assess interference between wells, in this case a fault was characterized as sealed; Well-1 drains from a different compartment as Wells-2 and 3.

Summary and Conclusions

This chapter presented several applications of the producer-based capacitance resistance model (CRMP) to characterize single and multiwell undersaturated oil reservoirs, in primary recovery. CRMP was systematically compared and validated against various well-reservoir analytical and numerical models. Productivity index (PI) definitions for popular reservoir models were incorporated. Also, successive time windows were used to study time-varying parameters. The well-reservoir cases discussed topics such as constant and variable rate production, transient flow, well location, well geometry, anisotropy and various forms of reservoir heterogeneity. These topics had not been previously discussed or deserved further explanation to include CRM into the reservoir engineering toolbox. The model results lead to the following conclusions:

- CRM is able to provide accurate and repeatable reservoir property estimates for variable production data, as long as the model assumptions are reasonably satisfied.
- CRM can be used with acceptable error when late transient flow measurements are used within a pressure-rate dataset of a developed field, as demonstrated by the synthetic and field examples.
- Incorporating PI definitions enabled performing CRM estimations, in terms of permeability and drainage radius. CRM permeability estimates were in excellent agreement for the ideal synthetic cases and were able to capture the effect of heterogeneity and anisotropy. For the real case, once we accounted for skin, we found good agreement between the CRM and PTA permeabilities.
- Using different time windows in the analysis can assess the effect of time-varying properties, such as the well drainage radius or PV, and permeability or skin in the field case example. A time-varying drainage size can reflect well interference or water influx.
- The drainage or reservoir volume estimate is the most important output from CRM. The results show that CRM accurately captures the connected/effective drainage volume for the well-reservoir examples of varying complexities, discussed throughout the chapter. The major advantage of CRM as compared to reservoir limit tests is that CRM can be used to calculate single-well drainage volumes in multiwell developed reservoirs. Furthermore, comparing the CRM drainage volume estimates with other techniques, such as volumetrics, can help assess infill drilling opportunities.
- Once the drainage volume has been obtained from CRM, the average pressure can be readily calculated from material balance. The major advantage of the CRM approach for calculating the average pressure is that it only requires pressure-rate data from routine field surveillance, i.e., there is no need to shut in wells. A comparison of the average pressure in the drainage volume of each well can help assess inter-well communication.

- For the field case, CRM estimated a reservoir volume of 141 million barrels, in excellent agreement with the estimation from static volumetrics. This also demonstrated that the assumed total compressibility is adequate and can be employed in other reservoir engineering analyses. The average pressures in the drainage volume of each well also demonstrated that the reservoir is compartmentalized by a sealing fault.

Chapter 5. Capacitance Resistance Producer Model with Aquifer and Fractional Flow (CRMPAF)

Introduction

This chapter presents a flow model that enables to characterize conventional undersaturated oil reservoirs with natural water influx in primary production. Again, the main application is to estimate the original oil in place (OOIP), but the model can also calculate the productivity index (PI), water influx, and heterogeneity factor.

Aquifers are common to many reservoirs and their diagnosis is relevant since they can serve as an important drive mechanism, but can also affect well productivity. Discerning between the reservoir and aquifer volumes is also a major challenge in many oil fields.

Reservoir-aquifer systems have been investigated with various dynamic characterization techniques such as the material balance equation (MBE), pressure transient analysis (PTA), and production/rate transient analysis (RTA). These methods have some limitations, e.g., requiring shut-in wells, and/or very large production histories, and high mobility and compressibility ratios to yield distinguishable responses in the diagnostic plots. The oldest and most widely applied method is the classical MBE. Several aquifer models have been developed for use in the MBE, dating back to Schilthuis (1936), going through the most rigorous van Everdingen and Hurst (VEH) model (1949), and similar approximations that have yielded accurate results (Carter and Tracy 1960, Fetkovich 1971, Allard and Chen 1988). These methods coupled with straight-line analysis techniques (Havlena and Odeh 1963) provide the most common way to simultaneously characterize the reservoir volume and perform water influx calculations (Dake 2001). However, they also have limitations, mainly because they require a long reservoir production/depletion history, and average pressure data obtained from buildup tests in shut-in wells.

In the field of PTA. Some authors assumed constant pressure boundary conditions (Muskat 1946; Abbaszadeh and Hegeman 1990; Bourdet 2002). Kumar (1977) introduced a parameter to account for the strength of water drive in finite systems. Composite models have also been used (Kaczorowski 1993; Chen et al. 1996; Houzé et al. 2022), however, these models usually require large mobility and compressibility contrasts between the reservoir and the aquifer, thus, they have been most effective in modeling gas reservoir-aquifer systems.

Water drive has also been investigated in the context of production analysis. Based on experience, Fetkovich (1996) associated the decline exponent with reservoir type and recovery mechanisms. Doublet and Blasingame (1995) developed analytical solutions to the diffusivity equation with

prescribed boundary conditions that represented water influx. Their solution provided good accuracy when compared to single and multiphase numerical simulations; however, accurate descriptions of real cases required very long production periods. Currently, a common approach is to couple the classical VEH or Fetkovich (1971) aquifer models to the transient or pseudosteady state (PSS) well-reservoir models, respectively (Anderson and Mattar 2004; Harmony 2022). This approach has been useful for gas wells, but is less satisfactory for oil reservoirs, again, because of the small compressibility and mobility contrast between oil and water.

The new flow model couples the producer-based capacitance resistance model (CRMP) with the Fetkovich aquifer model (CRMPA). It enables calculating the total instantaneous production flow rate from a well as a function of three mechanisms: reservoir depletion, changes in bottomhole pressure (BHP), and water influx. In addition, CRMPA is coupled with the Koval fractional flow model (CRMPAF) to calculate the individual oil and water rates, and to enhance the OOIP estimation for wells with two-phase production caused by water breakthrough from the aquifer.

As previously stated, there are few capacitance resistance model (CRM) applications for primary recovery, and only one investigated natural water influx (Izgec and Kabir, 2010). There are important differences between the previously published and the new CRMPA formulation. The former estimated the individual water influx to each well in a multiwell reservoir associated with an aquifer. The calculations were performed assuming the reservoir pore volume (PV) is known, whereas the present approach simultaneously calculates the PV and the water influx, tackling the major challenge of dynamically distinguishing between the reservoir and aquifer volumes. For example, reservoir limit tests (Jones 1956) are conducted to estimate hydrocarbon volume (HCPV), however, large errors are encountered in oil reservoir-aquifers having compressibility and mobility ratios close to unity. The former approach also required a priori knowledge of the average pressure, obtained from buildup tests, whereas the new method uses production data only, i.e., does not require shut-in wells.

Also, we note that CRMP and the Fetkovich aquifer model are derived from the same assumptions, and fit nicely together, e.g., they consider a finite volume; thus, this approach rigorously applies for small to medium-sized aquifers. In the original paper Fetkovich (1971) used a 20-year production period and showed the model was accurate for aquifers up to 100 times the reservoir volume and permeabilities from 10-1000 md, which comprise many conventional reservoirs. Here, we also present validation cases to discuss the range of utility of the model. CRMPA also requires that the average pressure is declining, thus, it is restricted to partial water drives. This is not a major limitation because most reservoirs show this behavior, otherwise, a simpler steady-state (SS) model can be used.

Furthermore, CRMPA was coupled with the Koval (1963) fractional flow model yielding the so-called CRMPAF. A similar approach was first reported by Cao et al. (2015) for the case of

waterflooding processes. Incorporating a fractional flow model aids discrimination between the individual oil and water production rates and results in more accurate OOIP estimations.

The CRMPAF solution begins by using CRMP to calculate the equivalent properties of a single medium corresponding to the reservoir-aquifer system. This procedure reduces the dimensions of the problem and constrains the limits of the reservoir and aquifer parameters. Next, storage and transmissibility relations are used to calculate the composite (reservoir and aquifer) properties that are required in the aquifer and well-reservoir models.

The next sections describe the derivation and the solution procedures of the new CRMPA/F approach. Afterwards, the model is used to characterize cases of reservoir-aquifer systems including a peripheral water drive model, an aquifer represented by pseudo injectors in a five-spot pattern, and a bottomwater drive with multiple wells. Finally, the model is used to characterize a field case.

CRMPA

The CRMPA solution for the total production flow rate of a single-well producing from three mechanisms: reservoir depletion, water influx and BHP fluctuations was given by Eq. 3.23:

$$q^n = q^{n-1} e^{-\frac{J_r \Delta t}{V_{pr} c_{tr}}} + \left(1 - e^{-\frac{J_r \Delta t}{V_{pr} c_{tr}}}\right)\left\{w_e^n - V_{pr} c_{tr}\left[\frac{p_{wf}^n - p_{wf}^{n-1}}{\Delta t}\right]\right\}, \tag{5.1}$$

Note that some water influx model must be used to find w_e in addition to the two matching parameters in CRMP. The Fetkovich aquifer model is simple, widely applied and consistent with the assumptions in CRMP, the model also couples an inflow equation for the aquifer:

$$w_e = \frac{dW_e}{dt} = J_a(\bar{p}_a - \bar{p}_r), \tag{5.2}$$

and the MBE for the aquifer:

$$W_e = V_a c_{ta}(p_a^0 - \bar{p}_a), \tag{5.3}$$

where W_e is the cumulative volume and w_e are the instantaneous rate of water influx encroaching from the aquifer, $\bar{p}_r$ and $\bar{p}_a$ are the average pressure in the reservoir and aquifer, respectively, V_a, J_a and c_{ta} are the PV, PI and total compressibility of the aquifer, respectively, and the superscript 0 refers to the initial aquifer pressure.

The water influx model can then be written analogous to CRM as follows:

$$W_e = V_a c_{ta}(\bar{p}_a - \bar{p}_r)\left(1 - e^{-\frac{J_a t}{V_a c_{ta}}}\right), \tag{5.4}$$

It must be noted that when the time tends to infinity the water influx model becomes:

$$W_e = V_a c_{ta}(\bar{p}_a - \bar{p}_r), \tag{5.5}$$

which indicates the maximum amount of water influx that can occur for the specified pressure drop.

The coupling of the aquifer model with CRMP is done by incorporating the reservoir MBE with the cumulative water influx as follows:

$$\bar{p}_r = p_r^0 - \frac{Q_p - W_e}{V_r c_{tr}}, \tag{5.6}$$

where Q_p is the total cumulative well production at reservoir conditions, V_r and c_{tr} are the reservoir PV and total compressibility, respectively.

CRMPA was solved using discrete time intervals and updating the average pressure at each timestep. The instantaneous rate of water influx was calculated as $w_e = \Delta W_e/\Delta t$, and then used in the CRMPA solution. Note that the water influx depends on the average reservoir pressure and vice versa; thus, an iterative procedure was used. Coupling the water influx model increases the number of matching parameters to be determined, because there are at least two highly uncertain variables (V_a and J_a) in the aquifer model, increasing the non-uniqueness of the solution.

The approach that was followed to minimize non-uniqueness consisted as follows. First, use CRMP (Eq. 4.1), which considers the reservoir and aquifer are a single medium and calculate two history match parameters (PV and J) for this effective medium:

$$q^n = q^{n-1} e^{-\frac{J_t \Delta t}{V_{p_t} c_t}} - \left(1 - e^{-\frac{J_t \Delta t}{V_{pt} c_t}}\right) V_p c_t \frac{p_{wf}^n - p_{wf}^{n-1}}{\Delta t}, \tag{5.7}$$

Next, auxiliary equations relating the storage and transmissibility of the equivalent and composite reservoir-aquifer systems are used.

The storage relationship is:

$$V_t c_t = V_r c_{tr} + V_a c_{ta} \tag{5.8}$$

The subscripts r, a, and t refer to the reservoir, aquifer, and total effective values. V_r is constrained to be $0 < V_r < V_t c_t / c_{tr}$.

The transmissibility relationship used here is obtained from the expression for flow in series at steady state, satisfying $\Delta p_t = \Delta p_r + \Delta p_a$. Multiple equations can be derived depending on the aquifer geometry. We used a transmissibility relationship assuming a vertical well located in the center of a cylindrical reservoir-aquifer system, rigorous for peripheral water drive, but which proved useful in other cases

$$J_t = \frac{\alpha \bar{k} h}{\bar{\mu}\, ln(r_e/r_w)} = \frac{\alpha k_r k_a h}{k_r \mu_w ln\,(r_e/r_r) + k_a \mu_o\, ln(r_r/r_w)}, \tag{5.9}$$

where k, h, μ, r and α are the permeability, thickness, viscosity, radius and a conversion factor (0.00708 in field units), respectively. The overlines indicates average properties. The middle and right equations assume a single-effective and a composite medium, respectively. In CRMPA, k_r was matched and used to calculate J_r and J_a. Eq. 5.9 is useful because it incorporates storage parameters,

is useful because it incorporates storage (r_e) parameters, thus, reducing the non-uniqueness as compared to directly matching V_r, V_a, J_r and J_a. If one uses Eq. 5.5 for the water influx. Note that using Eq. 5.5 for the water influx simplifies the analysis since it decreases the number of matching parameters to three and only requires the capacitance relationship.

CRMPAF

The CRMPA calculates the total production flow rate at the well, but cannot discriminate between the oil and water rates. To address this issue, the Koval fractional flow model was incorporated yielding CRMPAF. It collapses to CRMPA when there is single phase-flow at the production well, and to CRMP when the reservoir is volumetric.

Cao et al. (2015) were the first to couple CRM with fractional flow theory, namely with the Koval (1963) model to study undersaturated oil reservoirs during a waterflood. In this approach, CRM was first used to calculate the fraction of injected water that flows into the drainage volume of each producer. Next, the Koval model was used to calculate the oil and water production flow rates.

In the waterflooding case the volume of water influx is known, however, this is not the case with an aquifer. For the present case of an oil reservoir with natural water influx, the Koval model was applied after the CRMPA estimation of the reservoir volume (V_r) and cumulative water influx (W_e). The Koval model calculates the water fractional flow at the production well (water cut) as follows:

$$f_w = \begin{cases} 0, & t_D < 1/K_v \\ \dfrac{K_v - \sqrt{K_v/t_D}}{K_v - 1}, & 1/K_v < t_D < K_v \\ 1, & t_D > K_v \end{cases} \tag{5.10}$$

where $t_D = W_e/V_r$ represents the PVs of water influx into the reservoir, $K_v = H_k E$ is the Koval factor, the product of the heterogeneity factor (H_k) and the effective viscosity ratio between the oil and the displacing phase defined as.

$$E = \left(0.78 + 0.22\left(\frac{\mu_o}{\mu_w}\right)^{1/4}\right)^4. \tag{5.11}$$

Lake et al. (2014) stated that H_k is the most subjective feature of the Koval model and is usually regarded as a history match parameter. They also indicated that the Koval equation is equal to the Buckley-Leverett (1942) model for the case of straight-line relative permeabilities. The assumption of straight-line relative permeabilities is a major simplification to any flow problem. However, relative permeability data are often unknown, and even when measured, core-scale results might not be representative at the reservoir scale, especially in heterogeneous media. Recently, Salazar and

Lake (2020) investigated the physical meaning of the Koval factor and demonstrated that under some assumptions the Koval model can rigorously describe fractional flow at the interwell scale.

The advantages of the Koval model cannot be overemphasized: it is a single parameter model that has been extensively validated and successfully applied. **Fig. 1** shows the calculated fractional flow of water at the production well (water cut) for different K_v values as a function of PVs of water influx. The case of $K_v = 1$ represents a piston-like displacement. In the other cases, the breakthrough time occurs faster for higher values of K_v, or more precisely heterogeneity, considering a fixed viscosity ratio. The model also implies that in large reservoirs, where only small t_D values can be accomplished, K_v must be very large to cause water breakthrough.

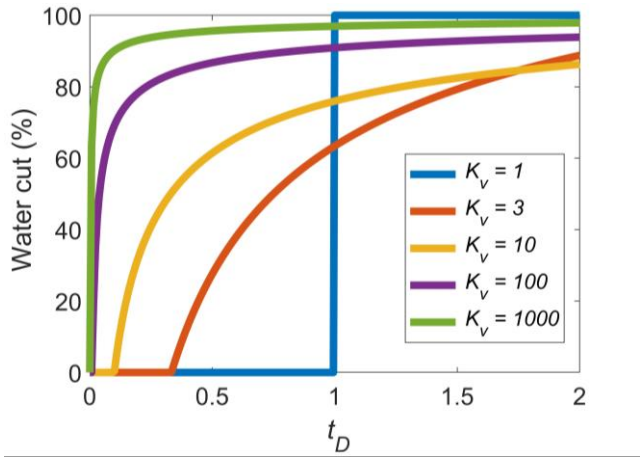

Fig. 5.1—Water cut as a function of K_v and t_D calculated with the Koval fractional flow model.

Solution procedure

The CRMPAF algorithm is summarized in **Fig. 5.2**. The optimum solution is obtained by nonlinear regression through a fitting process that minimizes the sum of the squared errors (SSE) between all the measured and calculated (total and oil) production flow rates (assumed constant during each timestep) over a time window with N timesteps:

$$\min\left[\sum_{n=1}^{N}\left(q_{t_{measured}} - q_{t_{CRMPA}}\right)^2 + \sum_{n=1}^{N}\left(q_{o_{measured}} - q_{o_{CRMPA}}\right)^2\right]. \qquad (5.12)$$

The minimization was conducted using the fmincon function in the MATLAB Optimization Toolbox, which uses an interior point algorithm, a gradient-based method. Note that when no water is produced from the aquifer, CRMPAF collapses to CRMPA and the optimization is conducted only using the first term in Eq. 5.11. Once again, the optimization process was made more robust by performing multiple realizations with different initial guesses.

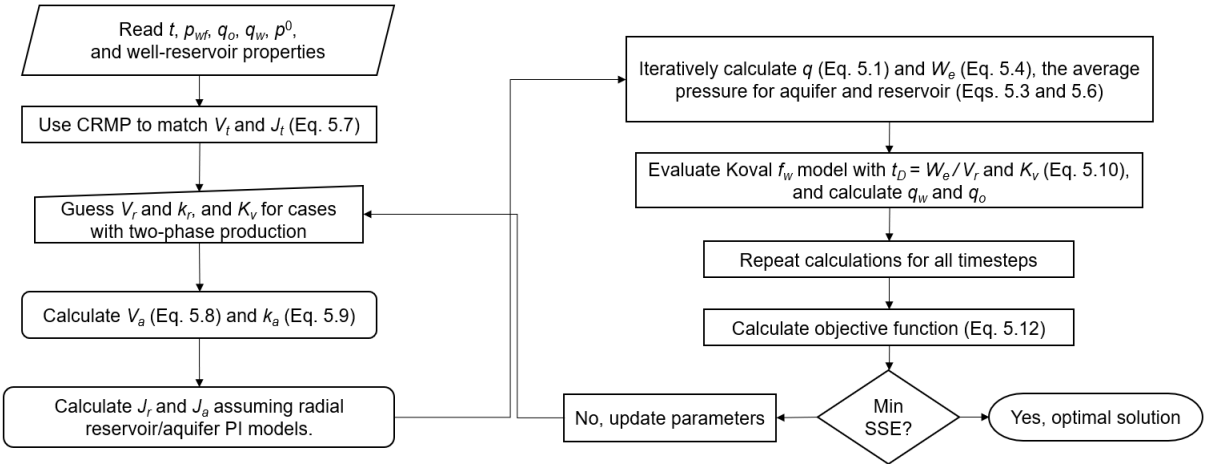

Fig. 5.2—Flow diagram of the new CRMPAF solution procedures.

Validation

In the following sections the CRMPAF models are compared and validated with three synthetic reservoir-aquifer systems: 1) a peripheral water drive, 2) an aquifer represented by pseudo injectors in a five-spot pattern, and 3) a bottomwater drive.

The synthetic reservoir-aquifer models were built using the CMG IMEX numerical simulator (CMG, Calgary, Canada). The three reservoir-aquifer models have a reservoir PV of ~180 million barrels including connate water, and an OOIP of ~160 million barrels. **Table 5.1** shows the general reservoir-aquifer properties of the numerical models, using the conventional symbols (defined in the Nomenclature section) and field units. The properties are independent of pressure, which is always greater than the bubble point. The models neglect capillary pressure and use straight-line relative permeabilities. The reservoir-aquifer properties are homogeneous. Permeability is isotropic. These conditions might appear restrictive, but they are also assumed in many of the available dynamic characterization models. The numerical reservoir-aquifer models were designed to aid test the utility of CRMPAF starting with these ideal cases.

The three base numerical simulation models were run for a production period of one year and using the monthly rate and BHP (12 data points) as input for CRMPAF. A relatively short production period was used because one of our objectives was to develop a model that can be applied early in the exploitation phase to aid reservoir management and development. The numerical models were constrained by a total bottomhole production flow rate. The rate constraint was changed every month. The BHP data at the last day of each month were extracted and used as input. In the first two aquifer models, water did not breakthrough, e.g., they produced single-phase oil and CRMPA was used. For

the bottomwater single and multiwell reservoir cases, water breakthrough because of coning from the aquifer (recall there is no injected water) occurred, thus, CRMPAF was applied.

Property and units	Reservoir - water drive model		
Case	Peripheral	Five-spot pseudo-injectors	Bottomwater
Numerical grid	Radial	Cartesian	Cartesian
Gridblocks	36×1×1	31×31×1	31×31×30
x_r (ft)	n/a	10,000	10,000
y_r (ft)	n/a	10,000	10,000
r_r (ft)	5600	n/a	n/a
r_e (ft)	18,000	n/a	n/a
h_r (ft)		100	
h_a (ft)	100	n/a	100
V_r (million barrels)	177	178	180
OOIP (million barrels)	159	160	162
V_a (million barrels)	1635	n/a	180
r_w (ft)		0.5	
ϕ		0.10	
S_o		0.90	
S_{wr}		0.10	
k (md)		100	
p^0 (psi)		4000	
c_o (psi^{-1})		30×10^{-6}	
c_w (psi^{-1})		3×10^{-6}	
c_f (psi^{-1})		3×10^{-6}	
$\mu_o = \mu_w$ (cp)		1	
$B_o = B_w$ (RB/STB)		1	
ρ_o (Kg/m^3)		850	
ρ_w (Kg/m^3)		1000	

Subscripts *a*, *e*, *o*, *r* and *w* denote aquifer, external or boundary, oil, reservoir and water properties, respectively. n/a = property does not apply for this model.

Table 5.1—Well, reservoir and aquifer properties used in the numerical simulation validation cases.

Table 5.2 shows the result comparison from the three base cases corresponding to each water drive model. The base reservoir-aquifer cases were also modified to investigate the range of utility of the model. The peripheral example was used to test the effect of transient flow by changing the permeability and production period for analysis. The five-spot pseudo-injector case was used to test the degree of pressure support from the aquifer, as the reservoir approximates SS flow. The bottomwater drive case was used to test a single-well and a more complex multiwell reservoir setting.

The paper also presents a field example starting with a single-well and finishing with a multiwell reservoir. The field case provides the final assessment for the model and inherently incorporates complexities, not accounted for in the validation cases.

Aquifer	Model	Production	OOIP (Million barrels)	Relative error (%)	J_t (B/D-psi)	Relative error (%)	W_e (Thousand barrels)	Relative error (%)
Peripheral	CRMPA	Single-phase	145	9	6.4	3	172	n/a
Five-spot pseudo-injector	CRMPA	Single-phase	161	1	6.7	2	163	10
Bottomwater	CRMPAF	Two-phase	163	1	2.0	2	170	n/a

n/a = property does not apply for this model.

Table 5.2—CRMPA/F characterization results for the synthetic reservoir-aquifer models.

Peripheral Water Drive

The first validation case is a peripheral water drive (**Fig. 5.3a**), which is one of most widely applied aquifer modeling geometries. The aquifer volume is ten times greater than the reservoir PV (Table 5.1). **Fig. 5.3b** shows the numerical BHP and rate data from the one-year production period that were used as input for CRMPA. The main objective of applying CRMPA was to accurately determine the OOIP, distinguishing it from the aquifer volume, but the model also enables the calculation of other reservoir and aquifer parameters, such as the PI and water influx

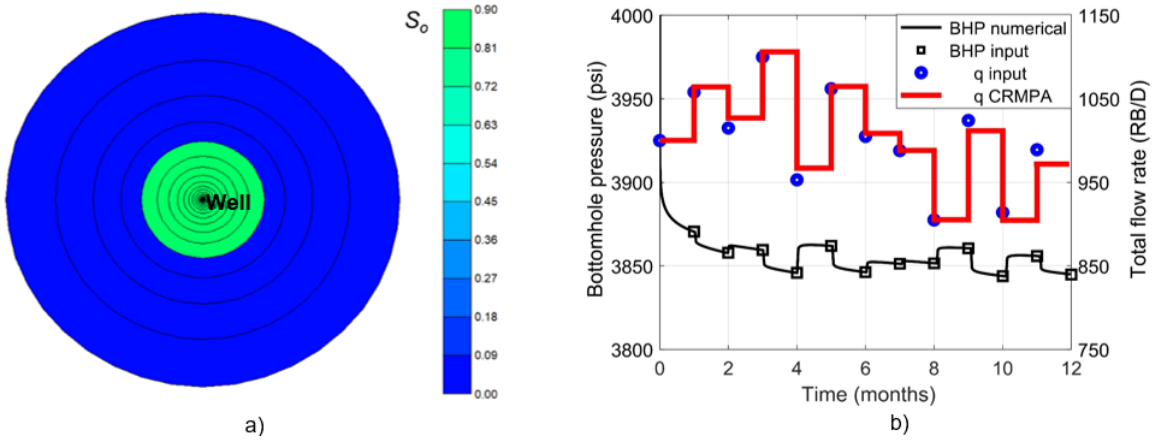

Fig. 5.3—a) Oil saturation for a reservoir with peripheral aquifer, b) Numerical and CRMPA BHP and rate match.

Fig. 5.3b shows the CRMPA production rate history match, displaying excellent agreement with the numerical values. The coefficient of determination is $R^2 > 0.99$. The calculated reservoir and aquifer parameters are in Table 2. These values are compared with the results from the other two base reservoir-aquifer cases (pseudo-injector and bottomwater), with the properties in Table 1. The OOIP is estimated to be 145 million barrels, which is 9% smaller than the actual value. The PI of the well considering the whole reservoir-aquifer system was calculated to be 6.4 B/D-psi, and was compared to the empirical PI definition ($J = q/\Delta p$) assuming a constant rate of 1000 B/D and a pressure drop of 150 psi, yielding J = 6.6 B/D-psi. The cumulative water influx was calculated to be 163 thousand

barrels. The aquifer PI and volume were estimated to be 51.2 B/D-psi and $1.05x10^9$ barrels, respectively. The water influx term looks reasonable but cannot be compared with a known value; the next reservoir-aquifer model (Five spot pseudo-injectors) was specifically designed for these purposes. The aquifer PI cannot be directly measured; but it can be compared with the analogous PI expression of Eq. 5.11 using the known aquifer properties and yielding 60.3 B/D-psi. The calculated aquifer PV is different from the actual value of $1.6x10^9$ barrels in the numerical model. This is because the transient flow regime in this reservoir-aquifer system lasted 230 days (based on the time to reach the late-time unit slope of the equivalent constant rate pressure derivative) and CRMPA is calculating a single average value that best represents the production history over the entire time window.

Transient flow

The peripheral example was used to investigate the range of utility of the model. Table 5.3 shows cases with a different permeability while maintaining the other reservoir-aquifer properties (Table 1). The cases simulated include permeabilities of 25, 50, 75 and 100 md. The time to reach PSS (based on the late-time unit slope of the equivalent constant rate pressure derivative) is shown in the second column of Table 3. The third column shows the OOIP estimation using the same one-year production flow-rate schedule (Fig. 3b). The fifth column shows the OOIP estimation using a production dataset of two years, which also has an average rate of 1000 B/D with ±10% fluctuations, as the one-year case. The OOIP results are compared with the actual numerical value of 159 million barrels. CRMPA estimations are much accurate at higher permeability and/or when using a longer period for analysis, because CRM is derived assuming PSS flow, which is the same requirement for correct application of the MBE (see Craft and Hawkins, 1959), however, transient effects are the dominant flow regime at low permeabilities and/or early times. Based on these results, it seems that the model works reasonably well (less than 10% error) when at least half of the data is in PSS flow. Fortunately, many conventional reservoirs with small to medium size aquifers will satisfy this condition when using data in the order of several months to years.

k (md)	t_{PSS} (days)	OOIP (Million barrels) 1 year of data	Relative error (%)	OOIP (Million barrels) 2 years of data	Relative error (%)
25	920	65	59	95	40
50	460	89	44	114	28
75	345	120	24	143	10
100	230	145	9	160	1

Table 5.3—CRMPA results in transient flow by changing permeability and production period in a peripheral aquifer.

Water Drive Represented by Pseudo-Injector Five Spot Pattern

In the previous peripheral case, CRMPA effectively calculated the OOIP when compared to the numerical input (as long as the model assumptions were reasonably satisfied); however, it was difficult to compare the water influx estimation with a known value. In this example, the aquifer is represented by a five-spot pattern with pseudo-injector wells located at the corners of the reservoir (**Fig. 5.4a**), thus, the cumulative water injected (W_i) is equal to the water influx (W_e). The production rate schedule is the same as in Fig. 5.3b. The cumulative oil production during the period for analysis was ~360 thousand barrels.

Several cases were considered using this five-spot pseudo-injector representation. The study cases differ in the volume of water injected, ranging from a voidage replacement ratio (VRR) of 0.00, 0.25, 0.50, 0.75 and 1.00. In all cases, the pseudo-injectors operated at a constant and equal water injection rate, from start to end of the analysis period to reach the desired VRR. Transient flow in the reservoir lasts ~37 days and does not introduce a significant error.

Table 5.4 shows the OOIP and water influx results from CRMPA, and the relative error with respect to the OOIP and the cumulative water injected from the numerical model. CRMPA is most accurate for partial water drives, which occur from the presence of medium size aquifers; CRMPA is not appropriate to model the extreme cases of a volumetric reservoir (VRR = 0), nor SS flow (VRR = 1). In the former case, the simpler CRMP version should be used. In the latter, the CRMPA solution will just converge to the specified upper constraint for the drainage volume.

The results for the case with a VRR = 0.50 are also in Table 5.2. The calculated numerical BHP for this model was very similar to the base peripheral case (Fig. 5.3b). The CRMPA production rate history match had an R^2 >0.99. The OOIP and W_e were calculated to be 161 million barrels and 177 thousand barrels, respectively. They have a relative error of ~1% from the actual values. Fig. 5.4b shows the water influx comparison with the numerical cumulative water injected. The water influx calculation from this example indicates that the model is accurately capturing this mechanism.

VRR	OOIP (Million barrels)	Relative error (%)	W_e (Thousand barrels)	Relative error (%)
0.00	116	27	104	∞
0.25	145	9	112	24
0.50	161	1	177	1
0.75	201	26	198	27

Table 5.4—CRMPA characterization results for the five-spot pseudo-injector aquifer representation.

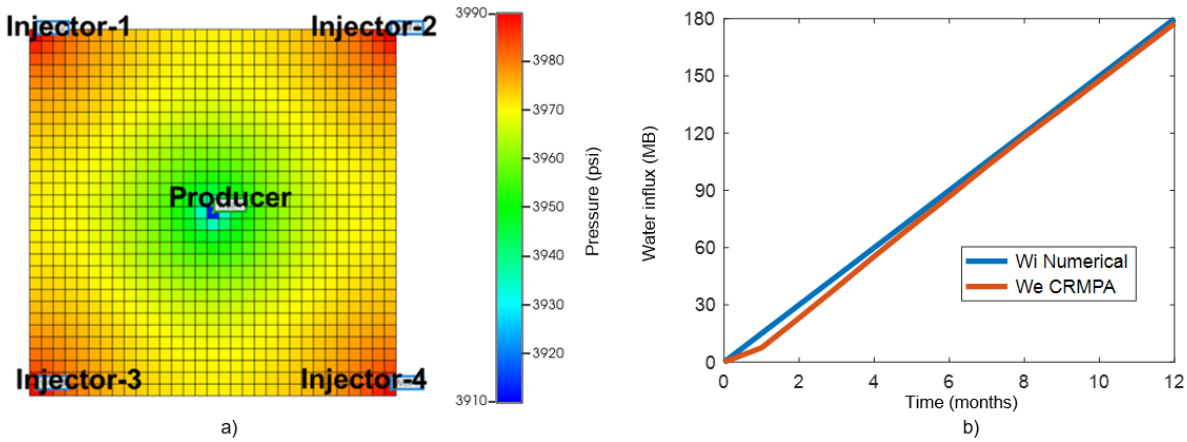

Fig. 5.4—a) Pressure profile after one year of production from a reservoir with five-spot pattern representing a natural water drive. b) Comparison between the numerical water injected and the water influx from CRMPA.

Bottomwater Drive

This section uses a bottomwater aquifer and introduces two-phase flow examples designed to test the CRMPAF approach which incorporates the Koval theory. Initially we discuss a single-well reservoir case, followed by a multiwell example, with the wells coming in at different times, which represents a more realistic scenario. Both cases use the same reservoir-bottomwater drive model. The reservoir and aquifer have the same PV of 180 million barrels and the properties in Table 5.1. The reservoir performance was simulated again with monthly rate variations, comprising at least 12 rate and BHP measurements, which is the minimum dataset required (as a rule of thumb) to estimate the three CRMPAF parameters (storage, transmissibility and the Koval factor). Increasing the number of data measurements should increase the quality of the estimations, as long as the model assumptions are reasonably satisfied.

Single Well Reservoir

Fig. 5.5a shows the well location and oil saturation profile at the initial time. The vertical well is located in gridblock (16,9) in the XY coordinates, and is completed in the four upper layers. This well is also used in the subsequent multiwell example. **Fig. 5.5b** shows the oil saturation at the end of the production period in the XZ plane where the well is located. Water coning from the aquifer is evident. Breakthrough occurred after five months of production.

The CRMPAF approach first requires the application of the single-phase and single medium CRMP formulation. This approach enhances the accuracy of the solution. Next, CRMPAF was applied to calculate the OOIP using the relationships with CRMP as described in previous sections. The BHP and CRMPAF total flow rate history match are in **Fig. 5.6a**. The OOIP and K_v were estimated to be 163 million barrels and 4096. The OOIP estimation is very close to the actual value of 162 million

barrels. The CRMPAF results are also in Table 5.2 for comparison with the other base aquifer drive models. The large K_v is a result of the extremely poor sweep efficiency caused by water coning (recall K_v = 1 for piston-like displacements). **Fig. 5.6b** shows the water cut comparison between the actual and the CRMPAF calculations. The water cut of 10% coming from the initial mobile connate water was summed to the Koval model expressions in Eq. 5.10. The water cut also shows good agreement with the numerical values. The cumulative oil and water production (not shown) calculated with the model are even more accurate. This is because the model calculates average parameters that result in the lowest error throughout the full-time window for analysis. Thus, some differences might occur at specific times, but the cumulative values will closely represent the data. This is relevant in practice, because both, BHP, and mostly rate measurements are prone to error.

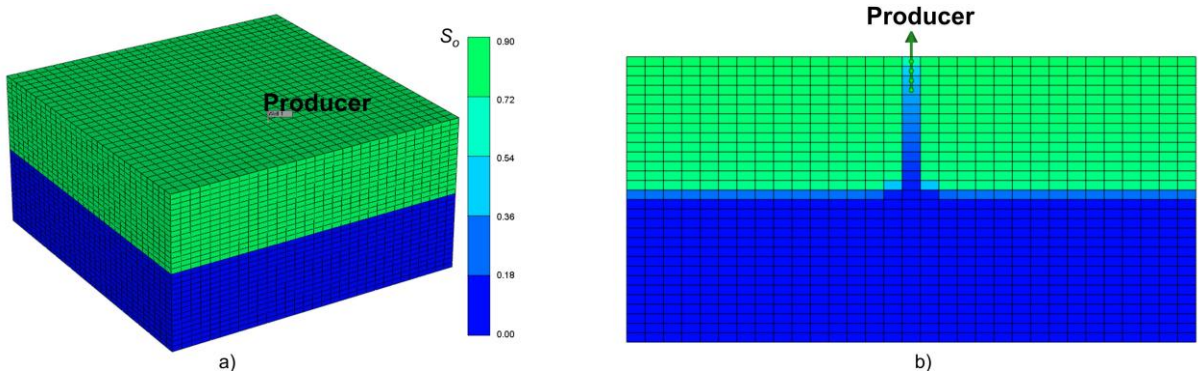

Fig. 5.5—a) Initial oil saturation and b) oil saturation after 18 months in the producer XZ plane location, for a single-well reservoir with a bottom-water aquifer.

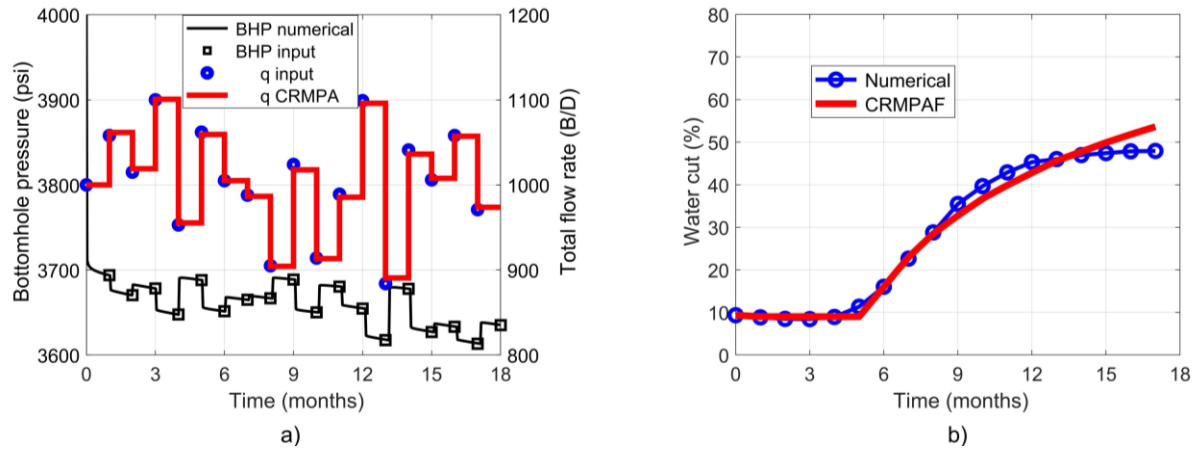

Fig. 5.6—a) Numerical BHP, total production flow rate input and CRMPAF history match, and b) Numerical and CRMPAF calculated water cut for a single-well reservoir with bottom-water drive.

Multiwell Reservoir

This example is used to characterize the OOIP in a more complex and realistic multiwell setting. The reservoir is produced with three wells, which come into production three months apart from each other, resembling a drilling program. The numerical model was run for a total of 18 months. The wells operated with a total production flow rate constraint, with averages of ~1000, 1200 and 1700 B/D, and ±15% monthly rate variations, for wells 1 to 3, respectively. Well-1 is the same as in the previous single-well example. Water breakthrough from the aquifer occurred after 5, 4 and 2 months, respectively. **Fig. 5.7a** shows the location of the wells and the pressure profile at the end of the simulation at the plane of the midpoint perforations depth. The numerical well production and BHP data were next used in CRMPAF to characterize the reservoir.

Fig. 5.7b shows the oil production history match for the three wells. The oil rate decreases after water breakthrough from the aquifer. The R^2 for the three wells is above 0.95. But most importantly, the reservoir OOIP calculated from the sum of the CRMPAF drainage volumes for the three wells is 167 million barrels (**Table 5.5**), which is only 5% different than the actual numerical input. K_v parameters are also in Table 5.5, the largest values are obtained for the highest rate wells, this is because in this example, the wells have the same completion and petrophysical properties, thus, water breakthrough depends on the production rate. We note that K_v for Well-1 in the previous single-well reservoir case was larger than in this case, because the well drainage volume was greater when it produced alone as compared to the multiwell example.

The CRMPAF calculations, particularly the OOIP estimation is relevant: the model proved useful regardless of the complexities of this case which include the presence of the aquifer, two-phase production, interference between wells and a relatively short production period for analysis. Overall, the application of CRMPAF in the study cases has provided accurate solutions when the assumptions are reasonably satisfied. Still, the study cases represent synthetic cases. ~~and make important simplifications~~. The next section presents a field example, which inherently includes several complexities and enables to further evaluate the new models

Well	OOIP (Million barrels)	k_v
1	48	1326
2	53	1467
3	66	1777
Total	167	

Table 5.5—CRMPA characterization results for a multiwell reservoir with bottomwater aquifer and two-phase production.

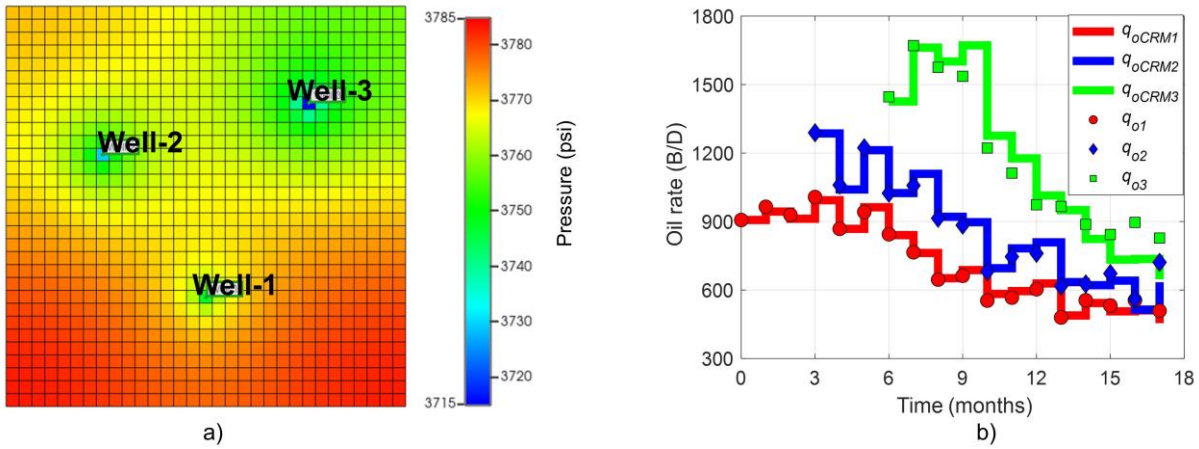

Fig. 5.7—a) Pressure profile at midpoint perforation depth at the end of the production period and b) CRMPAF oil production history match for a multiwell reservoir with a bottomwater aquifer.

Field case

This field case presents a two-well reservoir. Well-1 is the same as presented in the field case in Chapter 4, but Well-2 is new. The time period for analysis is 600 days. Well-1 was producing alone in this block for 227 days until Well-2 was drilled at a distance of 800 m and came into production. The block/reservoir is estimated to have 50 million barrels based on volumetrics. There are other wells in the field but they are not in pressure communication with the two wells in this block. The fluid, well and reservoir data are in **Table 4.10**. It is a conventional undersaturated reservoir producing black oil in primary recovery. The reservoir is associated with an aquifer, which provide pressure support, but also affect well productivity because of water channeling and coning.

The two wells are equipped with a permanent downhole gauge (PDG). All BHP measurements were above the bubble point pressure. Production flow rate measurements and back-allocation data were used to ensure consistency and improve the quality of the analysis. Data are sampled approximately every month. The discrete total production flow rate and BHP measurements for the whole production period are in **Figs. 5.8a** and **5.8b**, for Well-1 and 2, respectively. The cumulative oil production and water cut for the wells are also presented in **Figs. 5.9** and **5.10**, respectively.

Next, we discuss the application of the new CRM techniques corresponding to the single-well production (227 days) and to the total production period (600 days) with the objective to perform an accurate OOIP calculation.

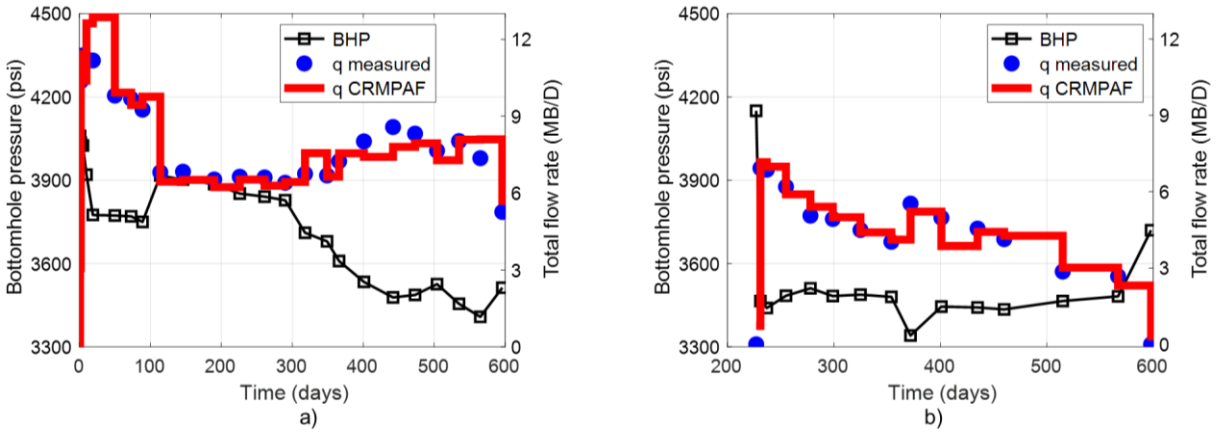

Fig. 5.8—Discrete BHP, measured and calculated CRMPAF total flow rate for a) Well-1 and b) Well-2 producing from an undersaturated reservoir in primary recovery with water influx.

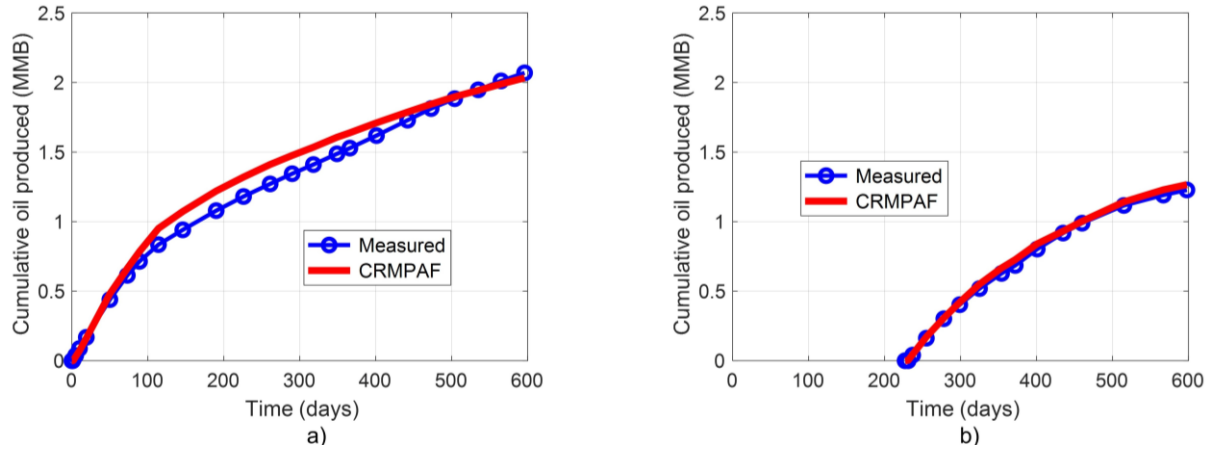

Fig. 5.9—Comparison of cumulative oil production between the measured and the CRMPAF calculation for a) Well-1 and b) Well-2, producing from an undersaturated reservoir in primary recovery with water influx.

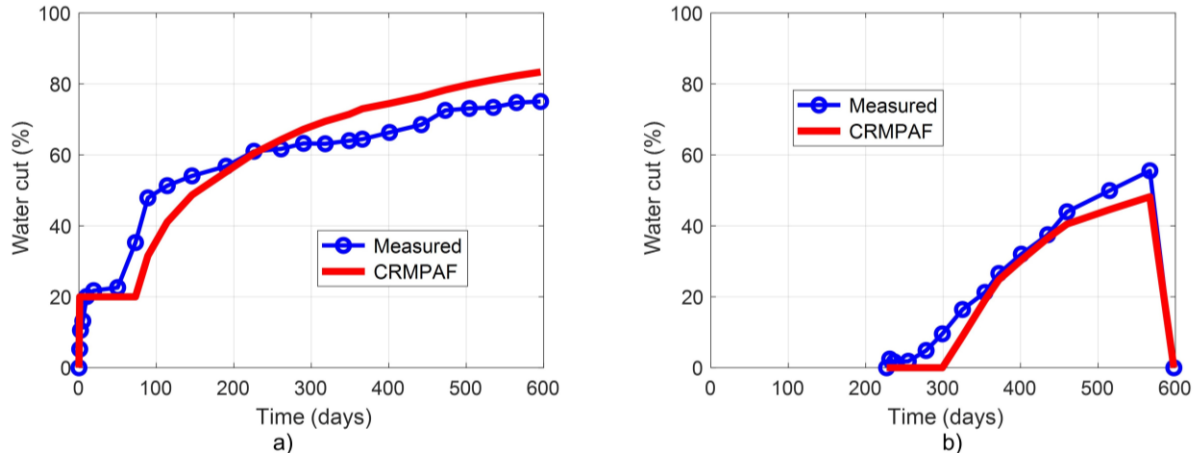

Fig. 5.10—Comparison of the water cut between the measured and the CRMPAF calculation for a) Well-1 and b) Well-2, producing from an undersaturated reservoir in primary recovery with water influx.

Single-Well Reservoir

CRMP, CRMPA and CRMPAF approaches were applied to calculate the OOIP for this reservoir-aquifer system. The OOIP comparison between the three models is in **Table 5.6**. Recall CRMP represents a volumetric reservoir with single-phase production, CRMPA incorporates water influx from an aquifer, and CRMPAF further accounts for two-phase production using the Koval fractional flow model. The OOIP estimation was 238, 82 and 57 million barrels, for the three CRM approaches respectively. These values are compared with the volumetric estimation of roughly 50 million barrels.

CRMP results in a very large OOIP estimation as compared to volumetrics, because it does not discriminate between the reservoir and the aquifer, i.e., it calculates the storage for the whole drainage volume (which is converted to OOIP with the properties in Table 4.10). As a basis for comparison, the traditional flowing material balance (FMB) technique was applied to the flowing pressure and rate data for Well-1 (Fig. 5.8a). The FMB plot (**Fig. 5.11**) shows a straight-line behavior at late times when the reservoir reaches PSS. Extrapolation to the x-intercept provides the reservoir volume; it is more than 200 million barrels for this case, which is also significantly greater than the actual volumetric estimate of 50 million barrels. The main reason is because the FMB does not consider a composite medium, it captures the total connected volume. In the case of gas reservoirs, the FMB can display a deviation from the straight line at late times, thus, it aids to distinguish the reservoir and aquifer volumes, because of the large compressibility/mobility differences (Anderson and Mattar 2004), but this is usually not the case for oil reservoirs, similarly as for the analysis reservoir limit tests (Chen et al. 1996).

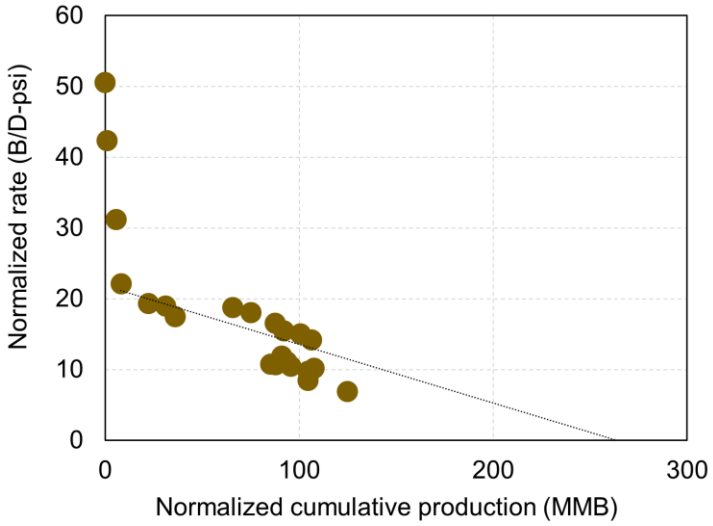

Fig. 5.11—Flowing Material Balance Plot for Well-1.

Model	OOIP (Million barrels)	Relative error (%)	W_e (Million barrels)	K_v
CRMP	238	376	n/a	n/a
CRMPA	82	64	1.08	n/a
CRMPAF	57	14	1.16	320
Volumetric	50			

n/a = property does not apply for this model

Table 5.6—Comparison of the calculated parameters for the single-well period reservoir-aquifer field case with the different CRM approaches.

The CRMPA estimation is better than CRMP (Table 5.7), but it is also in error as compared to volumetrics. CRMPA had resulted in very accurate parameters during the validation cases (peripheral and five spot pseudo-injector), because water breakthrough and multi-phase flow did not occur, even though they had an active water drive.

The CRMPAF approach provides the most accurate OOIP estimation of 57 million barrels, within engineering accuracy of the volumetric value. The CRMPAF history match for the total production flow rate, cumulative oil production and water cut are not shown, but are similar to the case considering the total production period in Figs. 5.8a, 5.9a and 5.10a. K_v was estimated to be 320. In this example, it is about the same as the heterogeneity factor, because the effective viscosity ratio is almost one. This value is in the range estimated by Salazar and Lake (2020) during a study using data from 112 wells from two different oil fields. Fig. 5.10a shows that Well-1 produced water from the start of exploitation (f_w ~ 20%), thus, it was summed to the three Koval model expressions in Eq. 5.10. The water breakthrough from the aquifer occurred after ~50 days. Other parameters estimated with the model are the aquifer PI and PV of 73 B/D-psi and more than 200 million barrels, respectively. **Fig. 5.12** shows the comparison between the average pressure using CRMP (assuming the reservoir-aquifer system behaves as an equivalent permeable medium) and the CRMPAF calculation, which accounts for the composite reservoir-aquifer nature and the fractional flow effects. At early times pressure depletes faster in the CRMPAF, because the aquifer has negligible effects and production mainly depends on the reservoir expansion. At later times both models show a similar rate of depletion; in CRMPAF, this is a result of the water influx, which provides a partial pressure support. Based on the reservoir-aquifer calculations, a drive index estimation was conducted, resulting in a water drive index of 68%; the additional drive is provided by the reservoir expansion.

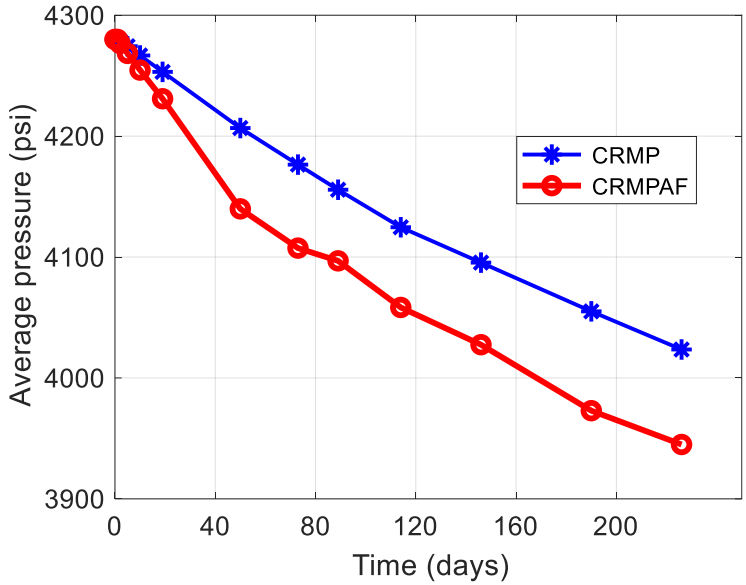

Fig. 5.12—Average reservoir pressure comparison between CRMP (equivalent model) and the new CRMPAF, for an oil well producing from an undersaturated reservoir in primary recovery with water influx.

Multiwell Reservoir

Finally, CRMPAF is applied to the total production period including the two wells. Figs. 5.8-5.10 show the total production flow rate, cumulative oil production and the water cut calculated with CRMPAF for both wells. The OOIP and K_v results are in **Table 5.7**. Using the whole production period results in a smaller OOIP for Well-1, because Well-2 is now draining a portion of the reservoir volume, this also results in a lower K_v estimation. The total reservoir OOIP is 61 million barrels, which has an error of 22% with respect to volumetrics, and that is also larger than the estimation for the single-well scenario. However, considering the uncertainty and complexity of the field case, this result is deemed useful. Recall we are using a simplified model to characterize a reservoir subject to water drive and two-phase production. Furthermore, we are using CRMPAF for a multiwell reservoir, which it does not explicitly account for, however it is accurate because this is a conventional reservoir with a medium size aquifer and most of the production data falls within the stabilized flow regime

Well	OOIP (Million barrels)	k_v
1	43	264
2	18	176
Total reservoir	61	
Volumetric	50	

Table 5.7—CRMPAF results for a multiwell reservoir field case with bottomwater aquifer and two-phase production.

Summary and Conclusions

This chapter presented two new approaches to characterize conventional oil reservoirs producing in primary recovery with natural water influx. These approaches combine the CRMP (a dynamic material balance) with the Fetkovich aquifer model resulting in the CRMPA. Next, CRMPA was extended to account for the oil and water fractional flow effects, by incorporating the Koval model and resulting in the CRMPAF. The model results and assumptions are discussed next.

All CRM approaches assume the permeable medium is finite; thus, they rigorously apply for boundary-dominated flow (BDF). This is not a major limitation, because conventional reservoirs spend most of their life producing in this flow regime (Walsh and Lake, 2003). The results using the peripheral aquifer model indicate that when approximately half of the data is in BDF, the model shows OOIP errors less than 10%. Note however, that the aquifer geometry in most real applications, is a mixture between peripheral and bottomwater drives, thus, the pressure signal will propagate simultaneously through the reservoir and the aquifer, complicating the analysis. Still, the field case demonstrated that CRMPAF is able to provide a reasonable OOIP value as compared to volumetrics; the major requirement is then having accurate production, fluid and formation compressibility data.

This work assumed pressure-independent reservoir properties, however, using multiple timesteps during the solution process enables accounting for pressure-dependent properties throughout the time window for analysis, analogous to reservoir simulation. Properties such as formation compressibility could be updated if a model is available from lab or correlations. Emphasis should be given to compressibility, because it can largely affect the PV estimations, particularly in reservoirs with significant compaction. Conversely, if the PV can be estimated with reasonable certainty from other sources, CRMPA could be used to calculate the total compressibility instead.

As previously described, the PTA and RTA models are usually not satisfactory for characterizing oil reservoir-aquifer systems, because they require very large compressibility and mobility ratios between the two mediums to yield detectable responses. The new CRM approaches showed good results when compared to the synthetic and field cases. This was most conspicuous in the field case for which both, the reservoir and aquifer compressibility and the oil-water viscosity are very similar. It is important to note that our results stem from simple storage and transmissibility relationships. Other transmissibility relationships including storage parameters could be applied, but considering the unknown nature (properties and geometry) of the aquifer, our simplified approach proves useful.

An improvement of the new models, as compared to the classical MBE and to the previous work on CRM with water influx (Izgec and Kabir 2010) is that CRMPAF can be effectively applied with production data only, i.e., they do not require the average pressure, nor shut-in wells. The new models actually calculate the average reservoir pressure, as shown in Fig. 5.12 for Well-1 in the field example.

Concerning the aquifer representation, it has been stated that the Fetkovich model fits nicely into CRM. The Fetkovich aquifer model is analogous to the case of a well producing via depletion (exponential decline). CRMPA rigorously applies to partial water drives in which the average pressure is declining; the quality of the solution diminishes as the model approaches SS flow, and collapses to CRMP in the limit of a volumetric reservoir. Thus, CRMPA can be rigorously applied to small and medium size aquifers for periods of several months to years; large aquifers will require a longer production dataset to ensure transient effects are minimized.

With respect to CRMPAF, we note that fractional flow models have been widely used to model secondary and tertiary recovery processes (Pope 1980), but their application has not been readily applied in the classical MBE. The Koval model used here is one of many available models; it was selected based on its simplicity and widespread use. From the examples discussed, only the bottomwater drive model and the field case produced water from the aquifer, enabling analysis with CRMPAF. The two cases resulted in large Koval factors, as expected for water coning scenarios which have extremely poor sweep efficiency. The OOIP result for the field case was greatly improved when the fractional flow model was incorporated.

Finally, it is worth mentioning that in this paper the model applications were restricted to history matching. As pointed out by Dake (2001), material balance methods, such as the CRM approaches, are better suited for characterization, to define the OOIP and drive mechanism, serving as a tool to build simulation models for the purpose of prediction.

The main conclusions are:

- CRMPAF enable the estimation of the OOIP associated with each well subject to natural water influx and two-phase production, using flowing pressure and production data only (no shut-in wells required). They also enable the calculation of the PI, water influx and a heterogeneity factor. They aid to discern between the reservoir and aquifer volumes, a major field challenge.
- The OOIP was calculated with reasonable accuracy when compared to the numerical values for three synthetic reservoir-aquifer models, and with respect to volumetrics during a field case.
- Incorporating the fractional flow model during the field case calculations improved the OOIP estimations, as compared to the single-phase CRMPA and the previous CRMP approaches.
- CRMPAF is useful to characterize conventional oil reservoirs with partial water drives from small to medium size aquifers, when the production data spans several months or years, and stabilized flow is the dominant regime in the reservoir. CRMPAF can also be used to characterize multiwell reservoirs under these conditions.

Chapter 6. 2D Multiwell Reservoir Model

Introduction

Knowledge of interwell properties is of major importance for reservoir exploitation. Some of its uses directly pertain to the design of infill drilling and the design of secondary and/or tertiary recovery processes, however, these properties are often unknown.

Interwell properties have been quantified by applying methods such as interferences or tracer tests. The output properties from the analysis of interference tests are the interwell permeability and total compressibility, while tracer tests yield estimates of interwell connectivity and swept pore volume (PV). Regardless of their enormous value, interference and tracer tests are not routinely conducted, this is because obtaining high quality interwell data usually requires to shut-in one or even more wells during interference tests, or demand a higher cost and a longer test period during tracer injection.

Interference test is the oldest form of pressure transient tests (Theis 1935; Jacob 1941). They used the line source solution assuming infinite acting radial flow with one active and one observation well to determine interwell permeability and total compressibility. Earlougher and Ramey (1973) presented solutions for a single active well with multiple observation points in a rectangular reservoir; analogous to an interference test in bounded reservoirs. Ramey (1975) based on the work of Papadopulos (1965) introduced the most popular method for analysis of interference tests in anisotropic reservoirs. It assumes transient flow, requires an active well and at least three shut-in observation wells in different directions (rays from the active well at the origin). The method enables calculation of 2D permeabilities, their orientation relative to the well axes and the ϕc_t product. When permeability is aligned with the well axes the model becomes the one proposed by Collins (1961).

Years later, Rodríguez and Cinco-Ley (1993) developed an analytical solution for a 2D closed reservoir producing with multiple wells. The model considered that the wells produced at constant but different bottomhole pressure (BHP). Later Camacho et al. (1996) relaxed this assumption. The previous authors used the model to investigate the rate production performance. Afterwards, Valko et al. (2000) used the model to generalize the productivity index (PI) definition for a multiwell reservoir. Umnuayponwiwat and Ozkan (2000) further extended the 2D model to include transient flow due to rate changes and new wells coming in production. They also included wells with horizontal geometry. The inclusion of transient flow was performed following the methods described by Ozkan (1988) and Raghavan and Ozkan (1994).

The previous references use the model in a forward manner and not in a reservoir characterization sense, some authors presented reservoir pressure profiles.

This chapter uses the microscopic 2D multiwell reservoir model. The model was first used as a basis for comparison with the CRM techniques, first in terms of the overall reservoir volume that was calculated as the sum of the individual drainage volumes, and next to quantify if CRM could give a measure of interwell connectivity, namely permeability, which was not attained. The approach that was followed instead was to use the 2D model to solve the inverse problem by quantifying the directional permeabilities and/or the total compressibility using long-term rate and flowing pressure data coming from a PDG (this data was not readily available in the past). In other words, the 2D model is used to characterize reservoir properties analogous to an interference test in a bounded reservoir as suggested by Earlougher but in a more straightforward manner.

The main advantage of the model is that it uses flowing pressure and rate data, coming from typical field surveillance, thus, it does not require a dedicated test. Since the model assumes BDF, it can incorporate longer periods of production data as compared to the transient methods, however, to work effectively it requires accurate estimation of the reservoir pore volume (PV), either from volumetrics or other sources, e.g., CRM. It is also important to state that the microscopic model inherently assumes communication between all the wells, i.e., the model cannot be used to simultaneously characterize or forecast the behavior of wells located in multiple blocks in one reservoir.

Solution

The microscopic model is a solution of the diffusivity equation for a 2D homogeneous reservoir in cartesian coordinates, under pseudosteady state (PSS) flow. It assumes single-phase flow of a fluid with small and constant compressibility. It incorporates the effect of multiple vertical wells and variable flow rates using superposition. The derivation of the model can be found in the cited references above. The solution is presented next:

$$\bar{p}(t) - p(x,y,z,t) = \frac{\beta q B \mu}{kh} \sum_{j=1}^{N_j} \sum_{n=1}^{N_t} \frac{q_{jk}}{q} a_j, \tag{6.1}$$

where q is a reference rate and a_j is a shape factor constant depending on the shape of the reservoir and the location of each well j, n is a timestep level and β = 141.2. The shape factor is defined as:

$$a_j = 2\pi \frac{y_e}{x_e}\left(\frac{1}{3} - \frac{y}{y_e} + \frac{y^2 + y_{wj}^2}{2y_e^2}\right) + \frac{2\sum_m^\infty \cos m\pi \frac{x}{x_e} \cos m\pi \frac{x_{wj}}{x_e}\left[\cosh m\pi\left(\frac{y_e - |y - y_{wj}|}{x_e}\right) + \cosh m\pi\left(\frac{y_e - |y + y_{wj}|}{x_e}\right)\right]}{m \sinh m\pi \frac{y_e}{x_e}}, \tag{6.2}$$

where the subscript w refers to the well location, e to the external boundary and m is the series index.

Eq. 6.2 is not particularly useful because the series has convergence problems. To avoid these problems, this research used the approach suggested by Ozkan and Raghavan (1991) and Raghavan and Ozkan (1994) to recast the solutions which include infinite series into useful expressions for computational purposes.

The 2D microscopic model was used as the validation case for multiwell CRMP examples in Chapter 4. In the following sections the model was also used for reservoir characterization purposes corresponding to real and synthetic cases. The cases build on complexity, the first example is in fact a field case with limited data, almost purely static BHP data. The following two are synthetic cases discussing isotropic and anisotropic reservoirs with sufficient flowing pressure data. The reference case for comparison of the synthetic cases is the same numerical model as used in Chapter 4, with the properties in Table 4.2. The model uses data from four production wells, the rate schedule consists of monthly rate changes as shown in Fig. 4.11. The production data was used for comparison with the 2D model.

Field Case

A first case was conducted using production rate and BHP data from an old volumetric oil reservoir. The production period for analysis comprises around 17 years, from the start of field exploitation to the time when the bubble point was reached. The reservoirs size has been reasonably determined by geoscience data to be 126 million barrels. The reservoir map and well locations is in **Fig. 6.1** and some reservoir properties are in **Table 6.2**. The rate and BHP data from five wells were considered in the analysis; they are in **Figs. 6.2** and **6.3**, respectively. Note there were very few available BHP measurements, almost all of them from pressure buildups.

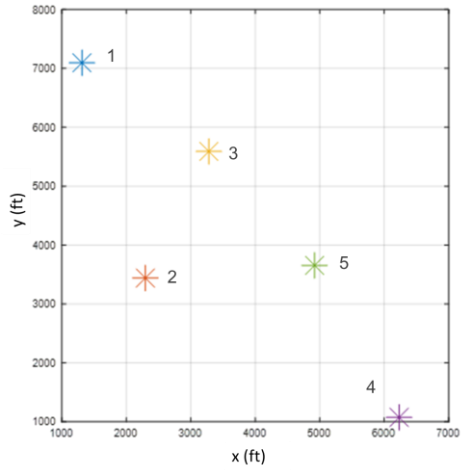

Fig. 6.1—Field case 2D reservoir map showing well locations.

Property	Value and units
x_e	6580 ft
y_e	8550 ft
h	395 ft
ϕ	0.06
S_w	0.20
k	35 md
μ	0.3 cp
Bo	1.5
$OOIP$	126 million barrels

Table 6.1—Field case reservoir properties for the use of the 2D model.

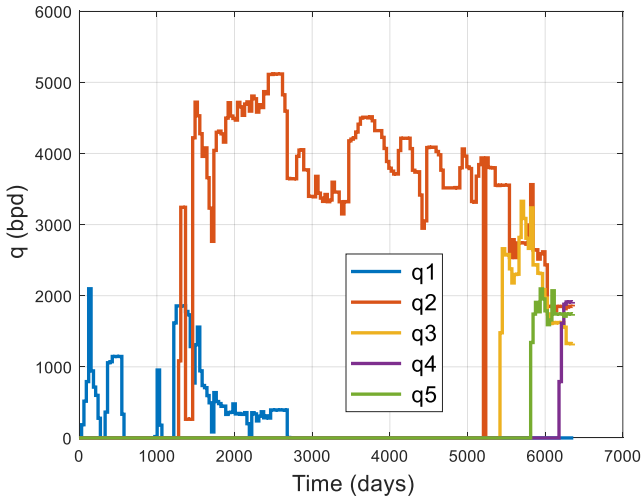

Fig. 6.2—Field case historical production rate.

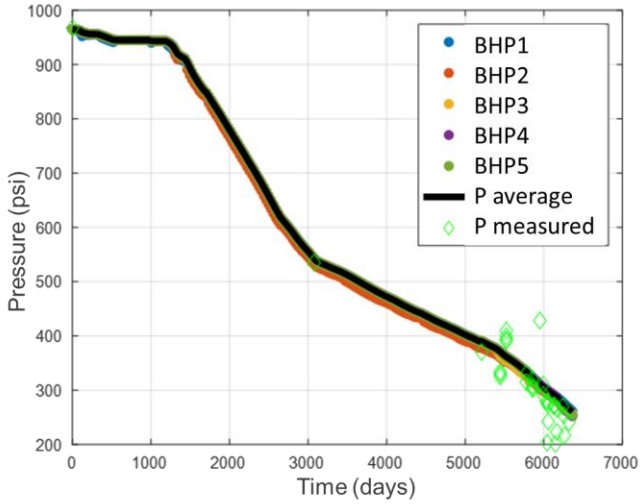

Fig. 6.3—Field case historical BHP and average pressure from the microscopic model vs measured data.

The 2D model was used to estimate the pressure in various locations of the reservoir, including the wells. **Fig. 6.4** shows the pressure profile at the end of the production period of analysis. The history matching process was performed using only the total compressibility. Fig. 6.3 shows the BHP history match, as well as the average pressure calculated from the model incorporating a MBE at each timestep. The best fit was obtained with a total compressibility ranging from 11 (during the first half of production) to 30e-6 psi^{-1} during the second half of the time period for analysis, as expected, c_t increases as the reservoir pressure decreases. In fact, using the model to history match c_t using static pressure data is analogous to performing a MBE analysis.

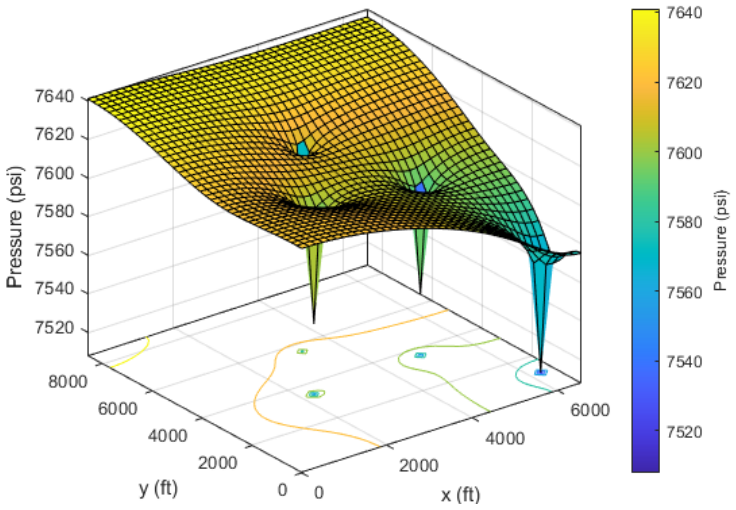

Fig. 6.4—Pressure profile at the end of the production period for analysis for a field case.

Isotropic Reservoir

The numerical reservoir simulator was also used to model an isotropic reservoir with four wells producing with variable flow rate as in Fig. 4.11. The reservoir pressure profile at the end of the one-year production period is in **Fig. 6.5**. Next the rate was used as input in the 2D model and the pressure data was calculated. A single permeability and the total compressibility were used as the matching parameters that best represent the pressure data. **Fig. 6.6** shows the pressure match. The model calculates an isotropic permeability of 99 md and a total compressibility of 2.99x10-6 psi^{-1}, the values are less than 1% off the actual values.

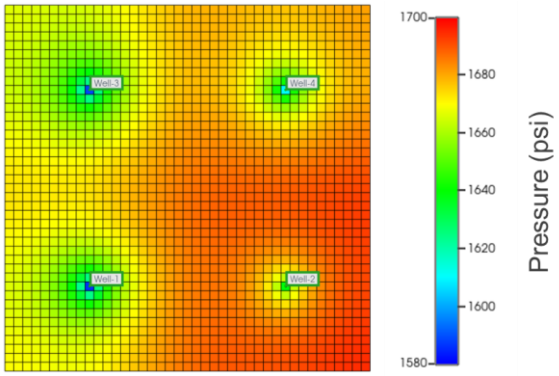

Fig. 6.5—Pressure profile at the end of the production period for analysis for an isotropic multiwell reservoir.

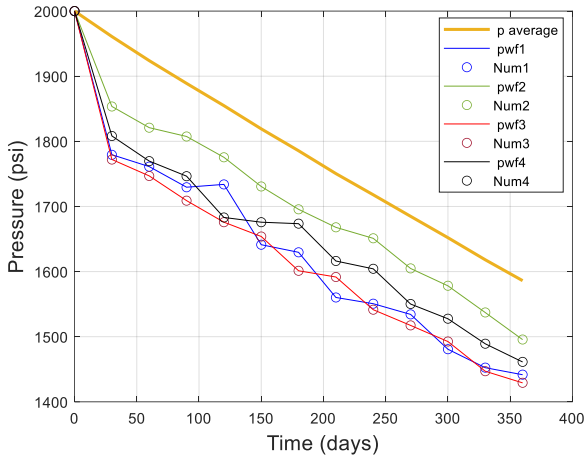

Fig. 6.6—BHP and average pressure calculated with the 2D model and comparison with isotropic numerical BHP.

Analogous to Kamal (2009) for multiple well tests, the suggestion is to first start considering an isotropic reservoir, if the data is well represented and congruent with other sources of information, such as geoscience or from other dynamic data, one can select this as the correct answer. Otherwise, the suggestion is to use the anisotropic reservoir model as described in the next cases.

Anisotropic reservoir

The numerical simulation model was first used to calculate the pressure profile in an anisotropic reservoir with a k_z/k_x = 0.20 as shown in **Fig. 6.7**, as well as the BHP data for the wells, displayed by the as shown in **Fig. 6.7**, as well as the BHP data for the wells, shown by the scatter data in **Fig. 6.8**. Next, the 2D model was used to calculate the anisotropic permeability and the total compressibility. Using the monthly production data results in the pressure match shown by the continuous line in Fig. 6. 8, the calculated reservoir parameters are 69 and 30 md, and 2.8x10-6 psi^{-1} for k_x, k_y and c_t respectively. The permeability values are compared to the actual values of 100 and 20 md; this is not

a very accurate calculation for permeability but it is at least in the right order of magnitude. The compressibility estimation is more accurate when compared to the actual value of 3x10-6 psi^{-1}, as expected for a PSS model.

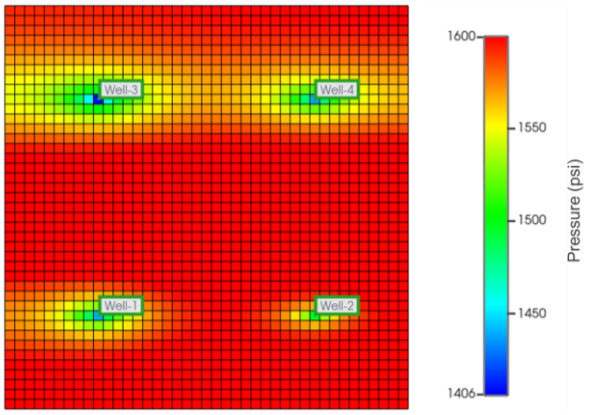

Fig. 6.7—Pressure profile at the end of the production period for analysis for an anisotropic multiwell reservoir.

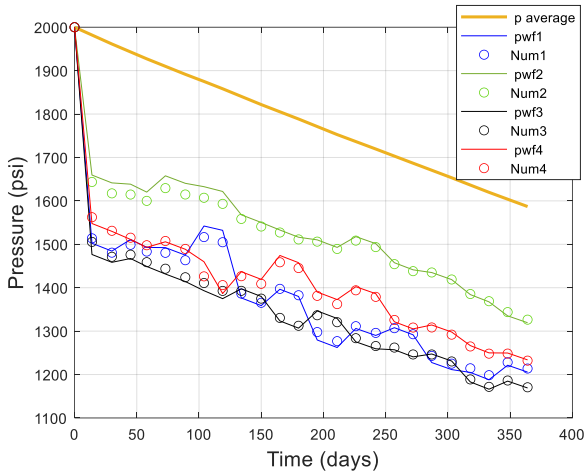

Fig. 6.8—BHP and average pressure calculated with the 2D model and comparison with anisotropic numerical BHP.

To further investigate the model utility, we investigated a case using twice as much rate-pressure data, e.g., using two production data measurements per month. Increasing the number of data measurements resulted in a better estimation of 78 and 25 md for the permeability in x and y directions, and $3x10^{-6}$ psi^{-1} for the total compressibility. It is important to note that one can use more rate-pressure data, this is not unreasonable considering that PDGs can record data in the order of one measurement per second, although the rate is usually reported with much less frequency. It is also worth noting that using more data increases the computation time, however, using the same computation power, as in reservoir simulation, the response for a block with four wells and daily data for one year can be obtained in the order of minutes.

Summary and conclusions

Three cases were presented to show the usefulness for reservoir characterization of a microscopic 2D multiwell reservoir model. The model was developed much earlier, but it was mainly applied for rate performance prediction and not for reservoir characterization, this is because BHP data was limited. The model makes several assumptions, but can be reasonably used for conventional multiwell reservoirs with relatively stabilized production. The model only requires rate and BHP data from day-to-day production operations

At the time of writing, the work on the 2D model is still being conducted, although the preliminary results look interesting, more cases are needed to evaluate the utility of the model to be used as part of the dynamic reservoir characterization toolbox.

Chapter 7. Conclusions and Future Work

Summary

This thesis has presented two dynamic material balance models for reservoir characterization. The first model is used to characterize single and multiwell undersaturated oil reservoirs in primary recovery. It is referred to as the producer-based capacitance resistance model (CRMP). The second model was developed to characterize conventional oil reservoirs producing in primary recovery with water influx from an aquifer and also includes fractional flow effects that occur from two-phase flow production caused by water breakthrough from the aquifer. The model is referred to as CRMPAF. Both of the models can be classified as macroscopic models, because they consider average drainage volume or reservoir properties.

The major advantage of the models is that they only require rate and pressure data from routine production operations. Their main purpose is to calculate the original oil in place (OOIP), but the. Their main purpose is to calculate the original oil in place (OOIP), but the models can also determine the productivity index (PI), water influx and a heterogeneity factor.

The two capacitance-resistance models (CRM) were systematically compared and validated against various analytical and numerical well-reservoir models of varying complexities, yielding very accurate results, as long as the model assumptions are reasonably satisfied, most importantly, that the reservoir is in boundary dominated flow (BDF) and contains slightly compressible fluids.

In addition to the macroscopic models, this work discussed a microscopic 2D multiwell reservoir model. It was initially used for validation purposes for the CRM technique, and later it was applied for dynamic characterization purposes to determine the total compressibility, permeability, and 2D directional permeabilities. The model also only requires rate and BHP data to work effectively.

Conclusions

1. The CRMP approach is essentially a production decline model with variable BHP. CRMP was enhanced by coupling PI definitions for popular reservoir models. Also, successive time windows to study time-varying parameters. The dissertation discussed topics such as constant and variable rate production, transient flow, well location, well geometry, anisotropy and various forms of reservoir heterogeneity. These topics had not been previously discussed or deserved further explanation to include CRM into the reservoir engineering toolbox.
2. It was concluded that CRMP can be used with acceptable error when transient flow measurements are used within a pressure-rate dataset of a developed field. Furthermore, the successive time

interval approach enables to estimate time-varying reservoir pore volume (PV) and PI, or skin/permeability when the well-reservoir model is defined from other sources; it also enables to update pressure-dependent parameters, e.g., fixing permeability one can determine the time-varying skin, otherwise one can determine the pressure-dependent permeability. The time varying nature of the reservoir parameters can reflect well interference or the presence of an aquifer.

3. The CRMP results demonstrated that it can accurately capture the connected/effective drainage volume. The major advantage as compared to reservoir limit tests is that CRMP can be used to calculate single-well drainage volumes in multiwell developed reservoirs. Further, comparing the CRM drainage volume estimates with other techniques, such as volumetrics, can help assess reservoir compartmentalization, interference effects or infill drilling opportunities when the static volume is much larger than estimated by the dynamic method. In addition, once the drainage volume has been obtained from CRM, the average pressure can be readily calculated from material balance. Note again that this calculation is performed using pressure-rate data from routine field surveillance, i.e., there is no need to shut in wells. A comparison of the average pressure in the drainage volume of each well can help assess inter-well communication.
4. CRMP estimated a reservoir volume of 141 million barrels for a field case application for a sandstone reservoir, in excellent agreement with the estimation from static volumetrics. This also demonstrated that the assumed total compressibility is adequate and can be employed in other reservoir engineering analyses. The average pressures in the drainage volume of each well also demonstrated that the reservoir is compartmentalized by a sealing fault.
5. CRMPAF is obtained from the coupling of CRMP, the Fetkovich aquifer model and the Koval fractional flow theory. The model also uses simple storage and transmissibility relationships between an equivalent medium and the composite reservoir-aquifer geometry to constrain the solution parameters.
6. CRMPAF was extensively validated with reservoir-aquifer models of different configurations and with different properties, with results well within engineering accuracy. The model estimated the OOIP within 10% error, even when only half of the data is in BDF.
7. CRMPAF was also very accurate when characterizing the field case which had very similar oil-water compressibility and mobility ratios, effectively distinguishing between reservoir and aquifer volumes, an important challenge.
8. CRMPAF provides an improvement as compared to the classical MBE and to the previous work on CRM aquifer formulation because it does not require average pressure, nor shut-in wells; in fact, this is an output of the model.

Future Work

In this work the CRM approaches were used for reservoir characterization, as is the case for most material balance type models, which best serve as a tool to define the OOIP and drive mechanisms that can later be used to build simulation models for the purpose of prediction.

The present models offer a very good balance between simplicity and results quality; thus, they could be potentially used by reservoir engineers. Some possible future developments include using CRM as a proxy within integrated asset models that couple the reservoir well and surface facilities; CRM is considerably simpler than a reservoir simulation model but offers more capabilities than traditional tank models. Another approach is to use CRM to characterize gas reservoirs, some work has already been with pseudo-functions but none has considered an aquifer yet. In addition, the model could be extended to represent all the complexities in primary recovery, analogous to the full MBE for reservoir with a gas cap and an aquifer, then it will require fractional flow models specific for the gas or water invaded wells.

On the other hand, the 2D microscopic model was only used for BDF conditions, using vertical wells producing with variable rates, it provided order of magnitude results in all cases, even for an anisotropic reservoir, and further research should be conducted. The model can be viewed as a simplified numerical simulation model, and although some might argue that it is not very useful since numerical simulation models are becoming more robust and faster every day, the value of analytical solutions cannot be overemphasized. The model can readily be extended to include more complexities, such as different well geometries, dual porosity, pressure-dependent properties and transient flow. Incorporating transient flow will likely lead to a much better estimation of reservoir parameters, although adding more data will increase the computational time. Another potential topic could be to explicitly include the presence of an aquifer and the effect of two-phase flow within the reservoir, as was done for the macroscopic case.

References

Abbaszadeh, M. and Hegeman, P. 1990. Pressure-Transient Analysis for a Slanted Well in a Reservoir with Vertical Pressure Support. *SPE Form Eval* 5 (03): 277–284. https://doi.org/10.2118/19045-PA.

Albertoni, Alejandro, and Larry W. Lake. 2003. Inferring Interwell Connectivity Only from Well-Rate Fluctuations in Waterfloods. *SPE Reservoir Evaluation and Engineering* 6 (01): 6–16. https://doi.org/10.2118/83381-pa.

Allard, D. R. and Chen, S. M. 1988. Calculation of Water Influx for Bottomwater Drive Reservoirs. *SPE Res Eng* 3 (02): 369–379. https://doi.org/10.2118/13170-PA.

Anderson, D. and Mattar, L. 2004. Practical Diagnostics Using Production Data and Flowing Pressures. Presented at the SPE Annual Technical Conference and Exhibition, Houston, Texas, September 2004. https://doi.org/10.2118/89939-MS.

Blasingame, T. A., and Lee, W. J. 1986. Variable-Rate Reservoir Limits Testing. Presented at the SPE Permian Basin Oil and Gas Recovery Conference, OGR, Midland, Texas, 13-14 March. https://doi.org/10.2523/15028-ms.

Bourdet, D. 2002. *Well Test Analysis: The use of Advanced Interpretation Models*. Amsterdam, Netherlands. Elsevier.

bp. 2022. bp Statistical Review of World Energy 2022. 71st edition. https://www.bp.com/content/dam/bp/business-sites/en/global/corporate/pdfs/energy-economics/statistical-review/bp-stats-review-2022-full-report.pdf.

Bruce, W.A. 1943. An Electrical Device for Analyzing Oil-Reservoir Behavior. *Transactions of the AIME* 151 (01): 112-124. https://doi.org/10.2118/943112-g.

Buckley S. E. and Leverett M. C. 1942. Mechanism of Fluid Displacement in Sands. *Trans.* AIME 146: 107–116. https://doi.org/10.2118/942107-G.

Camacho-V, R., Rodríguez, F., Galindo-N., A. and Prats, M. 1996. Optimum Position for Wells Producing at Constant Wellbore Pressure. *SPE Journal* 1 (02): 155–168. https://doi.org/10.2118/28715-pa.

Cao, F. 2014. The Development of a Two-Phase Capacitance Resistance Model. PhD Dissertation. The University of Texas at Austin, Austin, Texas.

Cao, F., Luo, H. and Lake, L.W. 2015. Oil-Rate Forecast by Inferring Fractional-Flow Models from Field Data with Koval Method Combined with the Capacitance/Resistance Model. *SPE Res Eval&Eng* 18 (2015): 534–553. https://doi.org/10.2118/173315-PA

Carter, R.D. and Tracy, G.W. 1960. An Improved Method for Calculating Water Influx. *Trans*., AIME 219: 415-417. https://doi.org/10.2118/1626-G.

Chen, C., Chu W. and Sadighi, S. 1996. Pressure-Transient Testing of Gas Reservoirs with Edge-Waterdrive. *SPE Formation Evaluation* 11 (4): 251–256. https://doi.org/10.2118/28381-PA.

Chitsiripanich, S. 2015. *Field Application of Capacitance-Resistance Models to Identify Potential Location for Infill Drilling*. MS Thesis, The University of Texas at Austin, Austin, Texas.

Cinco Ley, H. 2023. Caracterización Dinámica de Yacimientos. Lecture Notes. Universidad Nacional Autónoma de México, Mexico City, Mexico.

CoIlins, R. E. 1961. Flow of Fluids Through Porous Media. Reinhold Publishing Corp. New York.

Craft, B.C. and Hawkins, M.F., 1959. Applied Petroleum Reservoir Engineering. Prentice−Hall, Inc., Englewood Cliffs, New Jersey.

Dake, L. P. 2001. The Practice of Reservoir Engineering (Revised Edition). Developments in Petroleum Science, Elsevier.

Doublet L. E. and Blasingame, T. A. 1995. Decline Curve Analysis Using Type Curves: Water Influx/Waterflood Cases. Presented at the SPE Annual Technical Conference and Exhibition, Dallas, Texas, USA, 22-25 October, 1995. SPE 30774.

Earlougher, R.C. Jr. and Ramey, H.J. Jr. 1973. Interference Analysis in Bounded Systems. *J. Cdn. Pet. Tech*. (October–December 1973): 33–45. https://doi.org/10.2118/73-04-04.

Earlougher, R.C. Jr. 1977. *Advances in Well Test Analysis*. Monograph Series. Vol. No. 5. Richardson, Texas: Society of Petroleum Engineers.

Economides, M., Hill, D., Ehlig-Economides, C. et al. 2012. *Petroleum Production Systems*, second edition. Westford, Ma, USA: Pearson Education.

Fetkovich, M.J. 1971. A Simplified Approach to Water Influx Calculations—Finite Aquifer Systems *J Pet Technol* 23 (1971): 814–828. https://doi.org/10.2118/2603-PA.

Fetkovich, M. J., Fetkovich, E. J. and Fetkovich, M. D. 1996. Useful Concepts for Decline-Curve Forecasting, Reserve Estimation, and Analysis. *SPE Res Eng* 11 (1996): 13–22. https://doi.org/10.2118/28628-PA.

Fox, M.J., Chedburn, A. C. S., and Stewart, G. 1988. Simple Characterization of Communication Between Reservoir Regions. Presented at the European Petroleum Conference, London, United Kingdom, October 1988. https://doi.org/10.2118/18360-ms.

Hagoort, J., and Hoogstra, R. 1999. Numerical Solution of the Material Balance Equations of Compartmented Gas Reservoirs. *SPE Reservoir Evaluation and Engineering* 2 (4): 385-392. https://doi.org/10.2118/57655-PA.

Harmony Enterprise, 2022. Harmony Enterprise™ 2022.3 Help –PDF. https://www.ihsenergy.ca/support/documentation_ca/Harmony_Enterprise/latest/content/print_pdf_output/harmony_enterprise_help.pdf (accessed 6 April 2023).

Havlena, D. and Odeh, A. S., 1963. The Material Balance as an Equation of a Straight Line. *J Pet Technol* 16 (07): 815–822. https://doi.org/10.2118/869-PA.

Holanda, R. W., Gildin, E., Jensen, J. L. et al. 2018. A State-of-the-Art Literature Review on Capacitance Resistance Models for Reservoir Characterization and Performance Forecasting. *Energies* 11 (3368). https://doi.org/10.3390/en11123368.

Holanda, R. W., Gildin, E., and Jensen, J. L. 2018b. A Generalized Framework for Capacitance Resistance Models and a Comparison with Streamline Allocation Factors. *Journal of Petroleum Science and Engineering* 162 (2018): 260-282. https://doi.org/10.1016/j.petrol.2017.10.020.

Houzé, O., Viturat, D., Fjaere O. et al. 2022. *Dynamic Data Analysis* v5.50. Kappa Engineering. https://www.kappaeng.com/documents/flip/dda550/

Izgec, O. and Kabir C.S. 2010. Quantifying Nonuniform Aquifer Strength at Individual Wells. *SPE Res Eval & Eng* 13 (2010): 296–305. https://doi.org/10.2118/120850-PA.

Izgec, O., and Kabir, C. S. 2011. Quantifying Reservoir Connectivity, in-Place Volumes, and Drainage-Area Pressures During Primary Depletion. *Journal of Petroleum Science and Engineering* 81 (0): 7-17. https://doi.org/10.1016/j.petrol.2011.12.015.

Jacob, C.E. 1941. Coefficient of Storage and Transmissibility Obtained from Pumping Tests in the Houston District, Texas. Trans., American Geophysical Union, 744–756.

Jones, P. 1956. Reservoir Limit Test. *Oil and Gas Journal*, 184–96.

Joshi, S.D. 1988. Augmentation of Well Productivity with Slant and Horizontal Wells. *Journal of Petroleum Technology* 40 (06): 729-739. https://doi.org/10.2118/15375-pa.

Kaczorowski, N. J. 1993. Reservoir Limit Testing in Water-Drive Systems. Presented at the SPE Asia Pacific Oil and Gas Conference. February 1993. https://doi.org/10.2523/25336-ms.

Kamal, M. M. 2009. *Transient Well Testing*. Monograph Series. Vol. 23. Richardson, Texas: Society of Petroleum Engineers.

Kaviani, D., and Valkó, P. 2010. Inferring Interwell Connectivity Using Multiwell Productivity Index (MPI). *Journal of Petroleum Science and Engineering* 73 (1-2): 48-58. https://doi.org/10.1016/j.petrol.2010.05.006.

Kaviani, D., Soroush, M., and Jensen, J. L. 2014. How Accurate Are Capacitance Model Connectivity Estimates? *Journal of Petroleum Science and Engineering* 122 (0): 439-452. https://doi.org/10.1016/j.petrol.2014.08.003.

Koval, E. J. 1963. A Method for Predicting the Performance of Unstable Miscible Displacement in Heterogeneous Media. *SPE J*. 3 (2): 145–154. http://dx.doi.org/10.2118/450-PA.

Kumar, A. 1977. Strength of Water Drive or Fluid Injection from Transient Well Test Data. *J Pet Technol* 29:1497–1508. https://doi.org/10.2118/5054-PA.

Lake, L. W., Johns, R. T., Rossen W. R. et al. 2014. *Fundamentals of Enhanced Oil Recovery*. Richardson, Texas, Society of Petroleum Engineers.

Liang, X., Weber, D.B., Edgar, T.F. et al. 2007. Optimization of Oil Production Based on a Capacitance Model of Production and Injection Rates. Presented at the Hydrocarbon Economics and Evaluation Symposium, Dallas, Texas, USA., April 2007. https://doi.org/10.2118/107713-MS.

Marhaendrajana, Taufan, and T. A. Blasingame. 2001. Decline Curve Analysis Using Type Curves - Evaluation of Well Performance Behavior in a Multiwell Reservoir System. SPE Annual Technical Conference and Exhibition. https://doi.org/10.2118/71517-ms.

Martínez Romero, N. and Samaniego-V, F. Advances in the Analysis of Pressure Interference Tests. *J Can Pet Technol* 49 (12): 65–70. SPE-141028-PA. https://doi.org/10.2118/141028-PA

Mattar, L., and Anderson, D. 2005. Dynamic Material Balance (Oil or Gas-In-Place Without Shut-Ins). Presented at the Canadian International Petroleum Conference, Calgary, Alberta, June 2005. https://doi.org/10.2118/2005-113.

Matthews, C. S., and Russell, D. G. 1967. *Pressure Buildup and Flow Tests in Wells*. Monograph Series. Vol. No. 1. Richardson, Texas: Society of Petroleum Engineers.

Moreno, G. A., and Lake, L. W. 2014. Input Signal Design to Estimate Interwell Connectivities in Mature Fields from the Capacitance-Resistance Model. *Petroleum Science* 2014 (11): 563-568. https://doi.org/10.1007/s12182-014-0372-z.

Muskat, M. 1946. *The Flow of Homogeneous Fluids Through Porous Media*. Ann Arbor, Michigan, USA. J. W. Edwards, Inc.

Nguyen, A. P., Kim, J. S., Lake, L. W. et al. Integrated Capacitance Resistive Model for Reservoir Characterization in Primary and Secondary Recovery. Presented at the SPE Annual Technical Conference and Exhibition, Denver, Colorado, USA, October 2011. https://doi.org/10.2118/147344-MS.

Ozkan, E. 1988. Performance of Horizontal Wells. PhD dissertation, The University of Tulsa, Tulsa, Oklahoma.

Ozkan, E. and Raghavan, R. 1991. New Solutions for Well-Test-Analysis Problems: Part 1—Analytical Considerations. *SPE Formation Evaluation* 6 (1991): 359–368. https://doi.org/10.2118/18615-PA.

Ozkan, E. and Raghavan, R. 1991. New Solutions for Well-Test-Analysis Problems: Part 2—Computational Considerations and Applications. *SPE Formation Evaluation* 6 (03): 369–378. https://doi.org/10.2118/18616-PA.

Papadopulos, I.S. 1965. Non-Steady Flow to a Well in an Infinite Anisotropic Aquifer. Publication 73 presented at the International Association of Hydrological Sciences' Symposium of Dubrovnik, Dubrovnik, Yugoslavia, October 1965.

Parra, J. E., Samaniego-V, F. and Lake, L. W. 2023. Application of the Producer-Based Capacitance Resistance Model to Undersaturated Oil Reservoirs in Primary Recovery *SPE J.* Vol. 28 No. 5 (Oct): 2256–2273. https://doi.org/10.2118/214678-PA.

Parra, J. E., Samaniego-V, F. and Lake, L. W. 2023. CRM-Aquifer-Fractional Flow Model to Characterize Oil Reservoirs with Natural Water Influx. *SPE J.* https://doi.org/10.2118/217973-PA.

Pope, G. A. 1980. The Application of Fractional Flow Theory to Enhanced Oil Recovery. *SPE Journal* 20 (03): 191-205. SPE-7660-PA. http://dx.doi.org/10.2118/7660-PA.

Ramey, H. J., Jr., Kumar, A., and Gulati, M. S. 1973. *Gas Well Test Analysis Under Water-Drive Conditions*. Arlington, Va. USA: American Gas Association.

Raghavan, R. and Ozkan, E. 1994. A Method for Computing Unsteady Flows in Porous Media, Longman Scientific & Technical, Essex, U.K.

Rodriguez, Fernando, and Heber Cinco-Ley. 1993. New Model for Production Decline. In *Production Operations Symposium*. https://doi.org/10.2523/25480-ms.

Salazar, J. J. and Lake, L. W. 2020. The Physical Meaning of the Koval Factor. *Math Geoscience* 52, 1017–1033 (2020). https://doi.org/10.1007/s11004-020-09883-0.

Sayarpour, M. 2008. Development and Application of Capacitance-Resistive Models to Water/CO2 Floods. PhD dissertation. The University of Texas at Austin, Austin, Texas.

Sayarpour, M., Zuluaga, E., Kabir, C. S. et al. 2009. The Use of Capacitance-Resistance Models for Rapid Estimation of Waterflood Performance and Optimization. *Journal of Petroleum Science and Engineering* 69 (2009): 227-238. https://doi.org/10.1016/j.petrol.2009.09.006.

Schilthuis, R.J. 1936. Active Oil and Reservoir Energy. *Trans*., AIME, 118: 33–52. https://doi.org/10.2118/936033-G.

Soroush, M, and Rasaei, M. R. 2018. Application of the Capacitance Model in Primary Production Period before IOR Implementation. Presented at the SPE Trinidad and Tobago Section Energy Resources Conference, Port of Spain, Trinidad and Tobago, June 2018. https://doi.org/10.2118/191236-ms.

Theis, C.V. 1935. The Relation Between the Lowering of the Piezometric Surface and the Rate and Du ration of Discharge of a Well Using Groundwater Storage. Trans., American Geophysical Union, 519–524.

Umnuayponwiwat, S., and Ozkan, E. 2000. Evaluation of Inflow Performance of Multiple Horizontal Wells in Closed Systems. *Journal of Energy Resources Technology* 122 (1): 8-13. https://doi.org/10.1115/1.483155.

Valko P.P., Doublet, L.E., and Blasingame, T.A. Development and Application of the Multiwell Productivity Index (MPI). *SPE J.* 5 (01): 21–31. https://doi.org/10.2118/51793-PA

van Everdingen, A.F. and Hurst, W. 1949. The Application of the Laplace Transformation to Flow Problems in Reservoirs. *Trans*., AIME 186, 305-324. https://doi.org/10.2118/949305-G.

Wahl, W. L., Mullins, L. D., Barham, R. H. et al. 1962. Matching the Performance of Saudi Arabian Oil Fields with an Electrical Model. *Journal of Petroleum Technology* 14 (11). https://doi.org/10.2118/414-pa.

Walsh, M, and Lake, L. W. 2003. *A Generalized Approach to Primary Hydrocarbon Recovery*. Oxford, UK: Handbook of Petroleum Exploration and Production 4, Elsevier Science.

Yousef, A., Gentil, P., Jensen, J. L. et al. 2006. A Capacitance Model to Infer Interwell Connectivity from Production and Injection Rate Fluctuations. *SPE Reservoir Evaluation & Engineering* 9 (06): 630–46. https://doi.org/10.2118/95322-pa.